Application of polymer materials for development of artificial pancreas

Hao Chen

2011

Dedicated to my family

Hongjie Chen

Aihua Li

Table of Contents

Abbreviations

IBMIR	Instant blood-mediated inflammatory reactions
PEG	Poly(ethylene glycol)
DPPE	1,2-Dipalmitoyl-*sn*-glycerol-3-phosphatidylethanolamine
Tris	Tris(hydroxymethyl)aminomethane
ELISA	Enzyme-linked immunosorbent assay
PBS(-)	Phosphate Buffered Saline
HBSS	Hank's balanced salt solution
FITC	Fluorescein isothiocyanate
FBS	Fetal bovine serum
BSA	Bovine serum albumin
IgG	Immunoglobulin G
Tween 20	Polyoxyethylene sorbitan monolaurate
P-SH	Poly(acrylamide-*co*-*N*-acrylcysteamine)

General Introduction

The history of medicine is the history of human with disease, too. Because the advance of medicine is unrelenting, now many previous diseases without a cure can be recovered fully. However, while the type decreased, cancers heading the list of diseases that do not have an effective treatment still exist and many lives of people are being terrified by them.

One of them is diabetes; its main symptom is pathologic rising of blood glucose concentration that is brought on by the tumultus of control system in the body. The rapid rising brings on the disturbance of consciousness by diabetic ketoacidosis that expose patient to danger of life. In the case that concentration of blood glucose did not rise rapidly, the continuation of high blood glucose level damages peripheral vessel, the complication that is represented by diabetic neuropathy, diabetic retinopathy and diabetic nephropathy.

The diabetes have two types, one is the type 2 diabetes that is known as lifestyle disease. The plethoric consumption of sugar, adipose and salt turned down the insulin responsiveness, as a result rising of blood glucose concentration appeared. This type accounts 90% of total patients. In this case, if the disease is an early stage, alimentotherapy and ergotherapy were applied to patient. When they did not combat effectively, the oral antihyperglycemic drug that encourage the secretion of insulin is dosed, even so the symptom did not be change for the better, insulin injection is applied finally. On the whole, the control of blood glucose concentration is comparatively easy but the severe case.

The remaining 10% of patient is accounted by type 1 diabetes. The pathogeny

is the destruction of β cells that is brought on by the autoimmune disease, and the alimentotherapy and ergotherapy can not combat effectively because the insulin secretion with a capital is lost. So now only the insulin injection is effective as a pharmacological treatment. However, the insulin should be injected before 30 min of diet exactly, and it is a very long burden for patient. In the worse case, if the β cells are destructed completely, the control of blood glucose concentration only by insulin injection become hard and ketoacidosis will experience easily. Finally the patient needed a transplantation of pancreas or islets [1, 2].

It is possible for pancreas transplantation to let patient rid themselves completely of insulin injection. However, either the pancreas or islet transplantation, when the donated organ or tissue is moved into the body of recipient because they are foreign substance for recipient, after the activation the immune system began to attack the organ or tissue. As a result, transplanted organ can not be accepted by the body of recipient, graft survival rate decrease.

The transplantation of pancreas is organ transplantation so it has a high insulin secretion effect. However, because surgical operation is fundamental, it has high invasive for recipient, and the immune rejection is very strong. In contrast, islet transplantation is cellular transplantation so the burden of recipient is very little because it does not need a surgical operation but catheter to transplant.

The immune system is activated when the foreign substance invade to inside of the body. In the case that islets were transplanted into inportal, after the contact of blood the coagulation system and complement system were activated,

thrombus were made on the surface of islet and graft was damaged additionally by instant blood-mediated inflammatory reactions (IBMIR) [3–12].

As methods to protect islets from these systems, one is simply the physical isolation of islet by membrane, another is the biochemical protect by localizing drug that inhibit these systems around islets. If the former is the case, encapsulation of islets by algin acid and agarose is typical [13–27]. Of the latter, recombinant enzyme protein that introduced functional group is immobilized with surface of islets by crosslinker [28-40]. As each defect, in the case of microcapsulation, because the supply of oxygen and nutrition to encapsulated islets depends on osmosis, so the central necrosis appears after long term. And in the case of protein immobilization, because the functional group of enzyme was recombinant, there is a risk to apply to human body. Either way, polymer materials are almost used in these researches, the improvement of those materials is necessary.

The destination of this research is the improvement of polymer materials for artificial pancreas and it can be separated two parts. Part I is about the method to protect transplanted intravascular islets biochemically (Chapter.1-3). Part II is about the physical protection of transplanted islets and the securement of β cells expected donors (Chapter.4, 5).

In Chapter.1, the immobilization of nonrecombinant protein to islet surface by using PEG phospholipid conjugate was developed. Transplantation of islets of Langerhans is a promising method for treating patients with insulin-dependent diabetes mellitus. The major obstacle in clinical settings is early graft loss due to inflammation triggered by blood coagulation and complement activation on the

surface of the islets after intraportal transplantation. It is proposed a versatile method for modifying the surface of islets with the fibrinolytic enzyme urokinase and the soluble domain of the anticoagulant enzyme thrombomodulin. The surfaces of islets were modified with a poly(ethylene glycol) phospholipid conjugate bearing a maleimide group (Mal–PEG–lipid; PEG MW=5000 kDa). The Mal–PEG–lipid anchored to the cell membranes of islets, resulting in the presentation of functional maleimide groups on the islet surface. The surface was further treated with thiolated urokinase and thrombomodulin that conjugated by thiol/maleimide bonding. No practical islet volume increase was observed after surface modification, and the modifications did not impair insulin release in response to glucose stimulation. Furthermore, the activity of the immobilized urokinase and thrombomodulin was maintained. These modifications could help to improve graft survival by preventing thrombus formation on the surface of transplanted islets.

In Chapter.2, as a complementary method, the non protein low molecular weight drug was immobilized on islet surface by using encapsulation into liposome. An unresolved obstacle in transplantation of islets of Langerhans is the early graft loss caused by thrombotic reactions on the surface of islets after intraportal transplantation. It was investigated a versatile method for modifying the surface of islets with liposomes carrying the anticoagulant argatroban using an amphiphilic poly(ethylene glycol)-phospholipid conjugate derivative (PEG-lipid) and DNA hybridization. Argatroban was gradually released from the liposomes on the islets, and antithrombic activity was detected in culture medium. Modified islets retained the ability to control insulin release in response to

glucose concentration changes. Although it was mainly examined surface modification of islets, this technique may be useful for immobilizing various types of small molecules on cells and tissues and thus may have many applications in cell therapy and regenerative medicine.

In Chapter.3, because in these experiments PEG lipid was used, the control of cell attachment was tried by using oligoDNA PEG lipid conjugate. Cell–cell interactions play vital roles in embryo development and in homeostasis maintenance. Such interactions must be stringently controlled for cell-based tissue engineering and regenerative medicine therapies, and methods for studying and controlling cell–cell interactions are being developed using both biomedical and engineering approaches. In this study, it was prepared amphiphilic PEG-lipid polymers that were attached to oligoDNA with specific sequences. Incubation of cells with the oligoDNA–PEG-lipid conjugate transferred some of the oligoDNA to the cells' surfaces. Similarly, oligoDNA–PEG-lipid conjugate using oligoDNA with a complementary sequence was introduced to the surfaces of other cells or to a substrate surface. Cell–cell or cell–substrate attachments were subsequently mediated via hybridization between the two complementary oligoDNAs and monitored using fluorescence microscopy.

In Chapter.4, the polymer gel is useful for development of cell encapsulation, so the gelation rate of disulfide crosslink was determined. Kinetic analysis were carried out for formation of disulfide crosslinkages between thiol groups on linear polymers, poly(acrylamide-co-N-acrylcysteamine) (P-SH). Disulfide crosslinkages were formed by auto-oxidation of pendant thiol groups or through

the thiol-disulfide exchange reaction induced by addition of disulfide compounds gluthathione. In the auto-oxidation reaction, the rate constant for disulfide formation highly depended on pH values of the reaction mixtures and the P-SH concentrations. Gelation rate is too slow to enclose living cells into hydrogel under physiological pH 7.4. The hydrogel formation rate can be accelerated by addition of disulfides, such as oxidized glutathione. In the later case, oxygen in the reaction mixture is not consumed. The thiol-disulfide exchange reaction is much more suitable for the cell encapsulation than the thiol auto-oxidation reaction. These findings give a basis for enclosure of living cells in a hydrogel.

In Chapter.5, because the differentiation of β cells from stem cell is expected as a cell resource. The method to identify the special cells without killing them by secretion product from wide variety cells is developed. Embryonic stem (ES) cells hold promise as a source for cell transplantation treatment of diseases such as type I diabetes. Further, cells releasing bioactive substances from ES cell progeny may be concentrated and purified for clinical applications. Although ES cell lines that express reporter genes have been established to isolate cells releasing bioactive substances, other difficulties must be overcome before these genetically modified cells can be used for gene therapy in human patients. Fluorescence- or magnetic-activated cell sorters are commonly used to isolate specific cells using antibodies against cell surface antigens. However, for some cells, such as insulin-producing beta cells, specific surface antigens have not yet been identified. In this study, a simple and efficient method to identify and purify insulin- and alpha-fetoprotein-producing cells was developed. A nitrocellulose membrane treated with anti-insulin or anti-alpha–fetoprotein antibodies was

placed on a cell layer to trap insulin or alpha-fetoprotein released from the cells. The location of specific substance-producing cells was identified by immunostaining the membrane. The insulin-releasing cells were selectively collected from the culture dish using a cloning ring and transferred to another culture plate.

In summary, this thesis describes the approach on application of polymer materials for improvement of artificial pancreas from various fields. The author strongly believes that the results give some valuable information for the future clinical application of cell transplantation based diabetes therapy.

Reference

[1] A.M. Shapiro, J.R. Lakey, E.A. Ryan, G.S. Korbutt, E. Toth, G.L. Warnock, N.M. Kneteman, R.V. Rajotte, Islet transplantation in seven patients with type 1 diabetes mellitus using a glucocorticoid-free immunosuppressive regimen, N. Engl. J. Med. 343 (2000) 230–238.

[2] E.A. Ryan, J.R. Lakey, R.V. Rajotte, G.S. Korbutt, T Kin, S Imes, A. Rabinovitch, Elliott JF, Bigam D, Kneteman NM, Warnock GL, Larsen I, Shapiro AM, Clinical outcomes and insulin secretion after islet transplantation with the Edmonton protocol. Diabetes. 50 (2001) 710-719.

[3] S. Kizilel, M. Garfinkel, E. Opara, The bioartificial pancreas: progress and

[4] challenges, Diabetes Technol. Ther. 7 (2005) 968–985.

[5] J.T. Wilson, E.L. Chaikof, Challenges and emerging technologies in the immunoisolation of cells and tissues, Adv. Drug Deliv. Rev. 60 (2008) 124–145.

[6] A.S. Narang, R.I. Mahato, Biological and biomaterial approaches for improved islet transplantation, Pharmacol. Rev. 58 (2006) 194–243.

[7] L. Moberg, H. Johansson, A. Lukinius, C. Berne, A. Foss, R. Källen, Ø. Østraat, K. Salmela, A. Tibell, G. Tufveson, G. Elgue, E.K. Nilsson, O. Korsgren, B. Nilsson. Production of tissue factor by pancreatic islet cells as a trigger of detrimental thrombotic reactions in clinical islet transplantation. Lancet. 360 (2002) 2039-2045.

[8] H. Johansson, A. Lukinius, L. Moberg, T. Lundgren, C. Berne, A. Foss, M. Felldin, R. Källen, K. Salmela, A. Tibell, G. Tufveson, K.N. Ekdahl, G. Elgue, O. Korsgren, B.Nilsson, Tissue factor produced by the endocrine cells of the

islets of Langerhans is associated with a negative outcome of clinical islet transplantation. Diabetes. 54 (2005) 1755-1762.

[9] van der D.J. Windt, R. Bottino, A. Casu, N. Campanile, D.K. Cooper, Rapid loss of intraportally transplanted islets: An overview of pathophysiology and preventive strategies. Xenotransplantation. 14 (2007) 288-297.

[10] L. Ozmen, K.N. Ekdahl, G. Elgue, R. Larsson, O. Korsgren, B. Nilsson, Inhibition of thrombin abrogates the instant blood-mediated inflammatory reaction triggered by isolated human islets: Possible application of the thrombin inhibitormelagatran in clinical islet transplantation. Diabetes 51 (2002) 1779-1784.

[11] H. Johansson, M. Goto, D. Dufrane, A. Siegbahn, G. Elgue, P. Gianello, O. Korsgren, B.Nilsson, Low molecular weight dextran sulfate: a strong candidate drug to block IBMIR in clinical islet transplantation. Am. J. Transplant. 6 (2006) 305-312.

[12] B. Nilsson, O. Korsgren, J.D. Lambris, K.N. Ekdahl, Can cells and biomaterials in therapeutic medicine be shielded from innate immune recognition? Trends Immunol. 31 (2010) 32-38.

[13] Y. Sun, X. Ma, D. Zhou, I. Vacek, A.M. Sun, Normalization of diabetes in spontaneously diabetic cynomologus monkeys by xenografts of microencapsulated porcine islets without immunosuppression. J. Clin. Invest. 15 (1996) 1417-1422.

[14] P. Soon-Shiong, E. Feldman, R. Nelson, J. Komtebedde, O. Smidsrod, G. Skjak-Braek, T. Espevik, R. Heintz, M. Lee, Successful reversal of spontaneous diabetes in dogs by intraperitoneal microencapsulated islets.

Transplantation. 54 (1992)769-774.

[15] F. Lim, A.M. Sun. Microencapsulated islets as bioartificial endocrine pancreas. Science. 210 (1980) 908-910.

[16] T. Wang, I. Lacík, M. Brissová, A.V. Anilkumar, A. Prokop, D. Hunkeler, R. Green, K. Shahrokhi, A.C. Powers, An encapsulation system for the immunoisolation of pancreatic islets. Nat. Biotechnol. 15 (1997) 358-362.

[17] G.M. O'Shea, A.M. Sun, Encapsulation of rat islets of Langerhans prolongs xenograft survival in diabetic mice. Diabetes. 35 (1986) 943-946.

[18] C.J. Weber, M.K. Hagler, J.T.,Chryssochoos J.A. Kapp, G.S. Korbutt, R.V. Rajotte, P.S. Linsley, CTLA4-Ig prolongs survival of microencapsulated neonatal porcine islet xenografts in diabetic NOD mice. Cell. Transplant. 6 (1997) 505-508.

[19] V.F. Duvivier-Kali, A. Omer, R.J. Parent, J.J. O'Neil, G.C. Weir, Complete protection of islets against allorejection and autoimmunity by a simple barium-alginate membrane. Diabetes. 50 (2001) 1698-1705.

[20] H. Iwata, T. Takagi, K. Kobayashi, T. Oka, T. Tsuji, F. Ito, Strategy for developing microbeads applicable to islet xenotransplantation into a spontaneous diabetic NOD mouse. J. Biomed. Mater. Res. 28 (1994) 1201-1207.

[21] H. Iwata, H. Amemiya, T. Matsuda, H. Takano, R. Hayashi, T. Akutsu, Evaluation of microencapsulated islets in agarose gel as bioartificial pancreas by studies of hormone secretion in culture and by xenotransplantation. Diabetes. 38 (1989) 224-225.

[22] H. Iwata, T. Takagi, H. Amemiya, H. Shimizu, K. Yamashita, K. Kobayashi,

T..Akutsu, Agarose for a bioartificial pancreas. J. Biomed. Mater. Res. 26 (1992) 967-977.

[23] H. Iwata, H. Amemiya, T. Matsuda, H. Takano, T. Akutsu, Microencapsulation of Langerhans Islets in Agarose Microbeads and Their Application for a Bioartificial Pancreas. J. Bioact. Compat. Polym. 3 (1988) 356-369

[24] H. Tashiro, H. Iwata, G.L. Warnock, T. Takagi, H. Machida, Y. Ikada, T.Tsuji, Characterization and transplantation of agarose microencapsulated canine islets of Langerhans. Ann Transplant. 2 (1997)33-39.

[25] T. Ohyama, Y. Nakajima, H. Kanehiro, M. Hisanaga, Y. Aomatsu, T. Kin, K. Nishio, K. Ohashi, M. Sho, M. Nagao, Y. Tatekawa, N. Ikeda, H. Kanokogi, T. Yamada, H. Iwata, H. Nakano, Long-term normalization of diabetes by xenotransplantation of newly developed encapsulated pancreatic islets. Transplant. Proc. 30 (1998) 3433-3435.

[26] T. Tun, K. Inoue, H. Hayashi, T. Aung, Y.J. Gu, R. Doi, H. Kaji, Y. Echigo, W.J. Wang, H. Setoyama, M. Imamura, S. Maetani, N. Morikawa, H. Iwata, Y. Ikada, A newly developed three-layer agarose microcapsule for a promising biohybrid artificial pancreas: rat to mouse xenotransplantation. Cell. Transplant. 5 (1996) 59-63.

[27] T. Kin, H. Iwata, Y. Aomatsu, T. Ohyama, H. Kanehiro, M. Hisanaga, Y. Nakajima, Xenotransplantation of pig islets in diabetic dogs with use of a microcapsule composed of agarose and polystyrene sulfonic acid mixed gel. Pancreas. 25 (2002) 94-100.

[28] D. Rabuka, M.B. Forstner, J.T. Groves, C.R. Bertozzi, Noncovalent cell surface engineering: incorporation of bioactive synthetic glycopolymers into

cellular membranes. J. Am. Chem. Soc. 130 (2008) 5947-5953.

[29] M. G. Paulick,M. B. Forstner, J. T. Groves and C. R. Bertozzi, A chemical approach to unraveling the biological function of the glycosylphosphatidylinositol anchor. Proc. Natl. Acad. Sci. U S A. 104 (2007) 20332-20337.

[30] D.Y. Lee, S. Lee, J.H. Nam, Y. Byun, Minimization of immunosuppressive therapy after islet transplantation: combined action of heme oxygenase-1 and PEGylation to islet. Am. J. Transplant. 6 (2006) 1820-1808.

[31] S. Cabric, J. Sanchez, T. Lundgren, A. Foss, M. Felldin, R. Källen, K. Salmela, A. Tibell, G. Tufveson, R. Larsson, O. Korsgren, B.Nilsson, Islet surface heparinization prevents the instant blood-mediated inflammatory reaction in islet transplantation. Diabetes. 56 (2007) 2008-2015.

[32] C.L. Stabler, X.L. Sun, W. Cui, J.T. Wilson, C.A. Haller, E.L. Chaikof. Surface re-engineering of pancreatic islets with recombinant azido-thrombomodulin. Bioconjugate. Chem. 18 (2007) 1713-1715.

[33] J. L. Contreras, D. Xie, J. Mays, C. A. Smyth, C. Eckstein, F. G. Rahemtulla, C. J. Young, J. T. Anthony, G. Bilbao, D. T. Curiel, D. E. Eckhoff, A novel approach to xenotransplantation combining surface engineering and genetic modification of isolated adult porcine islets. Surgery. 136 (2004) 537-547.

[34] Y. Teramura, Y. Kaneda, H. Iwata, Islet-encapsulation in ultra-thin layer-by-layer membranes of poly(vinyl alcohol) anchored to poly(ethylene glycol)-lipids in the cell membrane. Biomaterials, 28 (2007) 4818–4825.

[35] S. Miura, Y. Teramura, H. Iwata, Encapsulation of islets with ultra-thin polyion complex membrane through poly(ethylene glycol)-phospholipids anchored

to cell membrane. Biomaterials, 27 (2006) 5828–5835.

[36] Y. Teramura, Y.Kaneda, T. Totani, H. Iwata, Behavior of synthetic polymers immobilized on a cell membrane. Biomaterials, 29 (2008) 1345–1355.

[37] Y. Teramura, H. Iwata, Islets surface modification prevents blood-mediated inflammatory responses. Bioconjugate. Chem., 19 (2008) 1389–1395.

[38] T. Totani, Y. Teramura, H. Iwata, Immobilization of urokinase on the islet surface by amphiphilic poly(vinyl alcohol) that carries alkyl side chains. Biomaterials, 29 (2008) 2878–2883.

[39] Y. Teramura, H. Iwata, Islet encapsulation with living cells for improvement of biocompatibility. Biomaterials, 30 (2009) 2270–2275.

[40] Y. Teramura, H. Iwata, Surface modification of islets with PEG-lipid for improvement of graft survival in intraportal transplantation. Transplantation, 88 (2009) 624–630.

Chapter 1

Co-immobilization of urokinase and thrombomodulin on islet surfaces by poly(ethylene glycol)-conjugated phospholipid

1. 1. Introduction

Transplantation of islets of Langerhans (islets) has been proposed as a safe and effective means of treating patients with insulin-dependent diabetes mellitus (type I), although it is still an experimental procedure [1, 2]. The Edmonton protocol demonstrates an increased rate of insulin independence and glycemic stability after intraportal transplantation of islets. However, large numbers of islets are needed to achieve insulin independence; thus, numbers of islets from only one donor for each recipient is not enough. This may be because many islets are lost early after intraportal transplantation [2]. It was reported that most transplanted islets are destroyed by instant blood-mediated inflammatory reactions (IBMIR) [3]. Systemic administration of anticoagulants such as low molecular weight dextran sulfate [4] and the thrombin inhibitor melagatran [5] inhibits IBMIR; however, patients who receive these anticoagulants may be at high risk for bleeding. Recently, it was reported that heparin coating the islets could be an alternative to the systemic administration of anticoagulants [6]. Biotin–avidin interactions were used to immobilize heparin on the islet surface. The immobilization of recombinant thrombomodulin (TM) onto the surface of islets was also achieved [7]; phosphine molecules were covalently conjugated to

the amino groups of membrane proteins by Staudinger ligation for immobilization of TM. Moreover, the immunogenic protein avidin, which is derived from xenogeneic spices, could induce unfavorable host immune reactions after transplantation of the modified islets.

To modulate the immunogenicity of cells and to immobilize anti-coagulant substances, our group and other groups has modified the cell surface with various amphiphilic polymers, such as poly(ethylene glycol)–phospholipid conjugates (PEG-lipids) [8-15]. Proteins have been immobilized on the cell surface through the amphiphilic polymer layer. In this chapter, this technology was extended to local release of anti-coagulant enzymes, urokinase (UK) and TM, from islets. There were no reports on the local release of anti-coagulants from islet surface in order to suppress the thrombogenic reactions. PEG-lipids for the surface modification by hydrophobic interaction were employed, which enabled us to release of anchoring UK and TM from the islet surface with function of time.

1. 2. Materials and methods

Materials

α-*N*-hydroxysuccinimidyl-maleimidyl PEG (NHS–PEG–Mal; 5,000 kDa) was purchased from Nektar Therapeutics (San Carlos, CA, USA). 1,2-Dipalmitoyl-*sn*-glycerol-3-phosphatidylethanolamine (DPPE) was purchased from NOF Corporation (Tokyo, Japan). Chloroform, dichloromethane, triethyl

amine, diethyl ether, heparin sodium salt, penicillin–streptomycin mixed solution (PC/SM), and 5,5′-dithiobis(2-nitrobenzoic acid) (Ellman's reagent) were purchased from Nacalai Tesque (Kyoto, Japan). Thrombin was from Kayaku Company (Saitama, Japan) and UK (high molecular weight, from human urine: 54 kDa, 80,000 U/mg) was from Calbiochem (Darmstadt, Germany). Medium 199 (for culture of islets) was from Invitrogen (Carlsbad, CA, USA). Anti-thrombin III (KENKETSU NONTHRON 500 (AT-III) was purchased from Nihon Pharmaceutical Company (Tokyo, Japan). Bovine albumin–fluorescein isothiocyanate conjugate (FITC–BSA), fibrinogen (type I), and plasminogen from human plasma were purchased from Sigma-Aldrich (St. Louis, MO, USA). Dulbecco's phosphate-buffered saline (PBS) was obtained from Nissui Pharmaceutical Company (Tokyo, Japan). Fetal bovine serum (FBS) was purchased from BioWest (Miami, FL, USA), and enzyme-linked immunosorbent assay (ELISA) kits for insulin were from Shibayagi Company (Gunma, Japan). Spectrozyme PCa, Spectrozyme uPA and human protein C were purchased from American Diagnostica (Stamford, CT, USA). Traut's reagent was obtained from MP Biochemicals (Solon, OH). Recombinant TM (Recomodulin Injection 12800) was kindly donated by Asahi Kasei Pharma (Tokyo, Japan). Recombinant TM (MW: 64 kDa) is obtained by expressing cDNA codes from 1st to 498th amino acid sequence of human TM in a Chinese hamster ovary cells.

Synthesis of maleimide–PEG–conjugated DPPE

Maleimide–PEG–conjugated DPPE (Mal-PEG-lipid) was synthesized from NHS–PEG–Mal and DPPE. NHS–PEG–Mal (180 mg), DPPE (20 mg), and

triethyl amine (10 μL) were dissolved in dichloromethane and stirred for 1 d at room temperature (RT) [9]. After precipitation in diethyl ether and freeze drying, Mal–PEG–lipid was obtained (190 mg, yield 80%).

Introduction of SH groups to FITC-BSA, UK and TM

In this experiment, FITC-BSA was used as a marker protein. FITC-BSA (2.5 mg) was dissolved in 150 μL of PBS. Traut's reagent (1.0 mg) was dissolved in 100 μL of 50 mM phosphate buffer (pH 8.0) containing 1 mM $MgCl_2$, 50 mM KCl, and 0.15 M NaCl. Specific amounts of the Traut's reagent solution was added to the BSA solution and shaken for 1 h at RT to introduce thiol groups. The molar ratios of Traut's reagent to BSA molecules ranged from 150 to 600. FITC–BSA carrying thiol groups (FITC–BSA–SH) was obtained by purification using a Sephadex™ G-25 M column. The concentration of thiol groups on BSA was determined by Ellman's reagent. Briefly, Ellman's reagent (0.25 μM in ethanol) was mixed with FITC–BSA–SH for 5 min at RT, and the absorption at 412 nm of the solution was measured. Based on the number of introduced thiol groups on BSA, the optimal concentration of Traut's reagent was determined for modification of UK and TM.

Traut's reagent (2.58 μL, 1.0 mg/mL) was added to a UK solution (50 μL, 3,000 units/mL). Traut's reagent (1.15 μL, 40 mg/mL) was also added to a TM solution (50 μL, 12 mg/mL). The molar ratio of Traut's reagent to the amino groups of both proteins was 10:1. The mixed solutions were shaken for 1 h at RT. Thiolated UK (UK–SH) and TM (TM–SH) was purified using a Sephadex™ G-25 M column.

Immobilization of proteins to cell surface with Mal–PEG–lipid

To demonstrate the immobilization of proteins on the cell surface using FITC–BSA–SH and Mal–PEG–lipid, a single-cell suspension of CCRF–CEM cells (established from acute lymphoblastic leukemia) which were obtained from the Health Science Research Resources Bank (Tokyo, Japan) and pancreatic islets were used in this experiment. The suspension of CCRF-CEM cells was cultured in RPMI-1640 medium supplemented with 10% FBS, 100 U/mL penicillin, and 0.1 mg/mL streptomycin (Invitrogen) at 37 °C under 5% CO_2. Islets were isolated from the pancreas of female Syrian hamsters (7–8 wk old; Japan SLC, Shizuoka, Japan) using the collagenase digestion method [20]. All animal experiments were approved and accepted by the animal care committee of Institute for Frontier Medical Sciences, Kyoto University. The islets were maintained in Medium 199 culture medium supplemented with 10% FBS, 8.8 mM HEPES buffer, 100 U/mL penicillin, 100 μg/mL streptomycin, and 8.8 U/mL heparin.

CCRF–CEM cells were centrifuged at RT and about 1.0×10^6 cells were collected. After removal of the supernatant, 50 μL of Mal–PEG–lipid (0.5 mg/mL) solution in PBS was added to the cell suspension and the suspension was incubated for 60 min with gentle agitation at RT. After washing with PBS using centrifugation, a solution of FITC–BSA–SH (100 μL, 3.3 mg/mL in PBS) was mixed with the cell suspension and left for 10 min at RT. After washing with PBS using centrifugation, the cells were observed under a confocal laser scanning microscope (FLUOVIEW FV500; Olympus, Tokyo, Japan).

The islets were cultured for 5-7 days after isolation to remove or sediment

cells that were damaged during the isolation procedure. Since the surface become smooth during culture, it is more appropriate to modify the surface with Mal-PEG-lipid. To modify islets, 0.5 mL of a Mal–PEG–lipid (0.5 mg/mL in PBS) solution was added to 400 islets and incubated for 30 min at 37 °C. After the Mal–PEG–lipid–modified islets were washed with PBS, 100 μL of FITC–BSA–SH (3.3 mg/mL in PBS), or 75 μL of a UK–SH and TM–SH mixture (600 U/mL and 2.4 mg/mL in PBS, respectively) was added and incubated for 30 min at 37 °C. FITC–BSA or UK/TM-immobilized islets were washed with PBS.

Measurement of UK and TM activities

To examine the fibrinolytic activity of UK in the UK/TM-immobilized islets, a fibrin plate assay [10] was performed as previously reported with slight modifications. Briefly, fibrinogen (type I, 80 mg) and lys-plasminogen (0.2 mg) were dissolved in saline (8 mL) and poured into a culture dish (10 cm diameter). Thrombin (6.7 mM, 30 μl) was added to the solution and the dish was rotated to mix. The plate was incubated for 3 h at RT to prepare a fibrin plate. The UK/TM-immobilized islets (100 islets) and non-treated islets (100 islets) were spotted on the fibrin plate. After incubation at 37 °C for 14 h, the fibrin plate was observed.

The activity of TM was determined from the amount of activated protein C (APC) that was produced [7]. TM-immobilized islets were suspended in 20 mM Tris-HCl solution (pH 7.4, 83 μL) containing 50 mM $CaCl_2$, 100 mM NaCl, and 1 mg/mL BSA. UK/TM-immobilized islets (50 islets) were transferred into a well in a 96-well plate. Then, 10 μM human protein C (2 μL in PBS) and 10 μM thrombin

(1 μL in PBS) were added, and the mixture was incubated at 37 °C. After 1 h incubation, the suspension was centrifuged and the supernatant was collected. Sodium heparin (100 μM, 2 μL in PBS) and 100 μM AT-III (2 μL in PBS) were mixed with the supernatant. After addition of 2 mM Spectrozyme PCa (10 μL), the mixture was incubated at 37 °C for 60 min, and absorption at 405 nm was measured.

Determination of released TM and UK from islets

UK/TM-immobilized islets (100 islets in 1 mL 20 mM Tris-HCl solution (pH 7.4, 83 μL) containing 50 mM $CaCl_2$, 100 mM NaCl, and 1 mg/mL BSA) were incubated at 37°C to determine the released UK and TM from islets. A part of the solution (200 μL) was taken at 0, 3, 6, and 24 h for the measurement and 200 μL of fresh buffer was added in replacement of the solution which was taken. The activity of TM in the buffer was measured as mentioned above. The activity of UK was measured. Briefly, after addition of 0.5 mM Spectrozyme uPA (10 μL) to 90 μL of the supernatant, the mixture was incubated 37 °C for 60 min, and then the absorption at 405 nm was measured.

Glucose-stimulated insulin release from islets

A static glucose-responsive insulin assay was performed to examine the effects of surface modification of islets on their viability and insulin-releasing ability. After the islets were washed several times with Krebs–Ringer solution, they were sequentially incubated in 0.1 g/L, 0.3 g/L, and then 0.1 g/L glucose in Krebs–Ringer solution for 1 h each at 37 °C. The supernatants at each step were

collected, and the insulin concentrations were determined by enzyme-linked immunosorbent assay (ELISA).

Statistical analysis

Comparisons between two groups were made using Student's *t*-test. $p < 0.05$ was considered statistically significant. All statistical calculations were performed using the software *JMP 5.0.1J*.

1. 3. Results

Mal–PEG–lipid and Traut's reagent for immobilization of proteins on cell surfaces

In a previous study [9], it was demonstrated that thiol groups on poly(vinyl alcohol) can react with maleimide groups that are introduced onto proteins under physiological conditions. In this chapter, proteins were immobilized on the cell surface through the same chemistry as shown in Scheme 1. The amino groups on the proteins were transformed into thiol groups using Traut's reagent. Cells were treated with the Mal–PEG–lipid to introduce maleimide groups onto the cell surface by interactions between hydrophobic residues of the Mal–PEG–lipid and the lipid bilayer of the cell membrane. The thiolated proteins were then immobilized on the cell surface by thiol/maleimide bonding.

To examine the efficacy of Traut's reagent, BSA was treated with Traut's reagent under various conditions and the number of thiol groups introduced onto

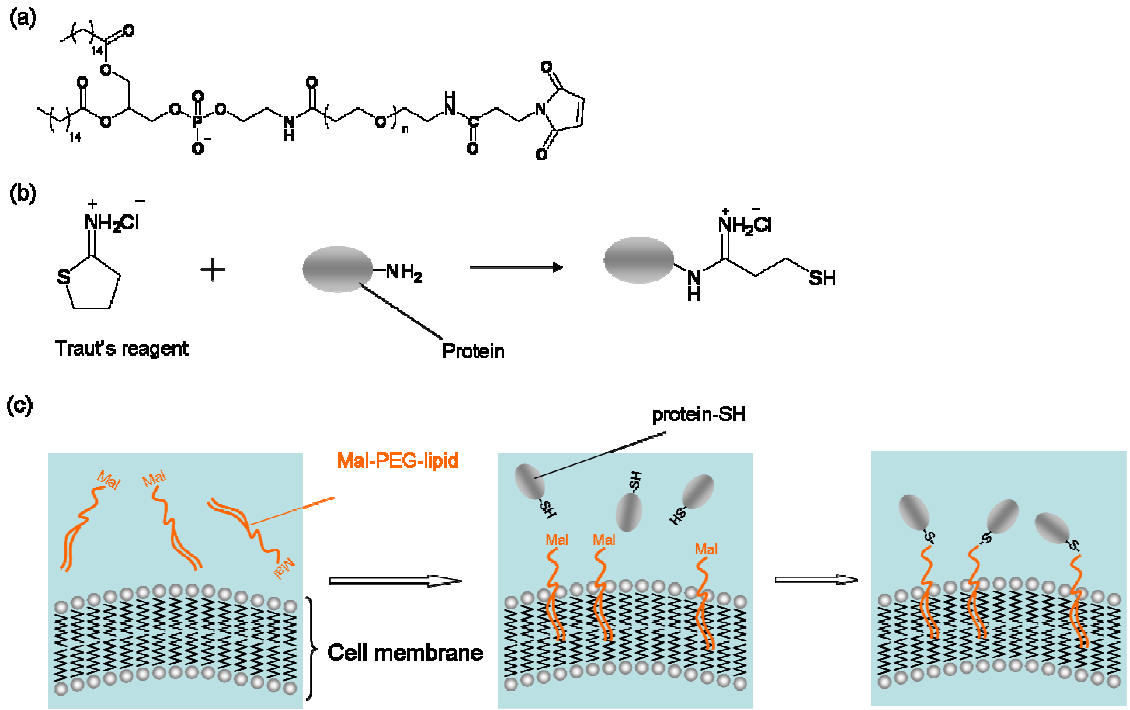

Scheme.1 Method for immobilization of proteins onto cell surface. (a) Chemical structure of Mal–PEG–lipid conjugate. (b) Introduction of thiol groups to protein using Traut's reagent. (c) Schematic illustration of immobilization of protein onto the cell surface through Mal–PEG–lipid. Mal–PEG–lipid anchored to the lipid bilayer membrane through hydrophobic interactions between the alkyl chains of Mal–PEG–lipid and the lipid bilayer. Thiol groups on the protein reacted with maleimide groups at the end of PEG chains on the cell membrane.

BSA was determined. Figure.1 shows the relationship between the amount of Traut's reagent and the amount of thiol groups on a BSA molecule. Thiol groups could be effectively introduced onto BSA with Traut's reagent. Referring these results, the proteins, urokinase and TM, were modified with Traut's reagent under 10:1 molar ratio of Traut's reagent and amino groups of the protein. 1.5 thiol groups were introduced per a protein molecule on average.

The surfaces of cells and islets were modified with Mal–PEG–lipid, followed by treatment with FITC-labeled BSA–SH (Figure.2 (a) and (b)). Fluorescence from

FITC–BSA was clearly seen at the periphery of each cell and islet. No fluorescence was observed on nontreated cells or naive islets treated with FITC–BSA (data not shown). BSA–SH could be immobilized onto the surface of cells and islets through Mal–PEG–lipid without damaging cell and islet morphology. Then the same method was applied to immobilize UK and TM on the surface of islets.

Immobilization of UK and TM on islets

Urokinase and TM were immobilized at the same time on the islet surface through Mal–PEG–lipid using the method described above. The morphology of the islets was well maintained as shown in Figure.2 (c) after the immobilization of UK and TM on the islet surface. This result suggested that the surface

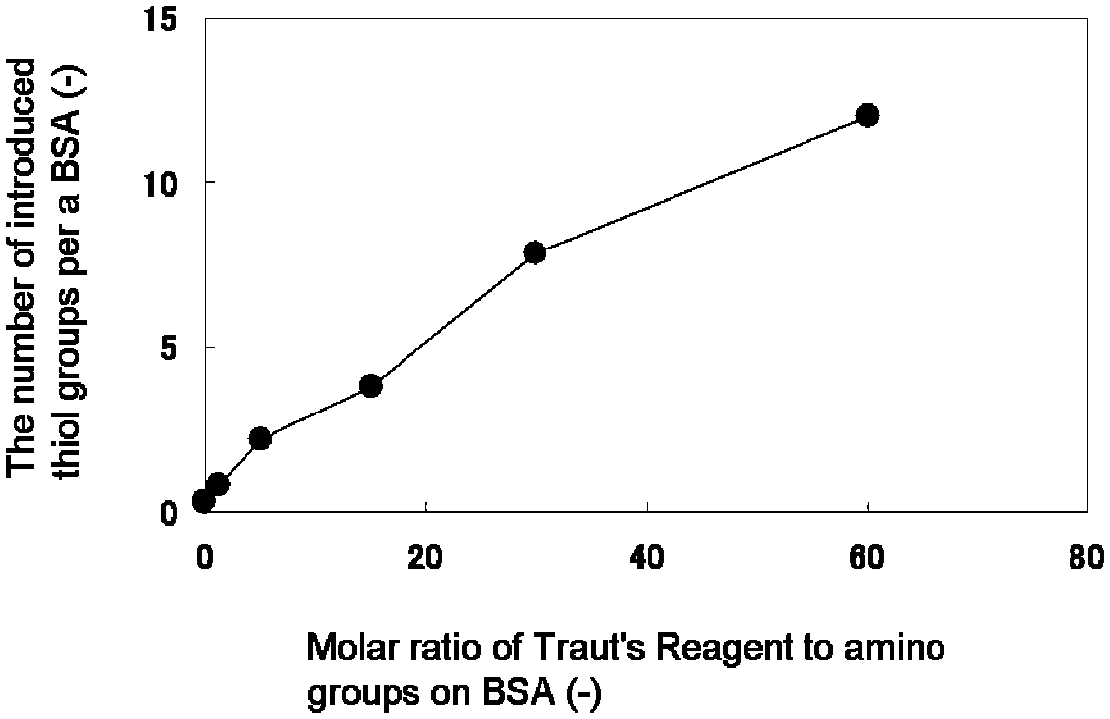

Figure.1 Effect of different concentrations of Traut's reagent on numbers of thiol groups added to BSA.

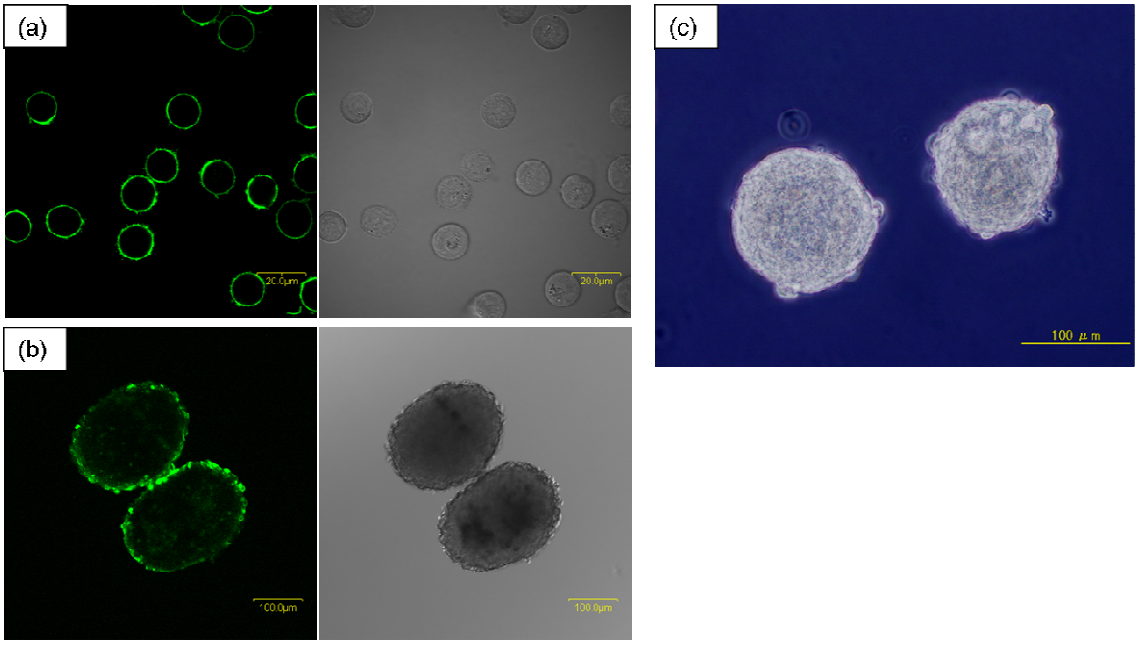

Figure.2 Microscopic images of modified cells and islets. (a); Fluorescent and phase-contrast microscopic image of CCRF–CEM cells modified with FITC–BSA–SH, (b); Confocal laser scanning and phase-contrast microscopic image of islets modified with FITC–BSA–SH, (c); Phase-contrast microscopic images of UK/TM-immobilized islets after 1 day culture.

modification did not damage to viability of islets. The activity of TM on UK/TM-islets was estimated from the amount of APC produced in the presence of human protein C and thrombin. The APC production of the 80 UK/TM-islets was 1.21 nM over 1 h, whereas it was 0.20 nM from 80 naive islets, as shown in Figure.3, indicating effective immobilization of TM on the islets. This indicates that TM was successfully immobilized onto the surface of islets using Mal–PEG–lipid. In addition, the fibrinolysis activity of UK on the UK/TM-islets was semiquantitatively determined by a fibrin plate–based assay. Figure.4 shows the fibrin plate after a 12 h incubation. Urokinase activates plasminogen, which produces plasmin in the fibrin gel; the plasmin then hydrolyzes fibrin gel,

yielding a transparent area in the fibrin gel plate. A large transparent area (2.0 cm^2, right bottom) was observed around the spotted islets, which reflected the fibrinolytic activity of UK immobilized on the islets. In contrast, the transparent area was small when naive islets were spotted (0.4 cm^2, right bottom). This small transparent area around the naive islets might be due to small amounts of tissue plasminogen activator secreted by the endothelial cells of capillaries in the islets. After the UK/TM-islets were incubated in culture medium for 1 d, the dissolved area (left bottom) decreased to that of the naive islets. This indicated that the UK released from the islet surface.

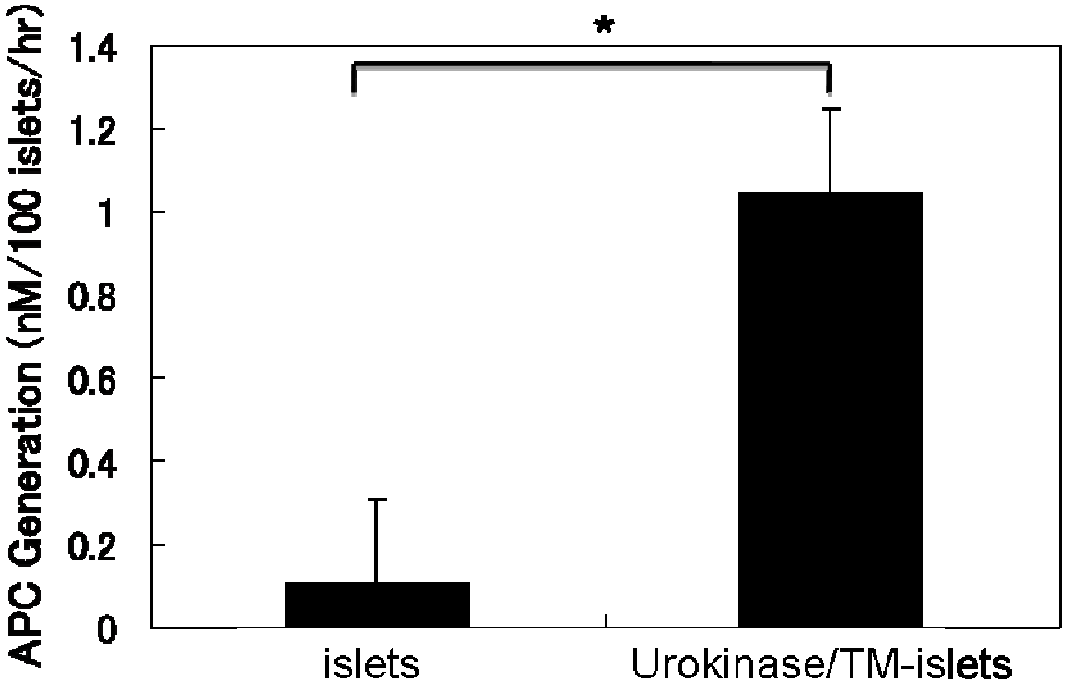

Figure.3 Activated protein C (APC) generation assay of UK/TM-immobilized islets. Amount of APC generation reflects TM immobilized on the islets. Data points represented by the mean ± standard deviation for n = 6. An asterisk represents a significant difference (p<0.05) between two groups.

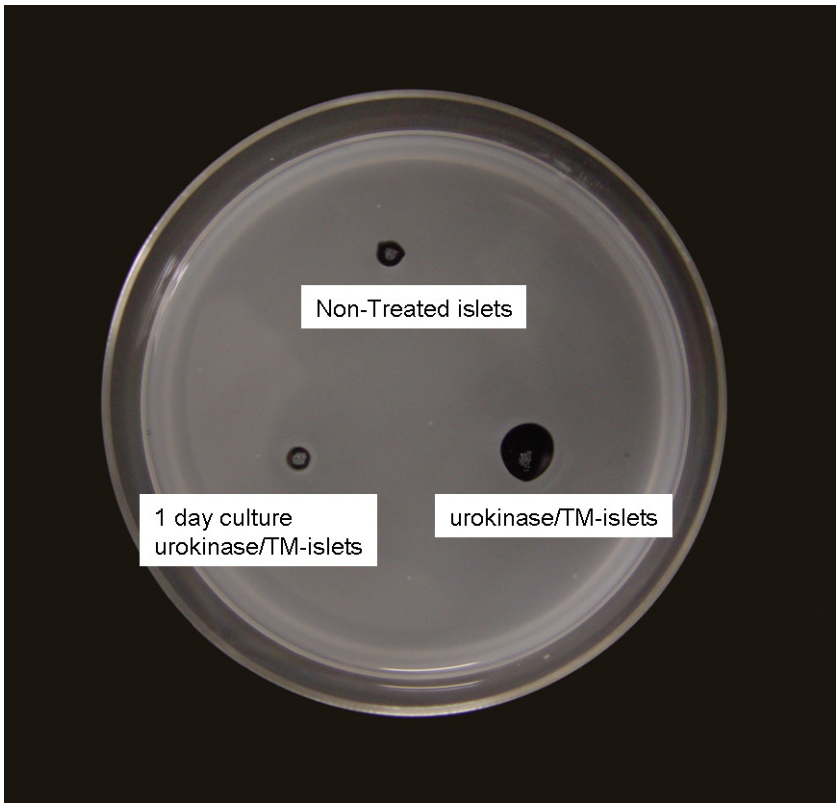

Figure.4 Fibrin plate assay of UK/TM-immobilized islets. One hundred UK/TM-immobilized islets (0 h for right bottom, 1 d culture for left bottom) and untreated islets (top) were placed on a fibrin gel plate and incubated at 37 °C for 14 h. A large, transparent area formed around the islets, indicating dissolution of the fibrin gel by plasmin, which was produced from plasminogen in the presence of UK.

Release of UK and TM from UK/TM-islets

The release behavior of UK and TM from UK/TM-islets was examined (Figure.5). 100 of UK/TM-islets were incubated in 1 mL buffer at 37°C. Aliquot of the buffer was collected from the islet suspension at pre-determined time and subjected to the assay for UK activity and TM activity with time. Urokinase and TM detected in the buffer increased with function of time, indicating that urokinase and TM anchored by PEG-lipid to the islet surface were gradually released from the surface and the enzyme activities were maintained well.

From the TM activity assay, about 83% TM on the islets was released during 6 h.

Glucose-stimulation test of UK/TM-islets

A glucose stimulation test was conducted to examine the effect of UK/TM immobilization on islet function. When the glucose concentration in the medium was increased from 0.1 g/dL to 0.3 g/dL, the amount of insulin released by islets in the three groups increased markedly in response (Figure.6). Islets of three groups, naïve, Mal-PEG-lipid modified islets and UK/TM-immobilized-islets, increased insulin release in response to high glucose concentration (0.3 g/dL glucose). Insulin release returned to basal levels when the islets were re-exposed to 0.1 g/dL glucose. No significant differences were seen in the

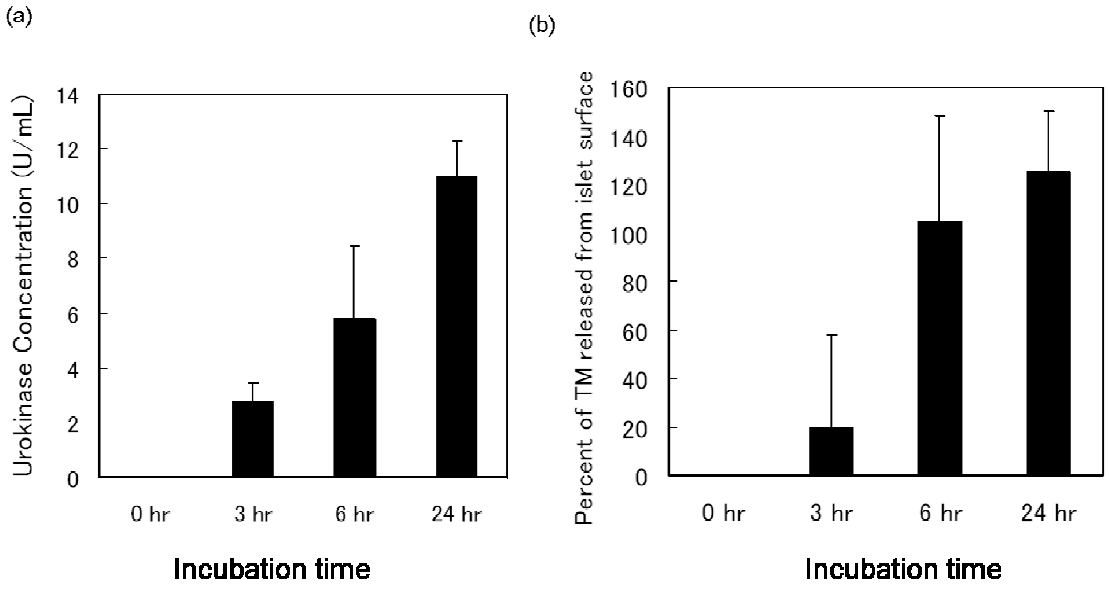

Figure.5 Release of UK and TM from UK/TM-immobilized islets. UK/TM-immobilized islets were incubated in buffer and then aliquots of the buffer were collected at certain time and were subjected to the assay for (a) UK activity and (b) TM relative activity. Percents of TM released were more than 100% at 6 and 24 h. The amounts of TM on islets varied in preparations. These values were calculated referring to the amount of APC generation shown in Fig. 3. Results are expressed as mean ± standard deviation for $n = 4$.

Figure.6 Glucose stimulation assays. Naive islets, Mal–PEG–lipid–modified islets, and UK/TM-immobilized islets (50 islets each) were incubated in solutions with different glucose concentrations for 1 h. The amount of insulin secreted from islets was determined by ELISA. Results are expressed as mean ± standard deviation for n = 5.

glucose stimulation indexes among the three groups. These results indicate that the PEG–lipid modification and UK/TM-immobilization did not influence the islets' ability to regulate insulin release in response to glucose concentration, and the protein layer on islets did not retard the diffusion of glucose and insulin.

1. 4. Discussion

When islets are transfused into the liver through the portal vein, they are exposed to fresh blood. The blood coagulation and complement systems are activated on the islet surface during the early post-transplantation phase, initiating the release of chemotactic factors, tissue factor, chemokines, and other inflammatory mediators. It has been reported that the majority of transplanted islets are destroyed by the IBMIR [3]. Islet graft loss at the early phase is one of

the most serious obstacles that remain to be solved in islet transplantation [2]. Several methods of regulating early coagulation and blood-mediated inflammatory reactions have been reported, such as administering the thrombin inhibitor Melagatran [5], activated protein C [16], low molecular weight dextran sulfate [4], and the water-soluble domain of complement receptor I (sCR1) [17, 18]. Successful transplantation has been demonstrated in animal models by reducing islet loss. However, it is difficult to use these methods in a clinical setting because systemic administration is associated with an increase in the risk of bleeding. An alternative method is the immobilization of bioactive substances, such as heparin, sCR1, UK, and thrombomodulin, on islet surfaces to suppress IBMIR.

Recently, Nilsson *et al.* reported that the graft survival of porcine islets could be improved by modifying the surface of islets with heparin [6], and Chaikof *et al.* reported immobilizing TM onto the surface of islets [7]. However, some aspects of their modification methods need to be improved prior to use in a clinical setting. Nilsson *et al.* employed the biotin–avidin reaction. Although this reaction can immobilize heparin on islet surfaces under physiological conditions, avidin, which is a xenogeneic protein, can induce unfavorable immune reactions. Chaikof *et al.* employed phosphine by Staudinger ligation. It is necessary to biosynthesize protein carrying a non-natural azido unit by a modified recombinant DNA technology. The phosphine-based method is tedious and cannot be applied some bioactive substances, such as heparin.

A versatile method to immobilize bioactive substances onto the surface of islets has been developed to avoid the problems described above. It was found

that a Mal–PEG–lipid conjugate anchored to the lipid bilayer of the cell membrane through hydrophobic interactions had no influence on islet morphology and function (Figures.2 and Figure.5). After this conjugate was anchored to the cell surface, thiolated bioactive substances—the fibrinolytic enzyme UK-SH or the anticoagulant TM-SH–were immobilized onto the end of the PEG chain through thiol/maleimide reactions. Since thiolation using Traut's reagent is an established technique, it is easy to prepare thiolated bioactive substances. The immobilized UK and TM retained their fibrinolytic properties and anticoagulant activity, respectively (Figures.3 and Figure.4), indicating that the thromboses that form immediately after islet transplantation may be prevented or dissolved on transplanted modified islets. Figure.4 shows UK on the islet surface did not stay there longer than 1 d. When modified islets are infused through the portal vein, the islets are hanged in small braches of veins. The results shown in Figure.6 indicates proteins, UK and TM, are released locally from the islet surface. From the release property of UK and TM from islet surface, most of them were released within 24 h. It was already reported that PEG-lipid on the cell membrane was gradually released from cell surface, which depends on the hydrophobicity of PEG-lipid [21]. Since enzymatic activities of released UK and TM were well maintained, they should inhibit the blood coagulation after intraportal transplantation. It was expect that the released enzymes effectively inhibit the blood coagulation surrounding the islets.

Thrombotic reactions initiate when islets come into direct contact with blood in the portal vein, resulting in early graft loss induced by IBMIR within a few hours [22]. It has been believed that islets can be rescued by our surface modification if

this early phase blood reaction is controlled. Recently, it could demonstrate that the immobilization of UK on islet surface could rescue the graft from IBMIR after intraportal transplantation in mice [23]. The co-immobilization of UK and TM should be more effective for suppress of IBMIR because of their potent anti-coagulant.

The results presented in this paper suggest that islet graft loss at the early phase caused by IBMIR will be effectively reduced by our method. The transplantation studies of modified islets is currently performing to demonstrate the efficacy of this method *in vivo*.

1. 5. References

[1] A.M. Shapiro, J.R. Lakey, E.A. Ryan, G.S. Korbutt, E. Toth, G.L. Warnock, N.M. Kneteman, R.V. Rajotte, Islet transplantation in seven patients with type 1 diabetes mellitus using a glucocorticoid-free immunosuppressive regimen, N. Engl. J. Med. 343 (2000) 230-238.

[2] E.A. Ryan, J.R. Lakey, R.V. Rajotte, G.S. Korbutt, T. Kin, S. Imes, A. Rabinovitch, J.F. Elliott, D. Bigam, N.M. Kneteman, G.L. Warnock, I. Larsen, A.M. Shapiro, Clinical outcomes and insulin secretion after islet transplantation with the Edmonton protocol, Diabetes 50 (2001) 710-719.

[3] O. Korsgren, T. Lundgren, M. Felldin, A. Foss, B. Isaksson, J. Permert, N.H. Persson, E. Rafael, M. Rydén, K. Salmela, A. Tibell, G. Tufveson, B. Nilsson, Optimising islet engraftment is critical for successful clinical islet transplantation, Diabetologia 51 (2008) 227-232.

[4] H. Johansson, A. Lukinius, L. Moberg, T. Lundgren, C. Berne, A. Foss, M. Felldin, R. Kallen, K. Salmela, A. Tibell, G. Tufveson, K.N. Ekdahl, G. Elgue, O. Korsgren, B. Nilsson, Tissue factor produced by the endocrine cells of the islets of Langerhans is associated with a negative outcome of clinical islet transplantation, Diabetes 54 (2005) 1755–1762.

[5] L. Moberg, H. Johansson, A. Lukinius, C. Berne, A. Foss, R. Kallen, O. Ostraat, K. Salmela, A. Tibell, G. Tufveson, G. Elgue, K. Ekdahl, O. Korsgren, B. Nilsson, Production of tissue factor by pancreatic islet cells as a trigger of detrimental thrombotic reactions in clinical islet transplantation, Lancet. 360 (2002) 2039–2045.

[6] S. Cabric, J. Sanchez, T. Lundgren, A. Foss, M. Felldin, R. Kallen, K.

Salmela, A. Tibell, G. Tufveson, R. Larsson, O. Korsgren, B. Nilsson, Islet surface heparinization prevents the instant blood-mediated inflammatory reaction in islet transplantation, Diabetes 56 (2007) 2008-2015.

[7] C.L. Stabler, X.L. Sun, W. Cui, J.T. Wilson, C.A. Haller, E.L. Chaikof, Surface Re-engineering of Pancreatic Islets with Recombinant azido-Thrombomodulin, Bioconjugate Chem. 18 (2007) 1713-1715.

[8] S. Miura, Y. Teramura, H. Iwata, Encapsulation of islets with ultra-thin polyion complex membrane through poly(ethylene glycol)-phospholipids anchored to cell membrane, Biomaterials 27 (2006) 5828-5835.

[9] Y. Teramura, Y. Kaneda, H. Iwata, Islet-encapsulation in ultra-thin layer-by-layer membranes of poly(vinyl alcohol) anchored to poly(ethylene glycol)-lipids in the cell membrane, Biomaterials 28 (2007) 4818–4825.

[10] Y. Teramura, H. Iwata, Islets surface modification prevents blood-mediated inflammatory responses, Bioconjugate Chem. 19 (2008) 1389–1395.

[11] Y. Teramura, H. Iwata, Surface modification of islets with PEG-lipid for improvement of graft survival in intraportal transplantation, Transplantation 88 (2009) 624-630.

[12] Y. Teramura, H. Iwata, Bioartificial pancreas Microencapsulation and conformal coating of islet of Langerhans, Adv. Drug. Deliv. Rev. 62 (2010) 827-840.

[13] M.V. Sefton, R.L. Broughton, M.E. Sugamori C.L. Mallabone, Hydrophilic polyacrylates for the microencapsulation of fibroblasts or pancreatic islets, J. Controlled Release. 6 (1987) 177-187.

[14] T. Takagi, H. Iwata , H. Tashiro, T. Tsuji, F. Ito, Development of a novel

microbead applicable to xenogeneic islet transplantation, J. Controlled Release. 31 (1994) 283-291.

[15] H. Uludag, J.E. Babensee, T. Roberts, L. Kharlip, V. Horvath, M.V. Sefton, Controlled release of dopamine, insulin and other agents from microencapsulated cells, J. Controlled Release, 24 (1993) 3-12.

[16] J.L. Contreras, C. Eckstein, C.A. Smyth, G. Bilbao, M. Vilatoba, S.E. Ringland, C. Young, J.A. Thompson, J.A. Fernandez, J.H. Griffin, D.E. Eckhoff, Activated protein C preserves functional islet mass after intraportal transplantation: a novel link between endothelial cell activation, thrombosis, inflammation, and islet cell death, Diabetes 53 (2004) 2804–2814.

[17] W. Bennet, B. Sundberg, T. Lundgren, A. Tibell, C.G. Groth, A. Richards, D.J. White, G. Elgue, R. Larsson, B. Nilsson, O. Korsgren, Damage to porcine islets of Langerhans after exposure to human blood in vitro, or after intraportal transplantation to cynomologus monkeys: protective effects of sCR1 and heparin, Transplantation 69 (2000) 711-719.

[18] W. Bennet, B. Sundberg, C.G. Groth, M.D. Brendel, D. Brandhorst, H. Brandhorst, R. G. Bretzel, G. Elgue, R. Larsson, B. Nilsson, O. Korsgren, Incompatibility between human blood and isolated islets of Langerhans: a finding with implications for clinical intraportal islet transplantation? Diabetes 48 (1999) 1907-1914.

[19] J.A. Gossage, J. Humphries, B. Modarai, K.G. Burnand, A. Smith, Adenoviral urokinase-type plasminogen activator (uPA) gene transfer enhances venous thrombus resolution, J. Vasc. Surg. 44 (2006) 1085-1090.

[20] H. Iwata, K. Kobayashi, T. Takagi, T. Oka, H. Yang, H. Amemiya, T. Tsuji, F.

Ito, Feasibility of agarose microbeads with xenogeneic islets as a bioartificial pancreas. J. Biomed. Mater. Res. 28 (1994) 1003–1011.

[21] O. Inui, Y. Teramura, H. Iwata, Retention dynamics of amphiphilic polymers PEG-lipids and PVA-Alkyl on the cell surface. ACS Appl. Mater. Interfaces. 2 (2010) 1514-1520.

[22] T. Eich, O. Eriksson, A. Sundin, S. Estrada, D. Brandhorst, H. Brandhorst, B. Langstrom, B. Nilsson, O. Korsgren, T. Lundgren, Positron emission tomography: a real-time tool to quantify early islet engraftment in a preclinical large animal model. Transplantation 84 (2007) 893-898.

[23] Y. Teramura, H. Iwata, Improvement of graft survival by surface modification with PEG-lipid and urokinase in intraportal islet transplantation. Transplantation 91 (2011) 271-278.

Chapter 2

Immobilization of anticoagulant-loaded liposomes on cell surfaces by DNA hybridization

2.1. Introduction

Type 1 diabetes is caused by the autoimmune destruction of insulin-producing pancreatic beta cells and inevitably leads to dependence upon exogenous insulin for control of blood glucose. Transplantation of islets of Langerhans (islets) has been proposed as a safe and effective treatment for type 1 diabetes patients and has been performed clinically for more than 15 y. Increased rates of insulin independence and glycemic stability after intraportal transplantation of islets have been achieved using the Edmonton protocol. However, some problems remain unresolved. For example, several pancreas donors are still necessary to achieve insulin independence in one recipient because more than 50% of islets are destroyed immediately after intraportal transplantation [1], [2] and [3]. Early graft loss is reported to be caused by the instant blood mediated inflammatory response (IBMIR) [4] and [5].

Systemic administration of anticoagulants and thrombin inhibitor have been administered to control IBMIR [6], [7], [8] and [9], and urokinase and soluble domains of thrombomodulin have been immobilized on islet surfaces [10], [11], [12], [13], [14], [15] and Chapter.1. The efficacy of these techniques has been examined in animal islet transplantation models, but a standard protocol has not

been yet established. In previous investigations, high molecular weight substances, such as heparin, thrombomodulin, and urokinase, were immobilized on islets. Low molecular weight drugs that act as inhibitors of blood coagulation enzyme, platelet, and complement are good candidates for immobilization and subsequent controlled release from the surface of islets. However, the methods that were used for immobilization of high molecular weight substances cannot be applied to immobilizing low molecular weight drugs on islet surfaces.

In this report, we investigated a new method to immobilize a small drug on the cell surface with subsequent sustained release from the cells. Liposomes, which can be used to encapsulate small drugs inside of a membrane, were used as the drug carrier. Poly (ethylene glycol)-phospholipid conjugates (PEG-lipids) carrying ssDNA (oligo$(dT)_{20}$ and oligo$(dA)_{20}$) were used to immobilize liposomes on the cell surface. When oligo$(dT)_{20}$- and oligo$(dA)_{20}$-PEG-lipids are applied to cells and liposomes, respectively, their lipid portions anchor into the lipid bilayers of cell membranes and liposomes; thus, the cells and the liposomes present oligo$(dT)_{20}$ and oligo$(dA)_{20}$ on their surface. We hypothesized that liposomes would be immobilized on the cell surface by hybridization between oligo$(dT)_{20}$ and oligo$(dA)_{20}$ when cells and liposomes were mixed. We applied this method to immobilize the thrombin inhibitor argatroban on the surface of islets and detected the release of argatroban by measuring antithrombin activity in the culture medium of the islets.

2.2. Materials and methods

Materials

α-*N*-Hydroxysuccinimidyl-*ω*-maleimidyl poly(ethylene glycol) (NHS-PEG--Mal, MW 5000) and 1,2-dipalmitoyl-*sn*-glycerol-3-phosphatidyl-ethanolamine (DPPE) were purchased from NOF Corporation (Tokyo, Japan). Chloroform, dichloromethane, triethyl amine, diethyl ether, heparin sodium salt, and penicillin–streptomycin mixed solution (PC/SM) were purchased from Nacalai Tesque (Kyoto, Japan). RPMI 1640 medium and Dulbecco's phosphate-buffered saline (PBS) were purchased from Invitrogen (Carlsbad, CA) and Nissui Pharmaceutical Company (Tokyo, Japan), respectively. Fetal bovine serum (FBS) was purchased from BioWest (Miami, FL, USA), and enzyme-linked immunosorbent assay (ELISA) kits for insulin were purchased from Shibayagi Company (Gunma, Japan). 1-Palmitoyl-2-[12-[(7-nitro-2-1, 3-benzoxadiazol-4-yl)amino]dodecanoyl]-*sn*-glycero-3-phosphoethanolamine (NBD-lipid) was purchased from Avanti Polar Lipids, Inc. (Alabaster, Alabama, USA). L-α-phosphatidylcholine from egg yolk, Type XVI-E (EggPC), Oligo(adenine)$_{20}$ (oligo(dA)$_{20}$), and oligo(thymine)$_{20}$ (oligo(dT)$_{20}$) carrying a protected SH group at the 5′-end (oligo(dA)$_{20}$-SH, oligo(dT)$_{20}$-SH) were purchased from Sigma-Aldrich Co. (St. Louis, MO, USA). The protecting group was removed from the -SH group by reduction of the disulfide bond with dithiothreitol (DTT) according to the manufacturer's instructions. Argatroban [16], a thrombin inhibitor, was purchased from Yoshindo, Inc. (Toyama, Japan). The

SensoLyte 520 Thrombin Activity Assay Kit was purchased from AnaSpec, Inc. (Fremont, CA), and the Phospholipids C-test Kit was purchased from Wako Pure Chemical Industries, Ltd (Osaka, Japan). Nitrocellulose membranes (0.8 μm pore size), Millex-GP 0.22 μm filter units, and Isopore 0.1 μm membrane filters were purchased from Millipore Co. (Billerica, MA, USA). Sephadex G-25 M was purchased from GE Healthcare (Little Chalfont, Buckinghamshire, UK). CCRF–CEM cells (established from acute lymphoblastic leukemia cells) were obtained from the Health Science Research Resources Bank (Tokyo, Japan).

Synthesis of oligo$(dA)_{20}$– or oligo$(dT)_{20}$– conjugated PEG lipids

Oligo$(dA)_{20}$- or oligo$(dT)_{20}$-conjugated PEG-lipids (oligo$(dA)_{20}$-PEG-DPPE or oligo$(dT)_{20}$-PEG-DPPE) (Scheme 1(a)) were synthesized following the method reported previously [14, 16]. They were used for the surface modification of liposomes and cells without any further purification.

Preparation of liposomes

EggPC (20 mg) was dissolved in 3.0 mL of chloroform , and the solution was dried in a vacuum to prepare a dry thin lipid film on the inner surface of a round-bottom flask using a rotary evaporator. The lipid film was hydrated with 2 ml of 0.1 mM argatroban in PBS solution and then the suspension was vigorously stirred for 3 h at room temperature (RT) to prepare the lipid vesicles. The suspension was extruded through a series of membrane filters with different pore sizes—0.8 μm, 0.22 μm (two times), and 0.1 μm (ten times)—to form small unilamellar vesicles or liposomes. The diameter of the liposomes was

determined by dynamic light scattering (DLS-7000; Otsuka Electronics Co., Ltd, Osaka, Japan). The resultant liposome suspension was applied to Sephadex G25 M to separate the liposomes carrying argatroban (liposome-argatroban) from free argatroban. The fraction was collected every 1.0 mL. The concentrations of argatroban and lipid in each fraction were determined by UV-VIS absorption at 331 nm (DU 640; Beckman Coulter Inc., Brea, California, USA) and with the Phospholipids C-test Kit, respectively. To prepare fluorescence-labeled liposomes, 20 mg of EggPC in 2 mL of chloroform was mixed with 0.4 mg of fluorescence-labeled lipid (NBD-lipid) yielding a final concentration of 1.8 mol%. The procedures to prepare small unilamellar liposomes carrying NBD (liposome-NBD) were same as those described above. Oligo$(dT)_{20}$ was introduced to the liposome surface by adding 20 μL of oligo$(dT)_{20}$-PEG-DPPE (0.5 mg/mL in PBS) to the liposome-argatroban suspension (10 mg/mL in PBS) and incubating for 2 h at RT.

Immobilization of oligo$(dA)_{20}$ on cell surfaces

CCRF–CEM cells were cultured in RPMI-1640 medium supplemented with 10% FBS, 100 U/mL penicillin, and 0.1 mg/mL streptomycin (Invitrogen) at 37°C under 5% CO_2. CCRF–CEM cells were collected by centrifugation. After 25 μL of oligo$(dA)_{20}$-PEG-lipid (0.5 mg/mL in PBS) solution was added to the cell pellet (1.0×10^6 cells), the suspension was incubated with gentle agitation for 1 h at RT. The cells were washed with PBS and collected by centrifugation. A suspension of oligo$(dT)_{20}$-liposome-NBD (25 μL, 10 mg/mL in PBS) was added to the cells, and the cell suspension was left to incubate for 10 min at RT. The cells carrying

liposome-NBD were washed with PBS and collected by centrifugation. The cells were resuspended in 2 mL of culture medium, observed over time under a confocal laser scanning microscope, and analyzed by a fluorescence-activated cell sorter (FACS) (Guava EasyCyte Mini; Millipore, Billerica, MA, USA) equipped with a 488 nm diode laser. Data collected from 50,000 cells were used to generate a histogram. Untreated cells were used as a negative control.

Immobilization of liposomes on islet surfaces by DNA hybridization

All animal experiments were approved and accepted by the animal care committee of the Institute for Frontier Medical Sciences, Kyoto University, Japan. Pancreatic islets were isolated from the pancreas of male BALB/c mice (6–7 wk old; Japan SLC, Shizuoka, Japan) by the collagenase digestion method. The islets were maintained in RPMI 1640 culture medium supplemented with 10% FBS, 100 U/mL penicillin, and 100 μg/mL streptomycin. The islets were cultured for 2 d after isolation to remove cells that were damaged during the isolation procedure. Since the surface of the cells becomes smooth during cell culture, it is more appropriate for surface modification. The basement membrane of isolated islets was lost immediately after enzymatic digestion, and laminin and collagen disappeared during culturing [17], [18]. The islets are suitable for surface modification using oligo$(dA)_{20}$-PEG-lipid. The cultured islets were collected by centrifugation and the supernatant was removed. A solution of oligo$(dA)_{20}$-PEG-lipid (0.5 mL, 0.5 mg/mL in PBS) was added to 100 islets, and the islet suspension was incubated for 1 h at RT. After the islet suspension was centrifuged and the supernatant was removed, 25 μL of

oligo$(dT)_{20}$-liposome-argatroban or 25 μL of oligo$(dT)_{20}$-liposome-NBD suspension was added to the oligo$(dA)_{20}$-islets. After 1 h of incubation, liposome-argatroban–immobilized islets or liposome-NBD-immobilized islets were washed with PBS. Liposome-NBD-immobilized islets were then observed over time under a confocal laser scanning microscope (FLUOVIEW FV500; Olympus, Tokyo, Japan).

Immobilization of liposomes on islet cells

After 1.0 mL of trypsin/EDTA solution (0.5 mg/mL) was added to an islet suspension (100 islets), the suspension was incubated for 2 min at 37°C. Islets were dissociated to single cells by pipetting gently and wash by HBSS. The immobilization of liposome-NBD was carried out as described in the former section (2.4). The modified cells were observed during culturing under a confocal laser scanning microscope. A line profile of fluorescence intensity across the cell was determined by Image J Version 1.37v. Average fluorescence intensities at the cell membrane and inside the cells were calculated using following equation (see also Figure. 4(b))

Fluorescence intensities at the cell membrane = (Area (M1 + M2))/(Width L1 + L2)

Fluorescence intensities inside the cell = (Area S)/(Width SL1)

Measurement of argatroban activity

Liposome-argatroban–immobilized islets (50 islets) were incubated in culture medium (2 mL) at 37°C and the supernatant was collected at predetermined times. Antithrombin activity was determined with the SensoLyte 520 Thrombin Activity Assay Kit. Briefly, 200 μL of sample, 25 μL of diluted standard thrombin solution, 25 μL of diluted substrate, and 15 μL of buffer were mixed and incubated for 1h at 37°C. After stop solution (50 μL) was added, fluorescence intensity was determined (excitation/emission = 490/520 nm). Fresh medium (200 μL) was added to replace the solution that was taken as samples at each time point.

Glucose-stimulated insulin release from islets

After the islets were washed several times with Krebs–Ringer solution, they were sequentially incubated for 1 h each in 0.1 g/dL, 0.3 g/dL, and then 0.1 g/dL glucose in Krebs–Ringer solution at 37°C. The supernatants were collected at each step, and the insulin concentrations were determined by enzyme-linked immunosorbent assay (ELISA).

Statistical analysis

Comparisons between two groups were made using Student's *t*-test. $p < 0.05$ was considered statistically significant. All statistical calculations were performed using the software JMP 5.0.1J.

2.3. Results

Immobilization of liposomes on cell surfaces

Liposomes were immobilized on CCRF–CEM cells and their stability during culture was examined. Oligo(dT)$_{20}$-liposome-NBD was applied to the surface of CCRF cells that had been pretreated with oligo(dA)$_{20}$-PEG-lipid. The cells were observed under a confocal laser scanning microscope. Fluorescence from NBD could be clearly observed at the periphery of each cell as shown in Figure.1 (a). By contrast, no fluorescence was observed on the surface of cells that were not

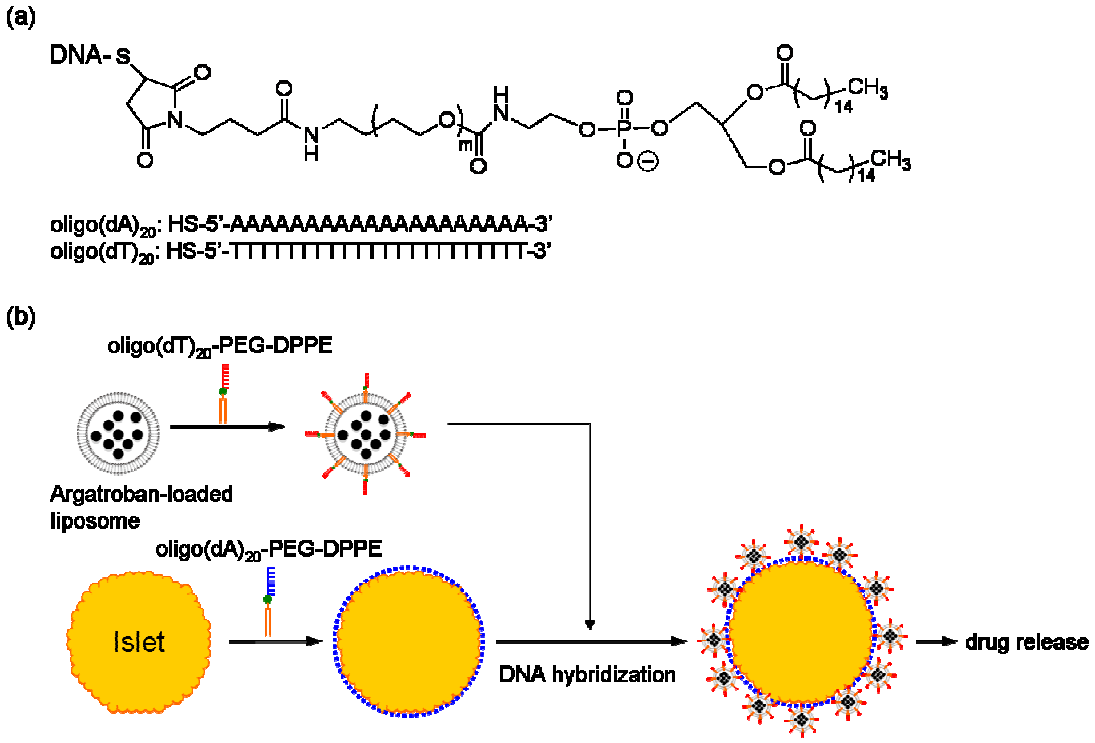

Scheme.1 Schematic illustration of immobilization of liposomes onto islet surfaces. (a) Chemical structure of DNA-PEG-lipid conjugate. (b) Schematic illustration of immobilization of liposomes onto islet surfaces via DNA-PEG-lipids. DNA-PEG-lipid anchored to the membrane through hydrophobic interactions between the alkyl chains of DNA-PEG-lipid and the lipid bilayer. Oligo(dT)$_{20}$ on liposomes hybridized with oligo(dA)$_{20}$ at the end of PEG chains on the islet surface.

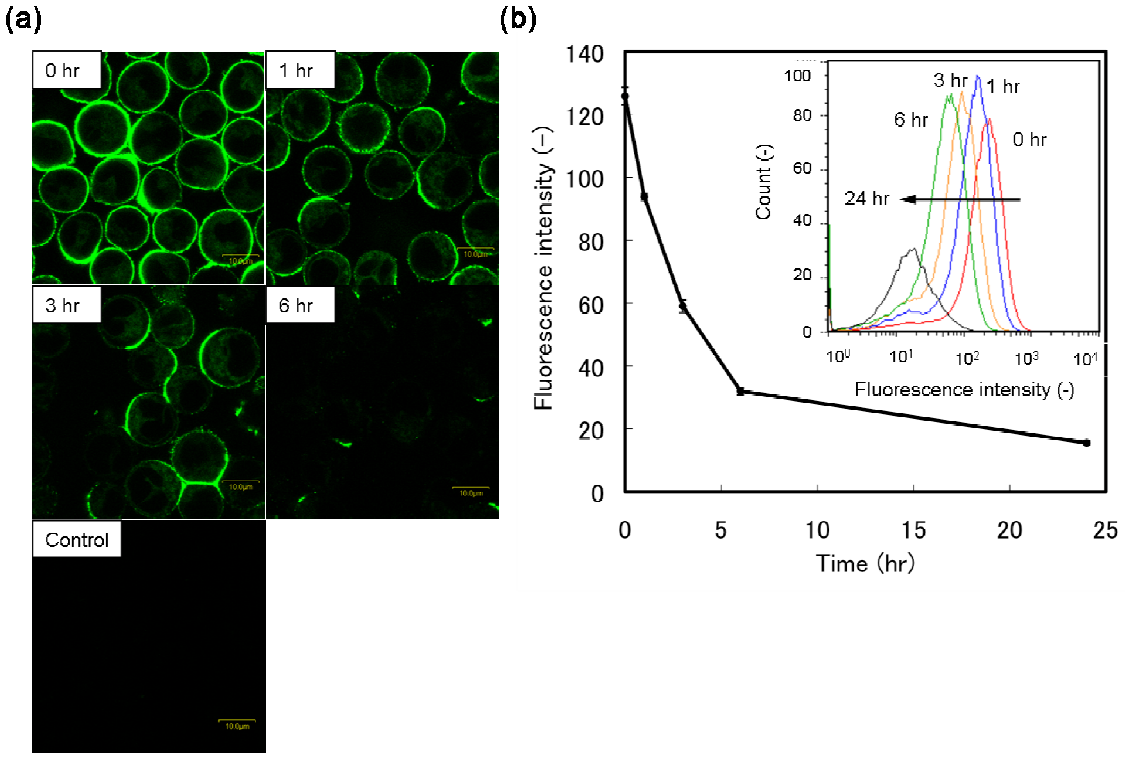

Figure.1 CCRF-CEM cells modified with oligo(dT)$_{20}$-liposome-NBD. (a) ; Fluorescence microscopic image of modified CCRF–CEM cells at 0 hr, 1 hr, 3 hr, 6 hr of incubation in medium at 37°C and control that were not pretreated with oligo(dA)$_{20}$-PEG-lipid (b) ; Flow cytometry analysis (FACS) for oligo(dT)$_{20}$-liposome-NBD-immobilized CCRF-CEM cells. Results are expressed as mean ± standard deviation for *n* = 3. Mean fluorescence intensities were plotted as a function of time. Inset shows the raw profiles of FACS.

pretreated with oligo(dA)$_{20}$-PEG-lipid (Figure.1 (a)). These results indicate that liposome-NBD is immobilized through hybridization between oligo(dT)$_{20}$ and oligo(dA)$_{20}$ as shown in Scheme.1.

Liposome-NBD–immobilized CCRF cells were cultured and observed by a confocal laser scanning microscope at different culture times. The fluorescent images became faint over the course of 6 h of observation, as shown Figure.1 (a). The cells were analyzed by FACS for more quantitative analysis. As shown

in the inset of Figure.1 (b), the profiles showing the relationship between fluorescence intensities and cell numbers shifted left with time over the 6 h observation. Average fluorescent intensities of the cells at each time point were calculated from the profiles shown in the inset and summarized in Figure.1 (b). At 6 h, about 75% of liposomes were detached from the cell surface.

Immobilization of liposome on islets

Immobilization of liposome on single islet cells was examined using liposomes modified with lipid-NBD. Oligo$(dA)_{20}$ was introduced onto the surface of islets using oligo$(dA)_{20}$-PEG-lipid. Liposome-NBD that had been previously modified with oligo$(dT)_{20}$-PEG-lipid was applied to the islets. The islets were observed under a confocal laser scanning microscope. The morphology of islets was well maintained after immobilization of the liposomes. Fluorescence from NBD could be clearly observed at the periphery of each islet as shown in Figure.2 (a), indicating that liposome-NBD was immobilized on the islet surfaces. Figure.2 also contains confocal laser scanning microscopic images of the modified islets after 3 and 6 h. The fluorescence on islets decreased with time during incubation, indicating that liposomes were release liposome from the islets over several hours of incubation.

Immobilization of liposome-argatroban on islets

The lipid film coating the inner surface of a round-bottom flask was hydrated with an argatroban solution and liposomes carrying argatroban were prepared by extruding the lipid suspension through a series of membrane filters. The

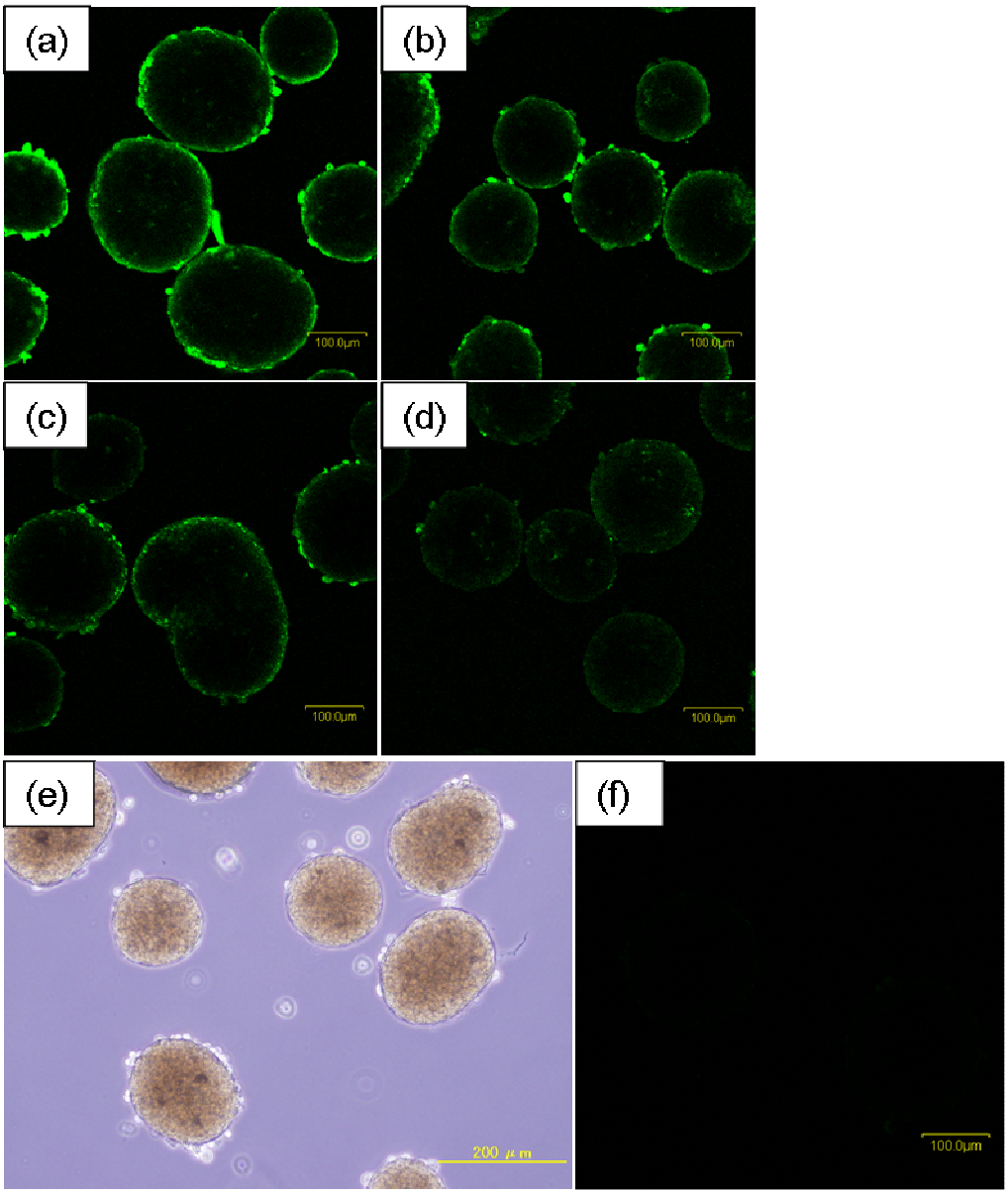

Figure.2 Immobilization of fluorescence-labeled liposomes on islet surface by DNA hybridization. Observation of liposome-immobilized islets at (a) 0 min, (b) 3 h, (c) 6 h, (d) 24 h and (e) 3 d of incubation in medium at 37°C. (f) Islets modified with oligo$(dT)_{20}$-liposome (NBD).

fractions of the resultant liposome suspension separated by the Sephadex G25 M column were analyzed for argatroban and liposome concentrations. The concentrations of lipid and argatroban are plotted against the eluted volume in

Figure.3. A single peak and two peaks were observed for lipid and argatroban, respectively. The concentration of argatroban was highest in the same eluted volume in which the lipid concentration was highest. This indicates that a liposome-argatroban complex was formed. Free argatroban was eluted from in the 7–15 ml fractions from the column.

Oligo(dT)$_{20}$-liposome-argatroban was prepared by the surface modification of liposome-argatroban with oligo(dT)$_{20}$-PEG-lipid. Oligo(dT)$_{20}$-liposome--argatrob

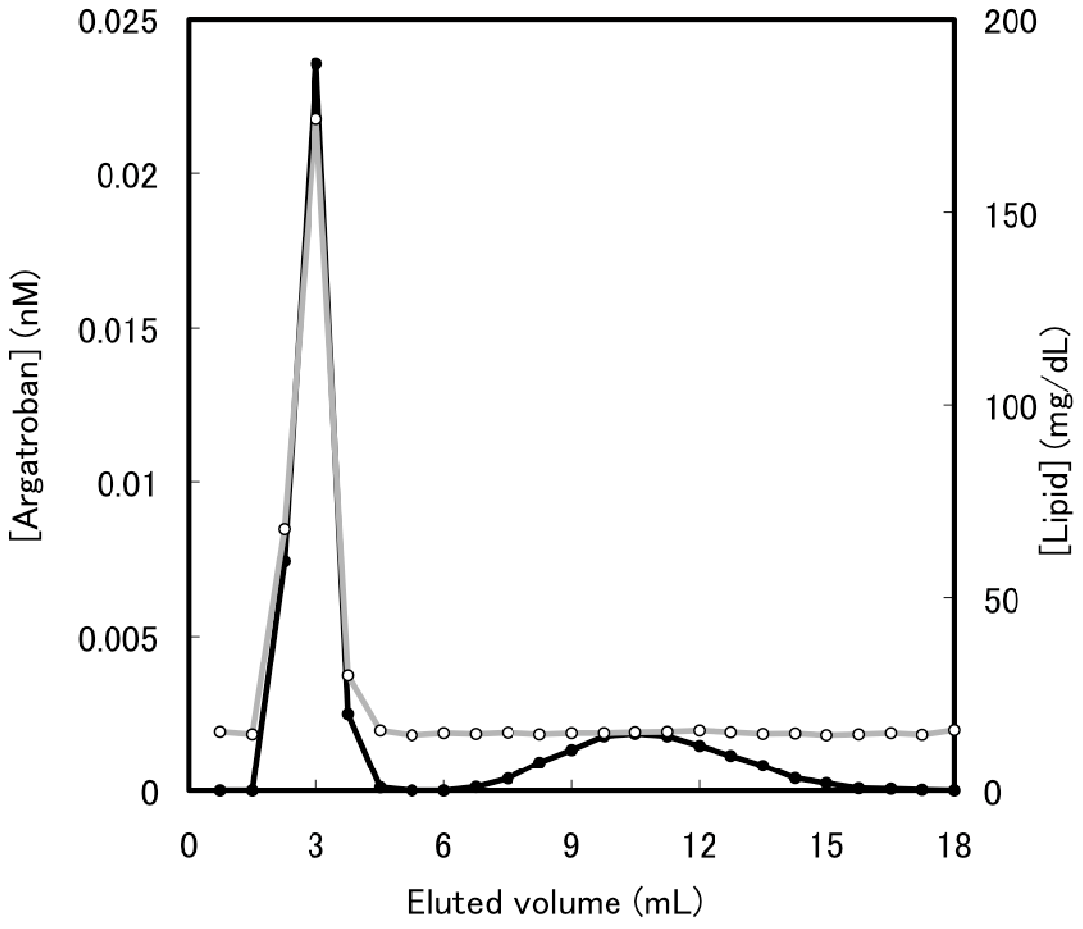

Figure.3 Elution profile of argatroban-loaded liposomes through a Sepadex G25 M column. The concentration of argatroban hydrate was estimated by UV-vis absorption spectra (331 nm) (●, left y-axis). The concentration of EggPC was estimated with the Phospholipids C-test Kit (○, right y-axis).

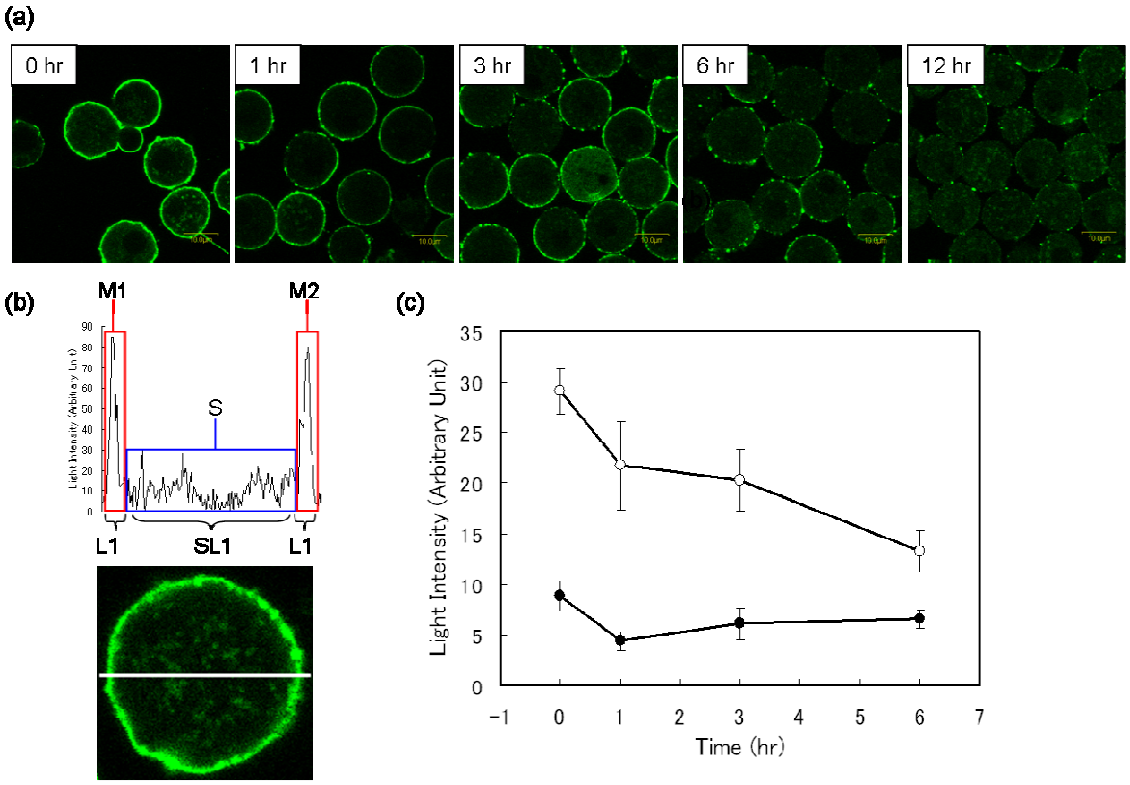

Figure.4 Immobilization of fluorescence-labeled liposomes on single cells dissociated from islets by DNA hybridization. (a); Fluorescence microscopic image of modified islet cells at 0 hr, 1 hr, 3 hr, 6 hr and 12 hr of incubation in medium at 37°C. (b); A line profile of fluorescence intensity across the cell. (c); Averaged light intensities at the cell membrane (○) and inside of cell (●). (*n* = 10).

-an was added to oligo(dA)$_{20}$-PEG-lipid–modified islets (Figure.2). The morphology of the islets was well maintained after they were treated with oligo(dT)$_{20}$-liposome-argatroban and after a 1 d incubation in culture medium.

Fate of liposomes on islet cells

Fate of liposomes on islet cells was observed using single cells dissociated from islets (Figure. 4 (a)). Oligo(dT)$_{20}$-liposome-NBD was immobilized to the surface of islet cells. Those cells were observed during culture under a confocal laser scanning microscope. Fluorescence from NBD was clearly observed at the

periphery of each cell just after immobilization. Then, fluorescence intensity at the cell membrane gradually decreased with function of time. On the other hand, no clear change of fluorescence intensity was observed inside of the cells. Most of liposomes were released from the cell surface, but not internalized into the inside of cells (Figure. 4 (c)).

Antithrombin activity of argatroban released from islets

Liposome-argatroban–immobilized islets were incubated in culture medium, and 0.2 ml of the medium was collected at predetermined periods of time. Antithrombin activity in the media increased with longer culture periods, indicating that argatroban was gradually released from the liposomes (Figure. 5). Antithrombin activity in medium in which naive islets were cultured was quite low.

Glucose-stimulated insulin release from islets

A static glucose-responsive insulin release assay [16] was performed to examine the effects of surface modification of islets on their insulin-releasing ability. Three samples were examined: naive islets, oligo$(dT)_{20}$ introduced islets, and liposome-argatroban–immobilized islets. The amount of insulin released from these islets is summarized in Figure.5. Insulin release markedly increased in all of these groups in response to an increase in the glucose concentration from 1.0 to 3.0 g/L in Krebs–Ringer solution. When the glucose concentration returned to basal levels, the insulin release in all of the samples also decreased to normal levels. No significant differences were seen among the three groups with regard to glucose stimulation indexes. This indicates that immobilization of

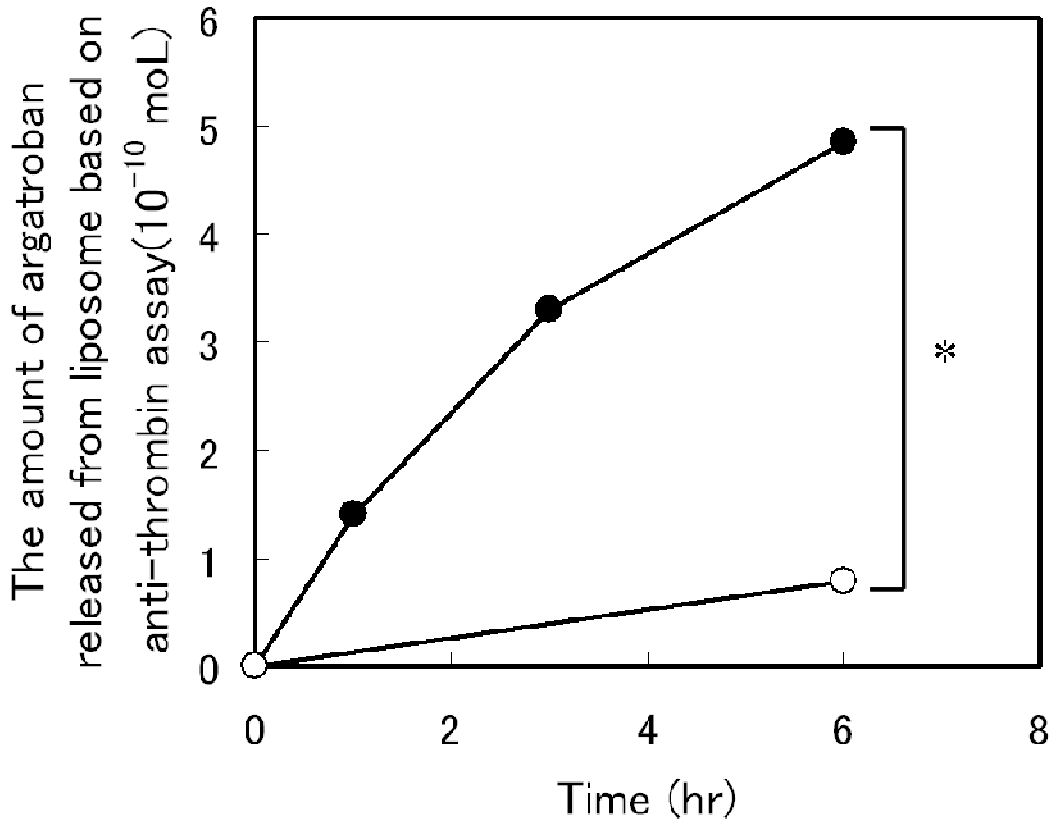

Figure.5 Antithrombin activity of argatroban released in the supernatant from oligo$(dT)_{20}$-argatroban-liposome immobilized islets (●) and untreated islets (○). During the incubation period, supernatant from the oligo$(dT)_{20}$-argatroban-liposome-immobilized islets was assayed for anti-thrombin activity. Results are expressed as mean ± standard deviation for n = 4. An asterisk represents a significant difference ($p<0.05$) between two groups.

liposomes on islet surfaces did not interfere with the islets' ability to regulate insulin release in response to glucose concentrations.

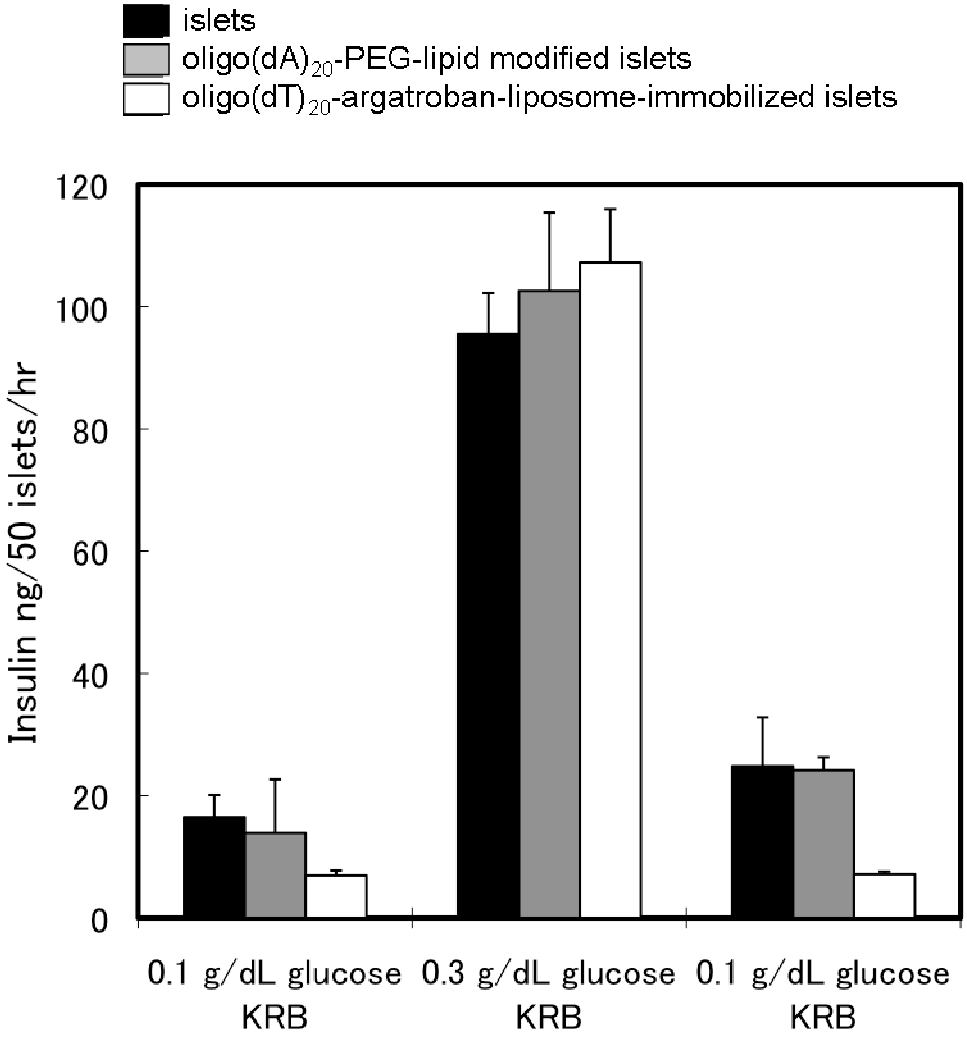

Figure.6 Glucose stimulation assays. Islets, oligo(dA)$_{20}$-PEG-lipid–modified islets, and argatroban-loaded liposome-immobilized islets (50 islets each) were incubated in solutions with different glucose concentrations for 1 h. The amount of insulin secreted from islets was determined by ELISA. Results are expressed as mean ± standard deviation for n = 4.

2.4. Discussion

Our group previously reported a method to immobilize living cells on islets using PEG-lipids carrying ssDNAs (oligo$(dT)_{20}$ and oligo$(dA)_{20}$) [19]. HEK293 cells were immobilized on islets. The cells stably persisted on the islets and after several days of culture, the HEK293 cells fully enclosed the islets. By contrast, liposomes that were immobilized on islets using the same molecules, PEG-lipid–carrying ssDNAs, were rapidly released from the islet surface, as shown in Figure. 2. It is not entirely clear why the cells remained immobilized on the islet surface while the lipids were released. The interactions between PEG-lipid–carrying ssDNAs or hydrophobic interactions between the part of lipids and cell membranes are not stable enough to immobilize liposomes or cells on islets for long periods of time. The HEK293 cells were initially immobilized on the islets through interactions between oligo$(dT)_{20}$ and oligo$(dA)_{20}$. However, cell–cell interactions through cadherins may play a role in stabilizing HEK293 cells on islet surfaces after several hours of culture.

We expected that argatroban would be released from liposomes on the islets. As shown in Figure.2 and 5, the release rate of argatroban, which was determined from antithrombin activity in the culture medium, was slightly higher than predicted based on the concentration of liposomes immobilized on islets; however, the difference was not significant. Anti-coagulant activity should remain on islets for about 1 day to rescue islets from IBMIR [21]. Argatroban release rate of our system is slightly higher. The lengths of the alkyl chains of the PEG-lipid molecules and the lipid compositions used to prepare liposome should be carefully examined to optimize the release rate of liposomes from the islets.

It is important to suppress blood coagulation triggered by the islet since IBMIR is involved in the early graft loss of islets. Systemic administration of anticoagulants and thrombin inhibitor has been done to control IBMIR [6], [7], [8] and [9], but patients may then be at a high risk for bleeding. Our approach is promising because argatroban can be released from the islet surface and blood coagulation can be locally suppressed around islets without affecting insulin release function of islets. However, it is expected that relatively high local concentration of the drug at the cell surface and high influx into cell due to activate endocytosis/phagocytosis can cause immediate cytotoxic effect in case of many active compounds. It is important to optimize a drug loading amount to liposomes without deteriorative effects on cells, but effectively exertion of medicinal effect surround the cell.

This is the first examination for the release of small drugs from the islet surface. A variety of anticoagulants and drugs can be available by the use of release from liposome. If an appropriate drug is selected, it is possible to suppress IBMIR effectively. We are currently performing transplantation studies to examine the efficacy for inhibiting IBMIR *in vivo*. And we will report near future.

2.5. References

[1] E.A. Ryan, J.R. Lakey, R.V. Rajotte, G.S. Korbutt, T. Kin, S. Imes, A. Rabinovitch, J.F. Elliott, D. Bigam, N.M. Kneteman, G.L. Warnock, I. Larsen, A.M. Shapiro, Clinical outcomes and insulin secretion after islet transplantation with the Edmonton protocol. Diabetes 50 (2001) 710-719.

[2] A.M. Davalli, L. Scaglia, D.H. Zangen, J. Hollister, S. Bonner-Weir, G.C. Weir, Vulnerability of islets in the immediate posttransplantation period. Dynamic changes in structure and function. Diabetes 45 (1996) 1161-1167.

[3] D.J. Van der Windt, R. Bottino, A. Casu, N. Campanile, D.K.C. Cooper, Rapid loss of intraportally transplanted islets: An overview of pathophysiology and preventive strategies. Xenotransplantation 14 (2007) 288-297.

[4] W. Bennet, B. Sundberg, C.G. Groth, M.D. Brendel, D. Brandhorst, H. Brandhorst, R.G. Bretzel, G. Elgue, R. Larsson, B. Nilsson, O. Korsgren, Incompatibility between human blood and isolated islets of Langerhans: A finding with implications for clinical intraportal islet transplantation? Diabetes 48 (1999) 1907-1914.

[5] L. Moberg, H. Johansson, A. Lukinius, C. Berne, A. Foss, R. Källen, Ø. Østraat, K. Salmela, A. Tibell, G. Tufveson, G. Elgue, E.K. Nilsson, O. Korsgren, B. Nilsson, Production of tissue factor by pancreatic islet cells as a trigger of detrimental thrombotic reactions in clinical islet transplantation, Lancet 360 (2002) 2039-2045.

[6] H. Johansson, A. Lukinius, L. Moberg, T. Lundgren, C. Berne, A. Foss, M. Felldin, R. Kallen, K. Salmela, A. Tibell, G. Tufveson, K.N. Ekdahl, G. Elgue,

O. Korsgren, B. Nilsson, Tissue factor produced by the endocrine cells of the islets of Langerhans is associated with a negative outcome of clinical islet transplantation, Diabetes 54 (2005) 1755–1762.

[7] H. Johansson, M. Gotoa, A. Siegbahnc, G. Elguea, O. Korsgrena, B. Nilsson, Lowmolecular weight dextran sulfate: A strong candidate drug to block IBMIR in clinical islet transplantation, Am. J. Transplant 6 (2006) 305-312.

[8] L. Ozmen, K.N. Ekdahl, G. Elgue, R, Larsson, O. Korsgren, B. Nilsson, Inhibition of thrombin abrogates the instant blood-mediated inflammatory reaction triggered by isolated human islets: Possible application of the thrombin inhibitormelagatran in clinical islet transplantation, Diabetes 51 (2002): 1779-1784.

[9] J.L. Contreras, C. Eckstein, C.A. Smyth, G. Bilbao, M. Vilatoba, S.E. Ringland, C. Young, J.A. Thompson, J.A. Fernández, J.H. Griffin, D.E. Eckhoff, Activated protein C preserves functional islet mass after intraportal transplantation: a novel link between endothelial cell activation, thrombosis, inflammation, and islet cell death, Diabetes 53 (2004) 2804-14.

[10] S. Cabric, J. Sanchez, T. Lundgren, A. Foss, M. Felldin, R. Kallen, K. Salmela, A. Tibell, G. Tufveson, R. Larsson, O. Korsgren, B. Nilsson, Islet surface heparinization prevents the instant blood-mediated inflammatory reaction in islet transplantation, Diabetes 56 (2007) 2008-2015.

[11] H. Johansson, A. Lukinius, L. Moberg, T. Lundgren, C. Berne, A. Foss, M. Felldin, R. Kallen, K. Salmela, A. Tibell, G. Tufveson, K.N. Ekdahl, G. Elgue, O. Korsgren, B. Nilsson, Tissue factor produced by the endocrine cells of the islets of Langerhans is associated with a negative outcome of clinical islet

transplantation, Diabetes 54 (2005) 1755–1762.

[12] C.L. Stabler, X.L. Sun, W. Cui, J.T. Wilson, C.A. Haller, E.L. Chaikof, Surface Re-engineering of Pancreatic Islets with Recombinant azido-Thrombomodulin, Bioconjugate. Chem 18 (2007) 1713-1715.

[13] T. Totani, Y. Teramura, H. Iwata, Immobilization of urokinase on the islet surface by amphiphilic poly(vinyl alcohol) that carries alkyl side chains, Biomaterials 29 (2008) 2878-2883.

[14] Y. Teramura, H. Iwata, Islets surface modification prevents blood-mediated inflammatory responses, Bioconjugate. Chem 19 (2008) 1389–1395.

[15] Y. Teramura, H. Iwata, Bioartificial pancreas Microencapsulation and conformal coating of islet of Langerhans, Adv. Drug. Deliv. Rev 62 (2010) 827-840.

[16] S. Okamoto, A. Hijikata, R. Kikumoto, S. Tonomura, H. Hara, K. Ninomiya, A. Maruyama, M. Sugano, Y. Tamao, Potent inhibition of thrombin by the newly synthesized arginine derivative No. 805. The importance of stereo-structure of its hydrophobic carboxamide portion, Biochem. Biophys. Res. Commun. 101 (1981) 440-446.

[17] G.G. Pinkse, W.P. Bouwman, R. Jiawan-Lalai, O.T. Terpstra, J.A. Bruijn, E. de Heer, Integrin signaling via RGD peptides and anti-beta1 antibodies confers resistance to apoptosis in islets of Langerhans. Diabetes. 55 (2006) 312-317.

[18] L. Rosenberg, R. Wang, S. Paraskevas, D. Maysinger. Structural and functional changes resulting from islet isolation lead to islet cell death. Surgery. 126 (1999) 393-398.

[19] S.L. Howell, K.W. Taylor, Potassium ions and the secretion of insulin by islets of Langerhans incubated in vitro, Biochem. J. 108 (1968) 17-24.

[20] Y. Teramura, LN. Minh, T. Kawamoto, H. Iwata, Microencapsulation of islets with living cells using polyDNA-PEG-lipid conjugate, Bioconjug. Chem 21 (2010) 792-796.

[21] Dr. Paul Johnson private communication.

Chapter 3

Control of cell attachment through oligoDNA hybridization

3.1. Introduction

In the past decade, therapeutic devices containing living cells or tissues have been studied extensively for tissue engineering and regenerative medicine applications. Stem cells, including embryonic stem (ES) cells, somatic stem cells, and induced pluripotent stem (iPS) cells, have been identified and studied [1–3] that show promise for treatment of diseases such as type I diabetes, Parkin-son's, Alzheimer's, ALS, and Huntington's disease [4–11]. Experimental manipulation of cell–cell interactions is a valuable method for inducing differentiation of stem cells for use in cell-based therapies. In addition, the differentiated cells can be manipulated further for use in regenerating tissues or organs. Cell–cell interactions must be tightly controlled for generating cell-type-specific tissues or organs. Cell–cell interactions are also used to develop pluripotent stem cells themselves. It was reported recently that somatic cells could be transformed into pluripotent stem cells by fusion with ES cells [12]. In this method, somatic cells and ES cell attachments formed first, and attachment was followed by induced cell fusion.

Cell–cell interactions are also very important in embryo development and in the maintenance of homeostasis. Methods for studying and controlling cell–cell

interactions are currently being developed using both biomedical and engineering approaches. Our group has studied the surface modification of living cells using amphiphilic polymers such as PEG-conjugated phospholipid (PEG-lipid) derivatives [13–19]. Specifically, our previous efforts were directed towards modification of cell surfaces and islets of Langerhans (islets) by introducing functional groups and polymers for improving graft survival after transplantation. Recently, immobilization of cells to the surface of islets using PEG-lipid and a biotin/streptavidin reaction resulted in encapsulation of the whole islet surface with layers of cells [19]. It seemed possible to use this method to induce cells to attach to a substrate. Although the biotin/streptavidin reaction is well characterized and is used frequently in biological studies, it has some disadvantages. Specifically, streptavidin is derived from bacteria and is a potent antigen in humans; further, the biotin/streptavidin association is so strong that it is difficult to be dissociated.

In the present study, DNA hybridization was employed rather than the biotin/streptavidin reaction as a novel method for inducing cell–cell attachment and cell immobilization on a substrate. PEG-lipid, an amphiphilic polymer, as a carrier for oligoDNA with a specific sequence was used. Cells treated with the oligoDNA–PEG-lipid conjugate incorporated the lipid (and thus the oligoDNA) onto the cell surface. OligoDNA with the complementary sequence was similarly transferred onto the surface or other cells or onto a substrate. Cell–cell or cell–substrate attachments were subsequently induced via hybridization between the two complementary oligoDNAs.

3.2. Materials and methods

Materials

α-*N*-Hydroxysuccinimidyl-ω-maleimidyl poly(ethylene glycol) (NHS-PEG-Mal, MW: 5000) was from Nektar Therapeutics (San Carlos, CA, USA). 1, 2-dipalmitoyl-sn-glycerol-3-phosphatidylethanolamine (DPPE) was from NOF Corporation (Tokyo, Japan). Dichloromethane, triethylamine, and diethyl ether was from Nacalai Tesque (Kyoto, Japan). Hanks' balanced salt solution (HBSS), minimum essential medium (MEM), and RPMI-1640 medium were from Invitrogen Co. (Carlsbad, CA, USA). Fetal bovine serum (FBS) was from Equitech-Bio, Inc. (TX, USA), and phosphate-buffered saline (PBS) was from Nissui Pharmaceutical Co. Ltd. (Tokyo, Japan). PKH67 Green Fluorescent Cell Linker Kit (PKH green) and PKH26 Red Fluorescent Cell Linker Kit (PKH red) were from Sigma–Aldrich Chemical Co. (St. Louis, MO, USA). *n*-Hexadecyl mercaptan was from Tokyo Chemical Industry Co., Ltd (Tokyo, Japan). Glass plates (22 mm × 26 mm; thickness: 0.12–0.17 mm) were from Matsunami Glass Ind., Ltd (Osaka, Japan). Dithiothreitol (DTT) was from Wako Pure Chemical Industries, Ltd (Osaka, Japan).

Synthesis of DNA-conjugated PEG-phospholipid (oligoDNA–PEG-lipid)

Mal-PEG-lipid was synthesized by combining NHS-PEG-Mal (180 mg), triethylamine (50 μL), and DPPE (20 mg) with dichloromethane and stirring for 36 h at room temperature (RT) [14]. After precipitation with diethyl ether, Mal-PEG-lipid was obtained as a white powder (190 mg, 80% yield). ^{1}H NMR

analysis ($CDCl_3$, 400 MHz, δ ppm): 0.88 (t, 6H, –CH3), 1.25 (br, 56H, –CH2–) 3.64 (br, 480H, PEG), 6.71 (s, 2H, –HC]CH–, maleimide). The DNA sequences used in this chapter are listed in Table 1. DNA was synthesized by Sigma–Aldrich Chemical Co. DNA-SH was prepared by reduction of the disulfide bond with DTT according to the manufacturer's instructions. A PBS solution of DNA-SH (1.0 mg) was mixed with Mal-PEG-lipid (5.0 mg) in PBS for 24 h at RT to prepare oligoDNA–PEG-lipid. OligoDNA–PEG-lipid (500 mg/mL in PBS) was used for surface modification of cells without purification.

Cell cultures

Two cell lines, CCRF-CEM cells (a human T cell lymphoblast-like cell line) and HEK293 cells (a human embryonic kidney cell line) were obtained from the Health Science Research Resources Bank (Osaka, Japan). Suspension culture of CCRF-CEM cells was performed in RPMI-1640 medium supplemented with 10% FBS, 100 U/mL penicillin, and 0.1 mg/mL streptomycin (Invitrogen) at 37°C under 5% CO_2. HEK293 cells that stably expressed enhanced green fluorescence protein (EGFP) (GFP-HEK) were the kind gift of Dr. K. Kato (Institute for Frontier Medical Sciences, Kyoto University). The GFP-HEK cells were maintained in MEM supplemented with 10% FBS, 100 U/mL penicillin, and 0.1 mg/mL streptomycin.

Surface modification of cells with oligoDNA–PEG-lipid and co-incubation of differentially modified cells

For visualization under a fluorescence microscope, CCRF-CEM cells were

labeled with PKH red or PKH green according to the manufacturer's instructions. To exchange the culture medium, CCRF-CEM or GFP-HEK cells (4×10^6 cells) were washed twice with HBSS and collected by centrifugation (180g, 5 min, 25°C). After the addition of oligoDNA–PEG-lipid solution (50 μL, 500 mg/mL in PBS) to the cell suspension, cells were incubated for 30 min at RT with gentle agitation. The cells were then suspended in 10mL HBSS, collected by centrifugation (180g, 5min, 25°C), washed with another 10mL HBSS, and re-centrifuged to obtain oligoDNA–PEG-lipid-modified cells.

After cells were treated with oligo(dA)–PEG-lipid or oligo(dT)–PEG-lipid, the oligoDNA–PEG-lipid-modified cells were mixed together in culture medium with the following ratios of oligo(dA)-cells:oligo(dT)-cells: 10:1, 4:1, 2:1, and 1:1. The cells were incubated with rotation at 100 rpm for 1 h at RT, followed by incubation at 37°C under 5% CO_2. The cells were observed over time using a confocal laser scanning microscope (FLUOVIEW FV500, Olympus, Tokyo, Japan) and a phase-contrast microscope (IX7, Olympus Optical Co. Ltd., Tokyo, Japan).

Immobilization of oligoDNA–PEG-lipid modified cells to patterned substrates

SeqA-conjugated PEG-lipid and SeqB-conjugated PEG-lipid were used for cell surface modification. For testing immobilization of the modified cells, substrate surfaces were modified using SeqA0 and SeqB0, the sequences complementary to SeqA and SeqB.

Glass plates were cleaned with a piranha solution (7:3 mixture of concentrated

sulfuric acid and 30% hydrogen peroxide solution), washed 3┐ with Milli-Q water, and stored in a 2-propanol solution. For experiments, glass plates were mounted on a rotation stage in a metal vapor deposition apparatus (V-KS200, Osaka Vacuum Instruments, Osaka, Japan). A 1.0-nm chromium layer was deposited on the glass, followed by deposition of a 19-nm gold layer. The resulting glass plates coated with a thin layer of gold were immersed in an ethanol solution of *n*-hexadecylmercaptan (1 mM) to produce a surface with SAM-carrying methyl groups (CH_3-SAM). The CH_3-SAM surface was irradiated with an ultraviolet (UV) light at 180 mW/cm^2 using an Optical ModuleX (SX-UI 501HQ, Ushio, Inc., Tokyo) equipped with a super-high-pressure mercury lamp (Ushio, Inc.) through a photomask with an array of transparent 1- or 2-mm circular dots in ambient air for 4 h. The plates were washed with ethanol to remove photodegradation products. A PBS solution of DNA-SH (600 mg/mL, SeqA0 and SeqB0), was applied to the UV-irradiated spots by manual pipetting and allowed to incubate for 2 h at RT. The substrate-coated glass plate was washed with HBSS before use.

In the first series of experiments, SeqA-PEG-lipid modified CCRF-CEM cells (SeqA-PEG-cells) and SeqB-PEG-lipid modified CCRF-CEM cells (SeqB-PEG-cells) were mixed at the following ratios: 4:1, 2:1, 1:1, 2:1, and 4:1. The cell suspensions were applied to UV-irradiated spots that had been incubated with a 1:1 mixture of $SeqA_0$ and $SeqB_0$ (see above); cells were incubated on the immobilized-DNA surface for 10 min at RT. In a second series of experiments, the UV-irradiated spots were incubated with $SeqA_0$:$SeqB_0$ at the following molar ratios: 4:1, 2:1, 1:1, 2:1, and 4:1. A 1:1 mixture of

SeqA-PEG-cells and SeqB-PEG-cells was then applied to the UV-irradiated spots containing immobilized DNA. After washing with HBSS, cells attached to the substrate were observed using an upright fluorescence microscope (BX51, Olympus, Tokyo, Japan) and a stereomicroscope (MZF LIII, Leica, Solms, Germany). The number of attached cells was analyzed using ImageJ software (NIH, Bethesda, MD, USA). An inhibition assay was also performed using a solution of $SeqA_0$ (200 mg/mL) that was added to the mixture of SeqA-PEG-cells and SeqB-PEG-cells. After incubation for 30 min, the mixture was applied to the $SeqA_0$ and $SeqB_0$-immobilized substrate and incubated for 10min at RT. After washing with HBSS, the cells attached to the substrate were observed using an upright fluorescence microscope.

Substrates for cell attachment were also prepared using a contact printing technique. Poly(dimethylsiloxane) (PDMS) stamps were prepared as follows: A ledge pattern was fabricated on a PDMS surface using a laser beam machine (VLS2.30, Universal Laser Systems, Inc., Scottsdale, AZ, USA): The pattern consisted of unidirectional ledges (1 mm × 1mm × 10 mm) with 1-mm intervals between ledges. The ledge surfaces on the stamps were coated with a solution of $SeqA_0$ or $SeqB_0$ DNA-SH (600 mg/mL) and applied to the gold-layered glass plates. A second stamp coated with a solution of $SeqA_0$ or $SeqB_0$ DNA-SH was applied to the surface perpendicular to the previous ledge design. The glass plate sat at RT for 2 h to dry. The glass plate was then immersed in an ethanol solution of *n*-hexadecylmercaptan for blocking with CH_3-SAM and washed with ethanol and Milli-Q water. A 1:1 mixture of

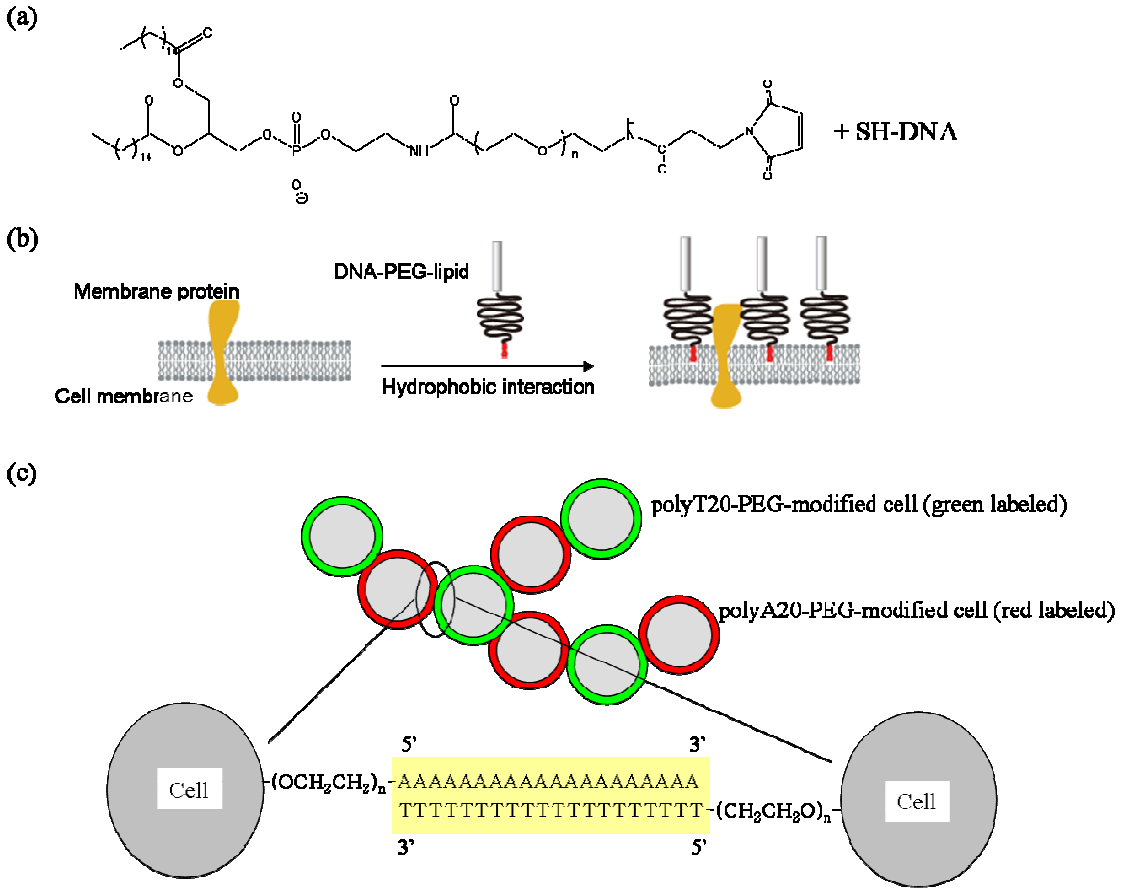

Scheme.1 (a) Synthesis of DNA-conjugated PEG-DPPE (oligoDNA-PEG-lipid) from maleimide-PEG-lipid and DNA-SH. (b) Schematic illustration of the interaction between oligoDNA-PEG-lipid and the lipid bilayer comprising the outer cell membrane. The oligoDNA-PEG-lipid inserts into the cell membrane due to hydrophobic interactions between the acyl chain and the lipid bilayer. (c) Schematic illustration of cell-cell attachment through DNA hybridization between complementary oligoDNA-PEG-lipids incorporated into the outer cell membranes.

SeqA-PEG-cells and SeqB-PEG-cells were applied onto the patterned substrate and incubated for 10 min at RT with gentle agitation. After washing with HBSS, cells attached to the glass plate were observed using an upright fluorescence microscope.

3.3. Results

Intercellular attachment through hybridization of complementary oligoDNA–PEG-lipid conjugates

Scheme 1 shows how cells carrying complementary oligoDNA–PEG-lipid conjugates were tested for intracellular attachment. oligoDNA–PEG-lipids were synthesized using a thiol/maleimide reaction between Mal-PEG-lipid and DNA-SH in which the SH group was introduced at the 50-end of the DNA sequence. The DNA sequences used in this chapter are listed in Table 1. oligoDNA–PEG-lipids carrying complementary sequences were prepared: oligo$(dA)_{20}$ and oligo$(dT)_{20}$, SeqA and $SeqA_0$, SeqB and $SeqB_0$. Our previous studies demonstrated that amphiphilic PEG-lipids are spontaneously incorporated into the cell membrane's lipid bilayer through hydrophobic interactions and that this incorporation has no cytotoxic effects [13–16,18,19].It was further showed that oligoDNA could be introduced onto the cell surface using a PEG-lipid (Scheme 1b). The strategy in the present study was to mediate cell–cell interactions by hybridization between complementary DNA sequences that were incorporated into the cells' outer membranes (Scheme 1c).

Incorporation of oligo$(dA)_{20}$–PEG-lipid into the cell membrane and its ability to

Table 1. Sequence of DNA for cell surface modification

	5'	3'
oligo$(dA)_{20}$	HS-AAA AAA AAA AAA AAA AAA AA	
oligo$(dT)_{20}$	HS-TTT TTT TTT TTT TTT TTT TT	
SeqA	HS-TGC GGA TAA CAA TTT CAC ACA	
SeqA'	HS-TGT GTG AAA TTG TTA TCC GCA	
SeqB	HS-TAG TAT TCA ACA TTT CCG TGT	
SeqB'	HS-ACA CGG AAA TGT TGA ATA CTA	

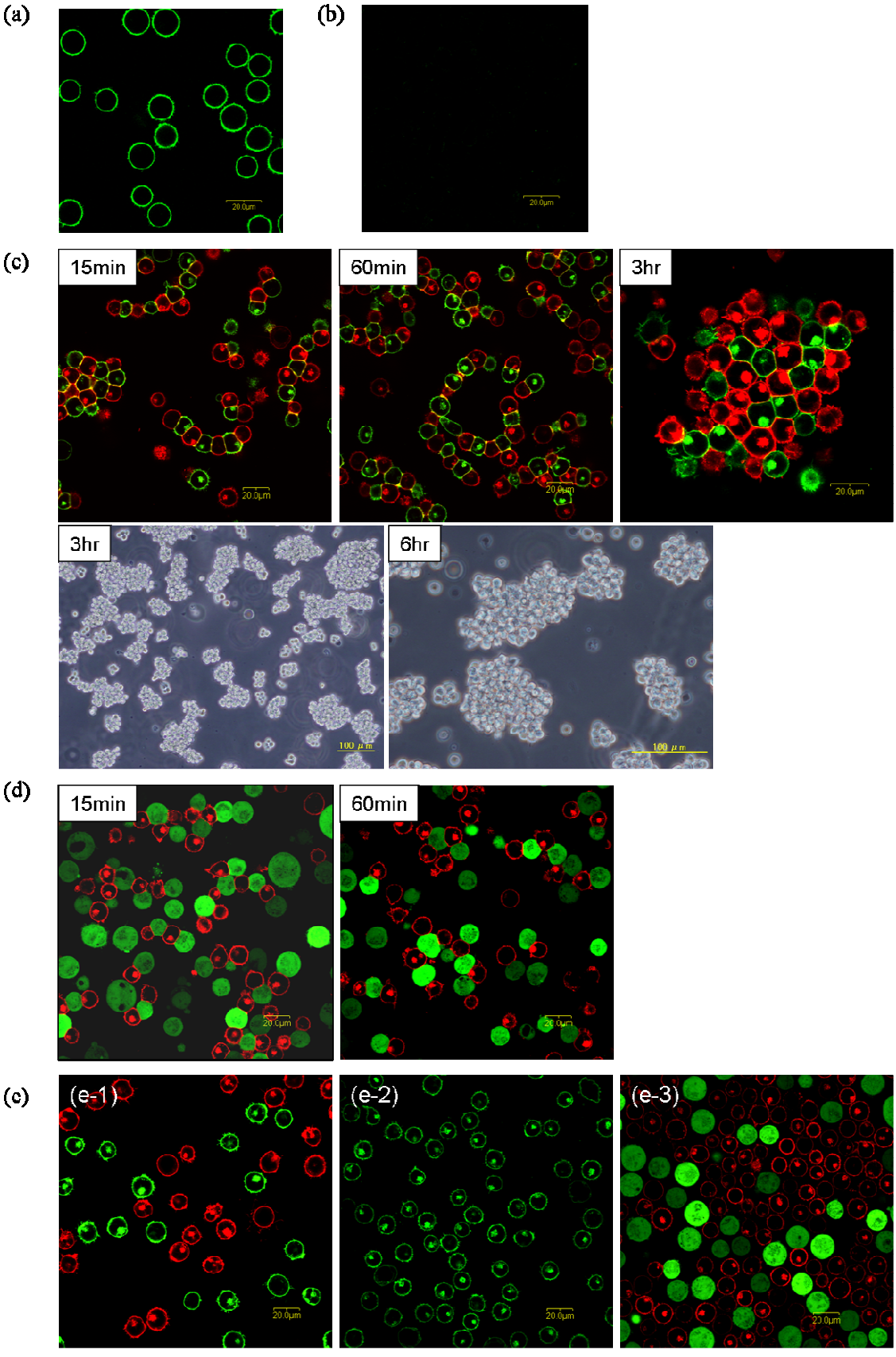
(a)
(b)
(c)
15min
60min
3hr
3hr
6hr
(d)
15min
60min
(e)
(e-1)
(e-2)
(e-3)

Figure.1 Cell-cell attachment via DNA hybridization between complementary oligoDNA-PEG-lipids on cell surfaces. CCRF-CEM cells incorporated oligo$(dA)_{20}$-PEG-lipid into the outer cell membranes. Cells were observed by a confocal laser scanning microscope after oligo$(dA)_{20}$-PEG-lipid modified CCRF-CEM cells were further treated with (a): FITC-labeled oligoT20 and (b): FITC-labeled oligo$(dA)_{20}$. (c): Cell-cell attachment between oligo$(dA)_{20}$-PEG-lipid modified CCRF-CEM cells labeled with PKH red and oligoT20-PEG-lipid modified CCRF-CEM cells labeled with PKH green in culture medium (cells were mixed in a 1:1 ratio). Cells were observed over time using a confocal laser scanning microscope and a phase contrast microscope. (d): Cell-cell attachment between oligo$(dA)_{20}$-PEG-lipid modified CCRF-CEM cells and oligoT20-PEG-lipid modified GFP-HEK293 cells (cells were mixed in a 1:1 ratio). (e): Control experiments for cell-cell attachment by surface modification with oligoDNA-PEG-lipid. (e-1): A mixture of CCRF-CEM cells labeled with PKH red and CCRF-CEM cells labeled with PKH green (no oligoDNA-PEG-lipid modification). (e-2): OligoT20-PEG-lipid modified cells. (e-3): A mixture of CCRF-CEM cells labeled with PKH green and GFP-HEK293 cells after rotation culture at 100 rpm (no oligoDNA-PEG-lipid modification).

hybridize with FITC-labeled oligo$(dT)_{20}$ was examined first. A solution of oligo$(dA)_{20}$–PEG-lipid was added to CCRF-CEM cells; after incubation, the cells were washed to remove unincorporated lipid, FITC-labeled oligo$(dT)_{20}$ was added, and cells were observed using a confocal laser scanning microscope. As shown in Figure.1 (a) the FITC fluorescence was observed at the periphery of all cells, indicating that oligo$(dA)_{20}$–PEG-lipids were incorporated into the outer cell membrane and that FITC-labeled oligo$(dT)_{20}$ hybridized with the incorporated oligo$(dA)_{20}$ DNA. When FITC-labeled oligo$(dA)_{20}$ was added to oligo$(dA)_{20}$–PEG-lipid modified cells, no fluorescence was observed on the cells. These results indicated that FITC-labeled oligo$(dT)_{20}$ hybridized specifically with oligo$(dA)_{20}$–PEG-lipids on the cell surface.

Intercellular attachments could also be mediated by hybridization between

oligo$(dA)_{20}$ and oligo$(dT)_{20}$, as shown in Figure.1 (c). CCRF-CEM cells labeled with PKH red were treated with oligo$(dA)_{20}$–PEG-lipids (oligo$(dA)_{20}$–PEG cells) and CCRF-CEM cells labeled with PKH green were treated with oligo$(dT)_{20}$–PEG-lipids (oligo$(dT)_{20}$–PEG-cells). Red oligo$(dA)_{20}$–PEG-cells and green oligo$(dT)_{20}$–PEG-cells were mixed at ratio of 1:1 and observed over time by a confocal laser scanning microscope (Figure.1 (c)). At 15 min after mixing, oligo$(dA)_{20}$–PEG cells (red) and oligo$(dT)_{20}$–PEG-cells (green) were attached to each other, with several cells attached in a linear fashion. At 60min, even more cells had attached to each other. At 3 h, the linear cell aggregates had gathered to form clumps of cells. At 6 h, the cellular clumps were still present in the culture medium. As a control experiment, PKH red- and PKH green-labeled cells with no oligoDNA–PEG-lipid treatment were mixed. These cells showed no attachment to each other (Figure.1 (e)). In addition, there was no self attachment between oligo$(dT)_{20}$–PEG-cells. These results clearly showed that the attachment of different cells could be induced by hybridization between oligo$(dA)_{20}$ DNA and oligo$(dT)_{20}$ DNA on the cell surfaces. The ratio of the number of attachments between oligo$(dA)_{20}$–PEG-cells and oligo$(dT)_{20}$–PEG-cells to the total number of attachments for all cells was approximately 1 at 15 and 60 min of incubation, indicating the alternating attachment of oligo$(dA)_{20}$–PEG-cells and oligo$(dT)_{20}$–PEG-cells. At 3 h, the ratio had decreased to approximately 0.6, indicating that larger aggregates of cells had formed. Cell–cell attachments could also be induced between oligo$(dA)_{20}$–PEG-lipid modified CCRF-CEM cells (red) and oligo$(dT)_{20}$–PEG-lipid modified GFP-HEK cells (green), as seen in

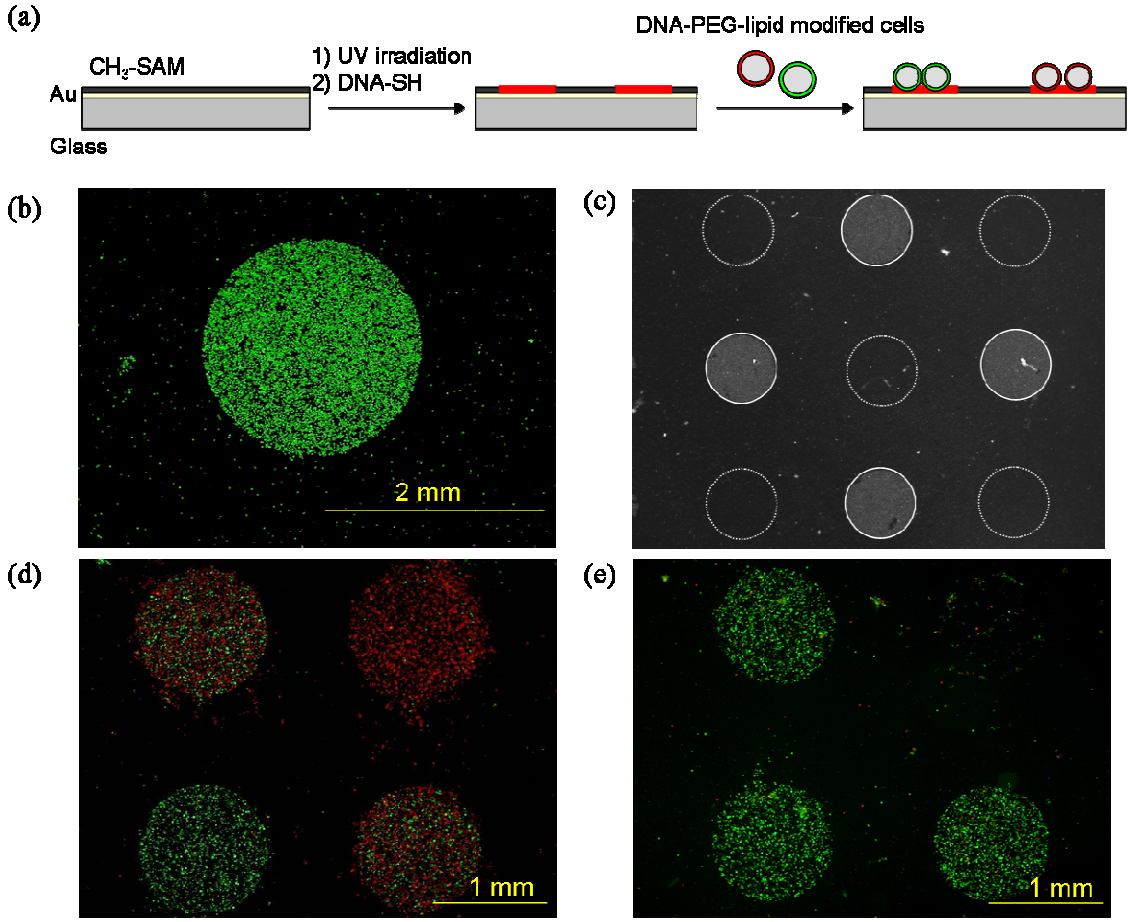

Figure.2 Immobilization of oligoDNA-PEG-lipid modified cells to a complementary oligoDNA' modified surface. (a): Scheme for preparation of DNA'-patterned substrate and immobilization of oligoDNA-PEG-lipid modified cells. (b): Immobilization of oligo$(dT)_{20}$-PEG-lipid modified CCRF-CEM cells labeled with PKH green to a single spot with immobilized oligo$(dA)_{20}$-SH. The spot on the substrate surface was observed using an upright fluorescence microscope. (c): Attachment of oligo$(dT)_{20}$-PEG-lipid modified CCRF-CEM cells to spots with immobilized oligo$(dA)_{20}$-SH (solid lines) and oligo$(dT)_{20}$-SH (dotted lines). The spots were observed using a stereomicroscope. (d): A mixture of SeqA-PEG-lipid modified CCRF-CEM cells and SeqB-PEG-lipid modified CCRF-CEM cells was incubated on DNA-immobilized spots where SeqA' (top right), SeqB' (bottom left), or a 1:1 mixture of SeqA' and SeqB' (top left and bottom right) were immobilized. (e): Inhibition assay for (d). A solution of SeqA'-SH was added to the mixture of SeqA-PEG-cells and SeqB-PEG-cells in advance and then the cells were incubated on the spots.

Figure.1 (d)). In contrast, no cell–cell attachments were observed between CCRF-CEM cells and GFP-HEK cells without oligoDNA–PEG-lipid modification (Figure.1 (e)). Thus, this method can be used to promote attachments between different kinds of cells.

Attachment of oligoDNA–PEG-cells to complementary DNA immobilized on a solid substrate

Glass plates with a thin layer of gold were modified with CH_3-SAM and irradiated with UV light through a photomask with an array of 1- or 2-mm transparent circular dots. After washing the plates to remove photodegradation products, a solution containing DNA-SH was spotted on the dots in order to immobilize DNA via the Au/thiol reaction (Figure.2 (a)). Oligo$(dT)_{20}$–PEG-cells labeled with PKH green were placed on the 2-mm spots where oligo$(dA)_{20}$ molecules were immobilized and incubated for 10 min. After removal of unattached cells by washing with HBSS, the surface was observed using an upright fluorescence microscope. As shown in Figure.2 (b), oligo$(dT)_{20}$–PEG-cells attached to the oligo$(dA)_{20}$-immobilized spot. Figure.2 (c) shows attachment of oligo$(dT)_{20}$–PEG-cells onto a substrate with oligo$(dA)_{20}$-SH and oligo$(dT)_{20}$-SH spots. After oligo$(dT)_{20}$–PEG-cells labeled with PKH green were applied and incubated for 10 min, and unattached cells were washed off with HBSS, the substrate was observed using a stereomicroscope (Figure.2 (c)). Oligo$(dT)_{20}$–PEG-cells selectively attached to the oligo(DA)20-immobilized spots, with practically no attachment of cells to the oligo$(dT)_{20}$-immobilized spots (dotted lines).

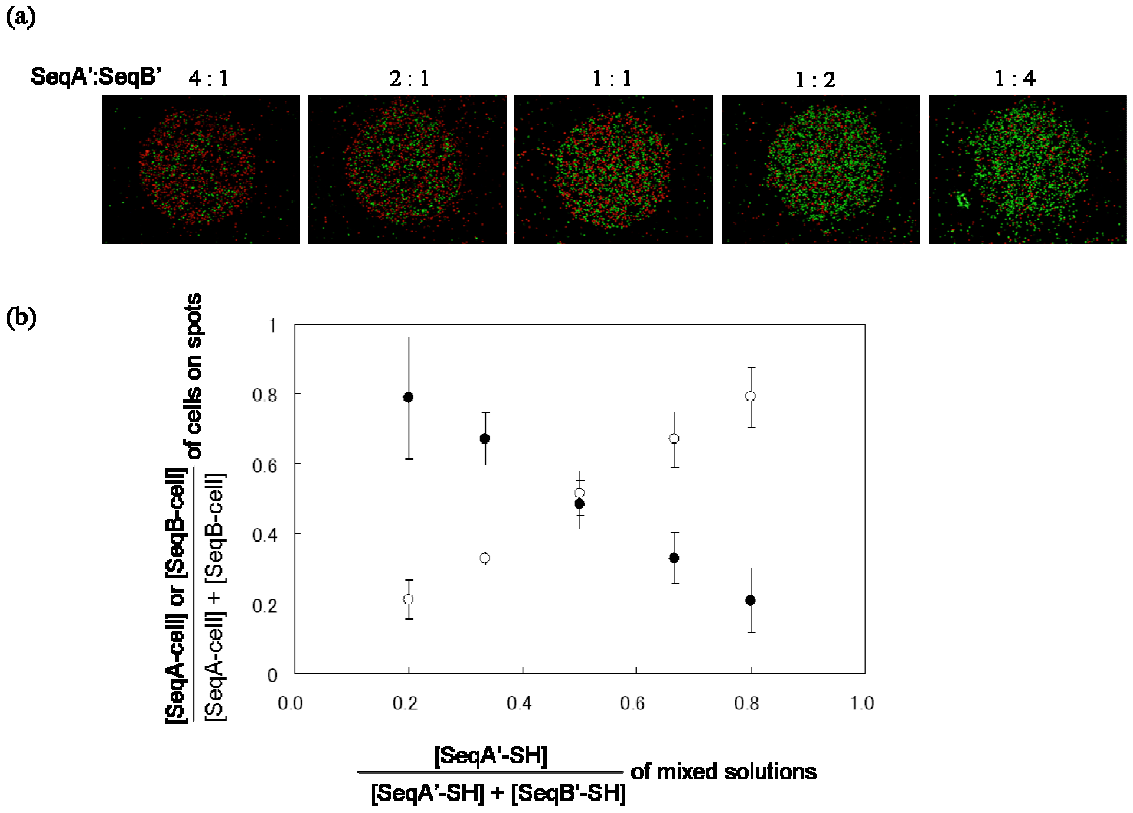

Figure.3 Varying the ratios of immobilized SeqA' and SeqB' DNA in spots on the substrate surface and the effect on cell attachment. A 1:1 mixture of SeqA-PEG-cells labeled with PKH red and SeqB-PEG-cells labeled with PKH green were applied to the spots. (a): The surface was observed using an upright fluorescence microscope. (b): The ratios of SeqA-PEG-cells (open circles) and SeqB-PEG-cells (closed circles) attached to each spot were determined from fluorescence images using ImageJ software. The composition of cells are plotted against the SeqA':SeqB' ratios in the spots.

These results showed that cells attached to the substrate through hybridization of DNA on the cell surface and on the substrate. Next, a similar array of spots with immobilized $SeqA_0$, $SeqB_0$, and a 1:1 mixture of $SeqA_0$:$SeqB_0$ were prepared. A 1:1 suspension of SeqA-PEG-cells labeled with PKH red and SeqB-PEG-cells labeled with PKH green was incubated on the spots for 10min. After removal of unattached cells with HBSS, the surface was observed using an

upright fluorescence microscope. Figure.2 (d) shows SeqA-PEG-cells and SeqB-PEG-cells attached to $SeqA_0$ and $SeqB_0$-immobilized spots, respectively, and both SeqA-PEG-cells and SeqB-PEG-cells attached to spots where a mixture of $SeqA_0$ and $SeqB_0$ was immobilized. To test whether this interaction could be inhibited, $SeqA_0$ was added to the mixture of SeqA-PEG-cells and SeqB-PEG-cells and the attachment of the cells to the substrate was examined. With the addition of $SeqA_0$, there was no attachment of SeqA-PEG-cells to the $SeqA_0$ spots, although SeqB-PEG-cells still attached to $SeqB_0$ spots (Figure.2 (e)). This inhibition assay indicated that cells were specifically attaching to the immobilized DNA via complementary DNA hybridization.

The effects on cell binding to different ratios of immobilized $SeqA_0$ and $SeqB_0$ on the substrate spots were examined. Five spots of immobilized DNA were prepared using the following molar ratios of $SeqA_0$:$SeqB_0$: 4:1, 2:1, 1:1, 1:2, 1:4. A 1:1 mixture of SeqA-PEG-cells labeled with PKH red and SeqB-PEG-cells labeled with PKH green was incubated on the spots, and unattached cells were removed by washing with HBSS. The substrate was observed using an upright fluorescence microscope (Figure.3 (a)). The number of cells that attached depended on the ratio of the complementary DNAs that were immobilized on the spots. The ratios of SeqA-PEG-cells to SeqB-PEG-cells attached to each spot were determined from fluorescence images using ImageJ software (open circles and closed circles in Figure.3 (b), respectively). The cell ratios correlated well with the mixture ratios of $SeqA_0$ and $SeqB_0$.

Next, the attachment of oligoDNA–PEG-cells to a pattern on the substrate was examined; the pattern was prepared by a contact printing method using a PDMS

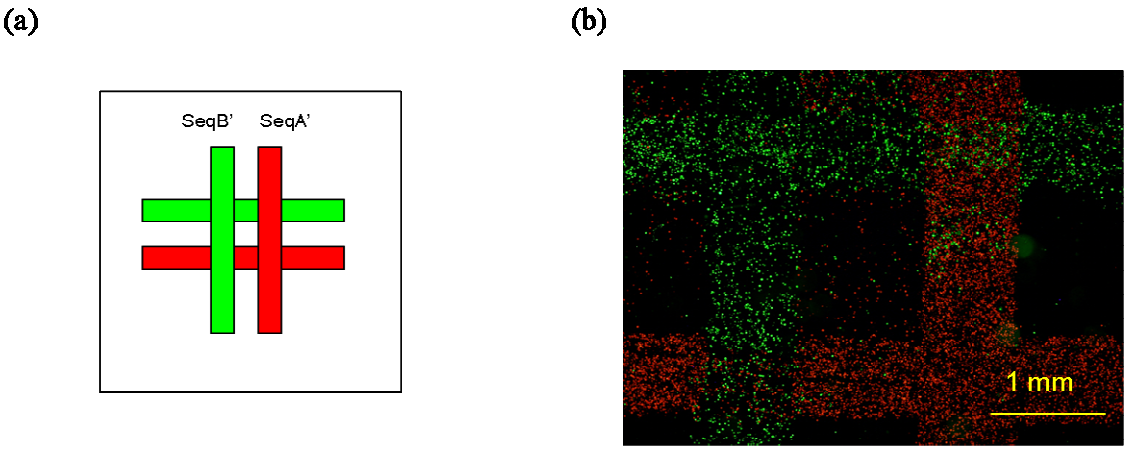

Figure.4 Immobilization of cells on a patterned substrate prepared by a contact printing method using a PDMS stamp. (a): SeqA'-SH and SeqB'-SH were immobilized (red and green lines, respectively) in the pattern shown here. (b): A 1:1 mixture of SeqA-PEG-lipid cells labeled with PKH red and SeqB-PEG-lipid cells labeled with PKH green was applied to the patterned substrate containing immobilized DNA. The substrate was observed using an upright fluorescence microscope.

stamp. As shown in Figure.4 (a), ledge surfaces on a PDMS stamp were coated with a solution of SeqA0 or SeqB0 DNA and pressed onto the gold surface. The same stamp was rotated 90° and again pressed to the surface, forming a cross pattern. A 1:1 mix of SeqA-PEG-cells and SeqB-PEG-cells was applied to the immobilized DNA, incubated, and washed with HBSS. Attached cells were observed using an upright fluorescence microscope. As shown in Figure.4 (b), SeqA-PEG-cells and SeqB-PEG-cells selectively attached to the stripes containing immobilized $SeqA_0$ or $SeqB_0$ DNA, respectively, demonstrating that cells could attach via DNA hybridization to a DNA pattern prepared using a contact printing technique.

3.4. Discussion

Cell surface modification is generally achieved three ways: by covalent conjugation to the amino groups of membrane proteins; by electrostatic interaction between cationic polymers and a negatively charged surface; and by incorporation of amphiphilic polymers into the lipid bilayer of the cell membrane by hydrophobic interactions [16]. It has been studied cell surface modification using amphiphilic polymers such as PEG-lipid derivatives that incorporate spontaneously into lipid bilayers [16,18]. Notably, this surface modification technique does not cause protein denaturation or have cytotoxic effects. Further, functional groups such as amino groups, maleimide, and biotin can be incorporated into the cell membrane using PEG-lipid derivatives bearing these groups [13–15].

In the present study, oligoDNA was introduced into the outer cell membrane using PEG-lipid. Cell–cell attachments between either the same types of cells or different types of cells were induced by incorporating complementary DNA sequences into two cell populations (Figure. 1); when mixed, the hybridization of the complementary sequences mediated cell–cell attachment. This DNA-hybridization technique was also used to attach DNA-modified cells to immobilized DNA on a substrate (Figure.2 and Figure.3). Anti-body–antigen reactions, cell-extracellular matrix interactions, and hydrophobic interactions with amphiphilic polymers have all been used to immobilize cells on surfaces [20–22]. Using these techniques, cell suspensions must be applied to each spot to prepare arrays of cells. Not only is this a tedious and time-consuming process, cell viability is lost during the preparation of the array. In contrast, the technique

described here is quite simple, since a suspension of cells with different DNA sequences can be applied to surfaces that have spots of immobilized complementary DNA sequences. Thus, this technique can be used for preparation of cell-based arrays for many types of studies.

To our knowledge, there are few previous studies that have achieved cell–cell attachment between different kinds of cells. It was previously reported the immobilization of living cells to the surface of islets of Langerhans for microencapsulation using PEG-lipids and the biotin/streptavidin reaction [19]. It is also possible to attach feeder cells to embryoid bodies for the analysis of differentiation of ES cells into neurons [Iwata et al., unpublished report]. The simple and versatile methods described here have many applications in both regenerative medicine and in tissue engineering.

3. 5. References

[1] G. Keller, H.R. Snodgrass, Human embryonic stem cells: the future is now, Nat Med. 5 (1999) 151–152.

[2] K. Takahashi, K. Tanabe, M. Ohnuki, M. Narita, T. Ichisaka, K. Tomoda, S.Yamanaka, Induction of pluripotent stem cells from adult human fibroblasts by defined factors. Cellule 131 (2007) 861–872.

[3] K. Takahashi, S. Yamanaka, Induction of pluripotent stem cells from mouse embryonic and adult fibroblast cultures by defined factors. Cell 126 (2006) 663–676.

[4] M. Lohr, A. Hoffmeyer, J. Kroger, M. Freund, J. Hain, A. Holle, P. Karle, W.T. Knöfel, S. Liebe, P. Müller, H. Nizze, M. Renner, R.M. Saller, T. Wagner, K. Hauenstein, W.H. Günzburg, B. Salmons, Microencapsulated cell-mediated treatment of inoperable pancreatic carcinoma. Lancet 357 (2001) 1591–1592.

[5] K.C. Wollert, H. Drexler, Cell-based therapy for heart failure. Curr. Opin. Cardiol. 21 (2006) 234–239.

[6] T. Visted, R. Bjerkvig, P.O. Enger, Cell encapsulation technology as a therapeutic strategy for CNS malignancies. Neuro. Oncol. 3 (2001) 201–210.

[7] S. Prakash, T.M. Chang, Microencapsulated genetically engineered live E. coli DH5 cells administered orally to maintain normal plasma urea level in uremic rats. Nat. Med. 2 (1996) 883–887.

[8] M.S. Shoichet, S.R. Winn, Cell delivery to the central nervous system. Adv. Drug. Deliv. Rev. 42 (2000) 81–102.

[9] D.F. Emerich, D.R. Winn, Immunoisolation cell therapy for CNS diseases. Crit. Rev. Ther. Drug. Carrier. Syst. 18 (2001) 265–298.

[10] S. Hao, L. Su, X. Guo, T. Moyana, J. Xiang, A novel approach to tumor suppression using microencapsulated engineered J558/TNF-alpha cells. Exp. Oncol. 27 (2005) 56–60.

[11] M.K. Lee, Y.H. Bae, Cell transplantation for endocrine disorders. Adv. Drug. Deliv. Rev. 42 (2000) 103–120.

[12] H. Matsumura, T. Tada, Cell fusion-mediated nuclear reprogramming of somatic cells. Reprod. Biomed. Online. 16 (2008) 51–56.

[13] S. Miura, Y. Teramura, H. Iwata, Encapsulation of islets with ultra-thin polyion complex membrane through poly(ethylene glycol)-phospholipids anchored to cell membrane. Biomaterials 27 (2006) 5828–5835.

[14] Y. Teramura, Y. Kaneda, H. Iwata, Islet-encapsulation in ultra-thin layer-by-layer membranes of poly(vinyl alcohol) anchored to poly(ethylene glycol)-lipids in the cell membrane. Biomaterials 28 (2007) 4818–4825.

[15] Y. Teramura, H. Iwata, Islets surface modification prevents blood-mediated inflammatory responses. Bioconjugate Chem. 19 (2008) 1389–1395.

[16] Y. Teramura, Y. Kaneda, T. Totani, H. Iwata, Behavior of synthetic polymers immobilized on cell membrane. Biomaterials 29 (2008) 1345–1355.

[17] T. Totani, Y. Teramura, H. Iwata, Immobilization of urokinase to islet surface by amphiphilic poly (vinyl alcohol) carrying alkyl side chains. Biomaterials 29 (2008) 2878–2883.

[18] Y. Teramura, H. Iwata, Surface modification of islets with PEG-lipid for improvement of graft survival in intraportal transplantation. Transplantation 88 (2009) 624–630.

[19] Y. Teramura, H. Iwata, Islet encapsulation with living cells for improvement of biocompatibility. Biomaterials 30 (2009) 2270–2275.

[20] K. Kato, K. Umezawa, M. Miyake, J. Miyake, T. Nagamune, Transfection microarray of nonadherent cells on an oleyl poly(ethylene glycol) ether-modified glass slide. Biotechniques 37 (2004) 444–448.

[21] I.K. Ko, K. Kato, H. Iwata, A thin carboxymethyl cellulose culture substrate for the cellulase-induced harvesting of an endothelial cell sheet. J .Biomater. Sci. Polym. Ed. 16 (2005) 1277–1291.

[22] K. Kato, K. Umezawa, D.P. Funeriu, M. Miyake, J. Miyake, T. Nagamune, Immobilized culture of nonadherent cells on an oleyl poly(ethylene glycol) ether-modified surface. (2003)35 Biotechniques 1014–1018. 1020–1021.

Chapter 4

Kinetic analysis of disulfide formation between thiol groups attached to linear poly(acrylamide)

4. 1. Introduction

Hydrogels are polymeric materials, which are formed by three dimensionally crosslinked polymer chains through chemical bonds and/or physical bonds and contain water as an extender. They have been used for various biomedical devices, such as contact lenses, drug delivery systems, scaffolds in tissue engineering, etc. However, some difficulties still remain in the preparation of suitable hydrogels for specific applications. In addition, chemical reactions used to crosslink polymer chains have destructive effects on living cells. Hydrogels are not still well characterized, because they are insoluble substances with few crosslinked points for gel formation. Our group has been working on development of a bioartificial pancreas in which islets of Langerhans (islets) are enclosed in various synthetic polymer hydrogels [1–5]. The hydrogels act as semipermeable membranes, which are expected to protect islets from attacks by the host immune system. The density of crosslinked points and their distribution determine permeability of oxygen and nutrients, which are required for survival of islets and also restrict access of antibodies and complement proteins that are harmful to islets. The mechanical properties of hydrogels, which are determined by the chemical characteristics of the main chains, the crosslinked bonds, and

the chain length between crosslinked points, exert large effects on tissue reactions and on the long term fate of the devices. Although crosslinkages can be controlled well, the characterization of chemical reactions are quite limited, which is important for enclosure of living cells and tissues.

In this chapter, detailed kinetic analysis were carried out on disulfide formation between thiol groups hanging from poly(acrylamide-*co*-*N*-acrylcysteamine) (P-SH) as side chains. As schematically shown in Scheme 1, P-SHs were prepared following the method previously reported [3]. Acrylamide and *N,N'-bis*-acrylcystamine (BAC) were copolymerized,and the copolymers obtained were reduced to linear P-SHs. Hydrogels were prepared through formation of crosslinkages between pendant thiol groups on the P-SH polymer chains. Detailed kinetic analysis were carried out by determining thiol concentrations in reaction mixtures.

4. 2. Materials and methods

Materials

Chemicals and their sources are the following; cysteamine dihydrochloride and 3,3'-dithiodipropionic acid from Aldrich Chemical, (Milwaukee, WI); acryloyl chloride, acrylamide, dithiothreitol (DTT), oxidized glutathione (GSSG), glutathione (GSH), and *o*-phthalaldehyde from Wako Pure Chemical Industries (Osaka, Japan); *N,N,N',N'*-tetramethylethylenediamine (TEMED), ammonium peroxodisulfate, 5,5'-dithio-*bis*(2-nitrobenzoic acid) (DTNB), cysteamine

hydrochloride and 2-hydroxyethyl disulfide from Nacalai Tesque (Kyoto, Japan). β-Nicotinamide adenine dinucleotide phosphate reduced form, (NADPH) and GSH reductase from Oriental Yeast (Tokyo, Japan).

Synthesis of Poly(acrylamide-co-N-acrylcysteamine)

The *N,N'*-BAC (bifunctional crosslinker monomer) was synthesized following the method reported by Hansen [6]. To purify BAC by recrystallization, it was dissolved in a minimum amount of chloroform at 50°C, and then cooled slowly to room temperature. Crystals were collected by filtration (49.9% yield). A solution (10%, w/v) containing acrylamide and BAC (44:1 and 22:1, by molar ratio) in distilled water was prepared. Copolymerization was carried out by adding TEMED (5.6%, w/v) and ammonium peroxodisulfate (0.08%, w/v) to a monomer solution at 60°C [7]. The obtained gel was crushed into small pieces and washed with phosphate buffer (0.1 M, pH 7.4) and then distilled water. The gel was solubilized by adding DTT in a proportion of 5 mol/mol of *N,N'-bis*-acryl-cysteamine. After adjusting the pH of the solubilized sol solution to 3, the polymer solution was poured into a large amount of methanol solution under a nitrogen atmosphere to collect the linear P-SH. This copolymer was dried and then stored *in vacuo* until use. In this article, the P-SH copolymers prepared from the acrylamide and BAC at 44:1 and 22:1 by molar ratio are expressed as P-SH44 and P-SH22, respectively. *N,N'-bis*-Acrylcystamine in copolymers was identified by ^{1}H NMR spectra (JNM-PMX60SI; JEOL, Tokyo, Japan) and elemental analysis [3].

The thiol content of P-SH copolymers was determined by the Ellman method

[10]. Briefly, P-SH was dissolved in distilled water at pH 3 (1.0%, w/v). An aliquot of the acidic solution of P-SH (20 μL of P-SH22 or 50 μL of P-SH44 aqueous solution) was added to DTNB solution (0.2 mL of a 1-mM solution prepared in 0.1 M phosphate buffer, pH 7.4). After 10 min incubation, the absorbance of the solution was measured at 412 nm using a 1-cm cuvette. The thiol concentration was determined using the extinction coefficient of 13,600 M^{-1} cm^{-1}. The average molecular weight of P-SHs was determined by gel permeation liquid chromatography (GPC), referring to a calibration curve of standard polyethylene glycols (Tosoh, Tokyo, Japan). Gel permeation liquid chromatography was performed for P-SHs using a series of columns of G6000PWXL and G3000PWXL (Tosoh, Tokyo, Japan) after the reduction of copolymers in phosphate buffer (0.2 M, pH 6.8) containing DTT (8.5 mg mL^{-1}).

Oxidation of P-SH by Oxygen

P-SH was dissolved in distilled water at pH 3 ([P-SH] = 10%, w/v). This solution was diluted using dilute hydrochloric acid solution, or phosphate buffer (pH 7), or Tris-HCl buffer solution (0.25 M, pH 9) to prepare the reaction mixture with different pH values. The P-SH solutions were incubated at 25°C with stirring. To evaluate the effects of dissolved oxygen in the reaction mixture on the oxidation rate of thiol groups, oxygen was continuously supplied to the reaction mixture by bubbling oxygen gas. An aliquot (20 μL) of the P-SH solution was withdrawn to determine thiol concentrations by the Ellman method as mentioned above.

Thiol-Disulfide Exchange between P-SH and GSSG

P-SH was dissolved in water ([SH] = 20 mM) and adjusted to pH 3 with dilute hydrochloric acid solution under a nitrogen atmosphere. GSSG (1 mM) was prepared in phosphate buffer (0.1 M, pH 7.4). The P-SH solution (4 mL) was added to GSSG solution (36 mL) at 37°C under a nitrogen atmosphere to start the reaction. Aliquots of the reaction mixture (1.8 mL) were taken out over time and mixed with metaphosphoric acid (10%, 0.3 mL) to stop the reaction.

Total Thiol

The sample (100 μL) was diluted with phosphate buffer (2.65 mL, 0.05 M, pH 7.4), and then DTNB solution (0.25 mL, 1 mM) was added. Total thiol concentration was determined from the absorbance at 412 nm as described above.

GSH

The sample was filtered using Ultracent-10 devices (TOSOH, Tokyo, Japan) for 30 min. The ultrafiltrate (50 μL) was mixed with phosphate buffer (4.9 mL, 0.1 M, pH 7.4) containing 0.01% *o*-phthalaldehyde [9].

After incubation for 30 min at 25°C, the fluorescence emission intensity (λ_{ex}: 350 nm, λ_{em}: 420 nm) was measured.

GSSG

The sample (100 μL) was diluted with phosphate buffer (1.5 mL, 0.1 M, pH 6.0). Solutions of NADPH (100 μL, 5 mg mL^{-1}) and GSH reductase (100 μL, 2

unit mL^{-1}) were added to the sample solution and incubated at 37°C for 30 min. Metaphosphoric acid solution (50 μL, 10%) was added to inactivate the reductase after cooling to 25°C. Phosphate buffer (3.75 mL, 0.125 M, pH 7.4) and DTNB solution (0.25 mL, 1 mM) were added. The absorbance was measured at 412 nm after incubation for 10 min. The concentration of GSSG was calculated from the difference between values with and without the reductase treatment.

Gelation of P-SH Solution by Thiol-Disulfide Exchange Reaction

Gelation was induced by a thiol-disulfide exchange reaction between P-SH and GSSG. P-SH was dissolved at 10%, w/v, into the phosphate-buffered solution adjusted to pH 3 by HCl. P-SH solution (0.5 mL) was pipetted into a glass test tube provided with a magnetic stirring bar, followed by incubation at 37 °C. The solution in the glass test tube was adjusted to pH 7.4 with 1N NaOH solution, and then GSSG solution was added to initiate the thiol-disulfide exchange reaction. The final concentrations of GSSG in the reaction mixtures were 1, 5, 10, and 50 mM. The time required until the magnetic bar stopped stirring was recorded as the gelation time of the mixed solutions.

4. 3. Results

Synthesis of Poly(acrylamide-co-N-acrylcysteamine)

N,N'-*bis*-Acrylcystamine was copolymerized with acrylamide by radical

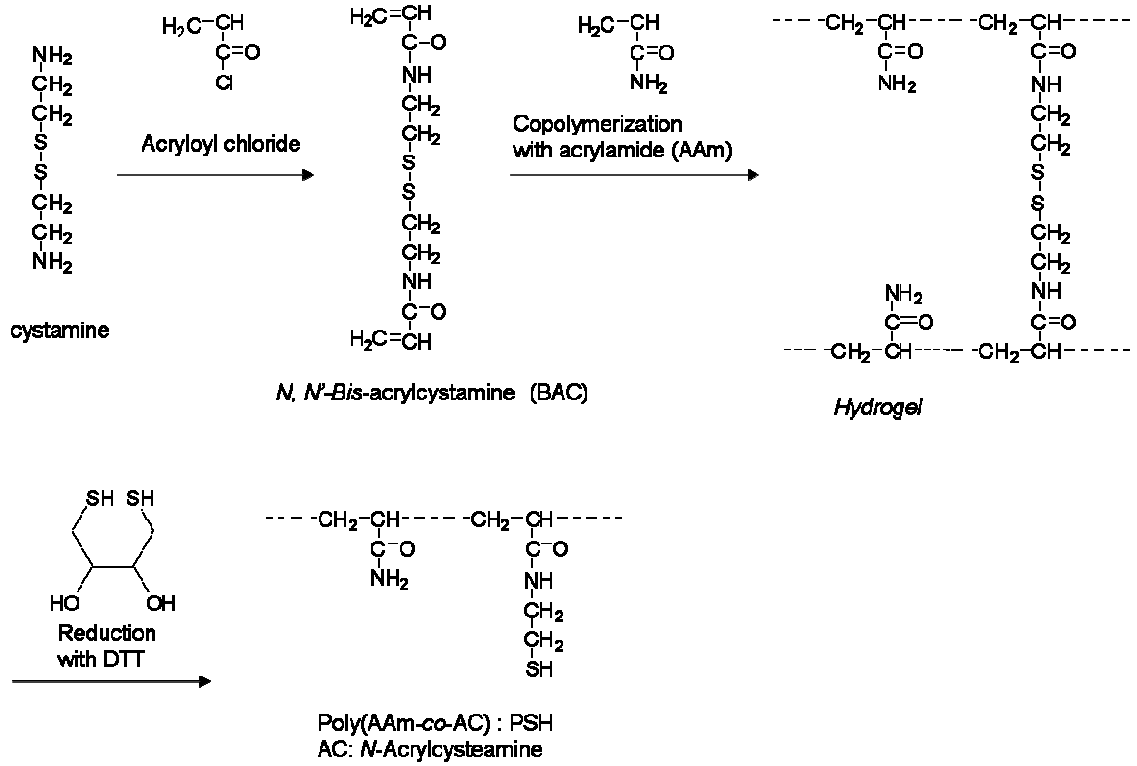

Scheme.1 Synthesis of poly(acrylamide-co-N-acrylcysteamine)

polymerization using ammonium peroxodisulfate and TEMED as a redox initiator, resulting in a hydrogel (Scheme 1). The hydrogel could be solubilized by reduction of disulfide bonds using DTT. The reaction mixture was poured into acidic methanol (pH = 3) to obtain a linear P-SH, because the rate of air oxidation of thiols to disulfides is very slow in acidic solution. The resulting P-SH precipitate could be dissolved in water even after drying and storage *in vacuo*.

The characteristics of the obtained P-SHs are listed in Table 1. *N*-Acrylcysteamine incorporated into the P-SH was linearly proportional to BAC/monomer ratios in the monomer solutions used for copolymerization. According to the GPC measurements, the weight average molecular weights of P-SH22 and P-SH44 were almost the same, approximately 1.0×10^6.

Table.1 Molecular Weight and thiol Content of Poly(acrylamide-*co*-*N*-acrylcysteamine)s.

Copolymer	AAm:BAC (mol:mol)	SH content ($x10^{-3}$ mol/g)		Mn	Mw	Mw/Mn
		Calculated	Observed	$x10^5$	$x10^5$	
P-SH22	22:1	1.10	1.12	2.09	10.0	4.78
P-SH44	44:1	0.590	0.615	2.93	10.4	3.55

Auto-oxidation of Pendant Thiol Groups

Pendant thiol groups of P-SH are expected to be oxidized by oxygen dissolved in its solution, resulting in disulfide bond formation as

$$2\text{P-SH} + 1/2\text{O}_2 \rightarrow \text{P-SS-P} + \text{H}_2\text{O}$$

The reaction can be deconstructed into the following reactions [10].

$$\text{P-SH} + \text{OH}^- \leftrightarrow \text{P-S}^- + \text{H}_2\text{O}$$

$$\text{P-S}^- + \cdot\text{O}_2\cdot \rightarrow \text{P-S}\cdot + \cdot\text{O}_2^-$$

$$\text{P-S}\cdot + \cdot\text{O}_2^- \rightarrow \text{P-S}\cdot + \cdot\text{O}_2^{-2}$$

$$2\text{P-S}\cdot \rightarrow \text{P-SS-P}$$

$$\text{O}_2^{-2} + \text{H}_2\text{O} \rightarrow 2\text{OH}^- + 1/2\text{O}_2$$

The thiol radicals, P-S$\cdot$, couple with each other and form a disulfide crosslinkage. It has been accepted that the rate determining step is a reaction of the anion ($P\text{-}S^-$) with oxygen [11]. The anion ($P\text{-}S^-$) concentration is linearly proportional to the thiol concentration [SH] due to the equilibrium between P-SH and $P\text{-}S^-$. Thus, the rate of oxidation follows first-order kinetics with respect to [SH]. The rate of thiol disappearance under the constant oxygen concentration can be expressed by

$$-\frac{d[\mathrm{SH}]}{dt} = k[\mathrm{SH}] \qquad (1)$$

$$\ln\frac{[\mathrm{SH}]}{[\mathrm{SH}]_0} = -kt \qquad (2)$$

where $[SH]_0$ and [SH] are thiol concentrations at times 0 and t, respectively, and k is a reaction rate constant of the oxidation reaction. Concentrations of pendant thiol groups, [SH], were determined by the DTNB method. Changes of thiol group concentrations were plotted against reaction time using eq 2 in Figure.1 and Figure.2. The rate of auto-oxidation of the thiol groups was dependent on pH (Figure.1). A decrease in thiol group concentration was not observed at pH 3 during 6-h observation, but when the pH was increased to 7.4 and 9.0, the concentration of free thiols decreased more rapidly. Figure.2 (a) and (b) shows

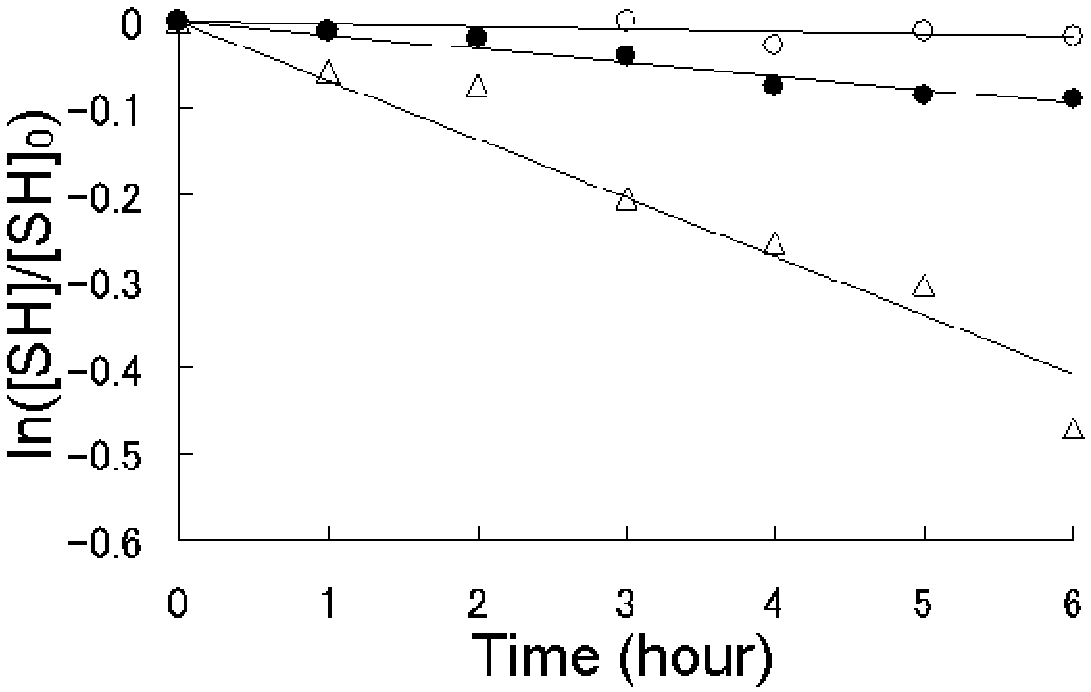

Figure. 1 Effect of solution pH on auto-oxidation rates of thiol groups in P-SH44 at 25 °C. Lines in the figure were derived from linear regression analysis of experimental points using the least-squares method. [P-SH44] = 1% (w/v); (○): pH 3; (●): pH 7; (Δ): pH 9.

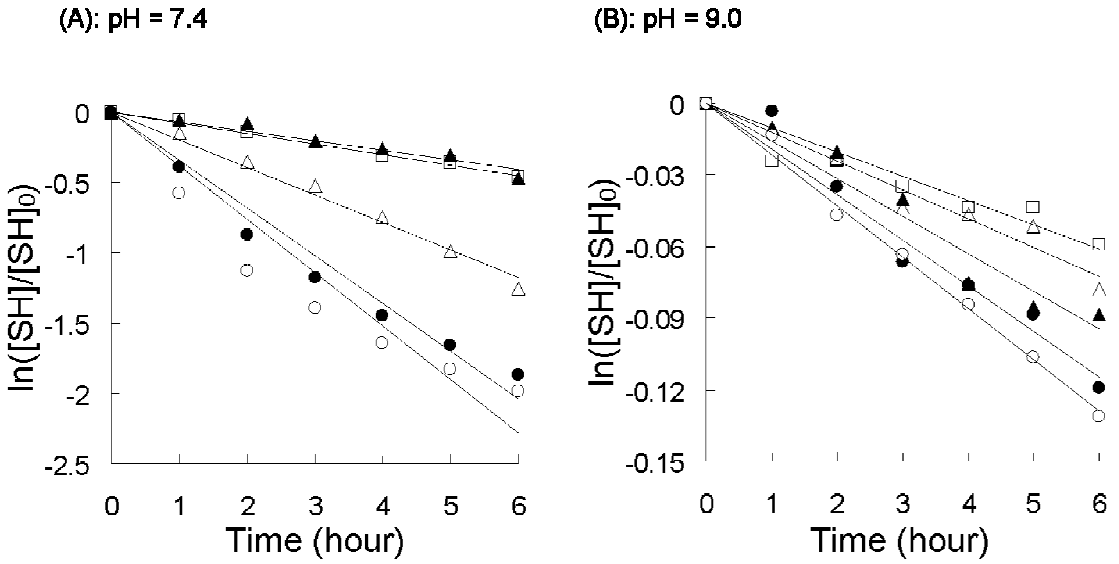

Figure.2 Effect of polymer P-SH44 concentrations on auto-oxidation rates at pH 7.4 and pH 9 at 25 °C. Lines in the figure were derived from the linear regression analysis of experimental points using the least-squares method. Figure key: (○): 0.05%; (●): 0.1%; (Δ): 0.5%; (▲): 1%; (□): 2%.

analysis of decreases of thiol group concentrations at different polymer concentrations at pH 7.4 and 9.0 using eq 2. The first-order reaction rate constants determined from the slope of these plots (Figure.2), increased sharply with decreasing levels of the polymer P-SH, at concentrations less than 0.55%, w/v. At pH 9, the rate constant at 0.05%, w/v, was about eight times greater than that at 2%, w/v (Figure.3).

As indicated above, a half mole of molecular oxygen is required for conversion of two moles of thiol groups to 1 mole of disulfide compound. Oxygen in the reaction mixture is consumed in advance of the reaction. For example, the thiol group concentrations in 0.5% PH-44 solution and the oxygen concentration in water at 25°C equilibrated with air are 2.9 and 0.25 μmol mL^{-1} , respectively. Thus, the apparent reaction rate constant is expected to decrease with

increasing P-SH concentration due to insufficient oxygen supply. To demonstrate the effect of oxygen consumption on the reaction rate, oxygen was bubbled into reaction mixtures and the reaction rate constants were determined. With oxygen bubbling, the rate constant increased by about twofold (Figure.3). Even under oxygen bubbling, the rate constant in 0.05%, w/v, P-SH solution was about 2.5 times higher than that in the 0.5%, w/v, P-SH solution. The great dependence of the rate constants on polymer concentration in dilute solutions could not simply be explained by oxygen consumption in the reaction mixtures.

Thiol-Disulfide Exchange Between P-SH and Oxidized Glutathione

Thiol-disulfide exchange spontaneously occurs when thiol and disulfide compounds coexist in a reaction mixture. Disulfide crosslinkages between P-SH can be induced by the thiol-disulfide exchange reaction. In this chapter, GSSG was used as a disulfide compound. Two thiol-disulfide exchange reactions are

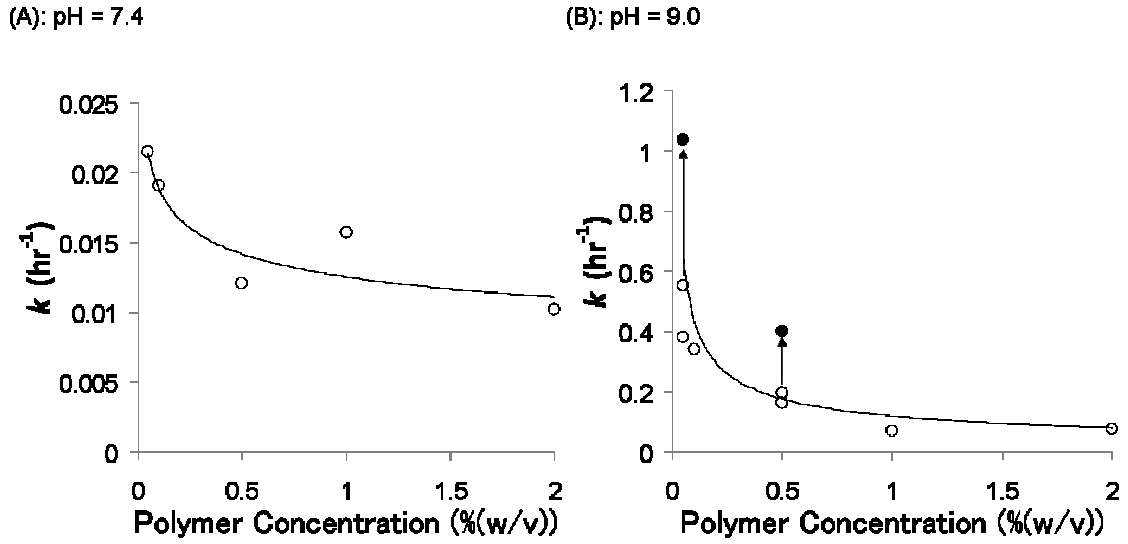

Figure.3 Dependence of rate constants for the auto-oxidation of thiol to disulfide on the polymer concentrations of P-SH44 at pH 9 and 25 °C. Figure key: (○): without oxygen bubbling; (●): with oxygen bubbling.

expressed by

$$\text{P - SH} + \text{GSSG} \underset{k_2}{\overset{k_1}{\rightleftarrows}} \text{P - SS - G} + \text{GSH}$$

$$\text{P - SH} + \text{P - SS - G} \underset{k_4}{\overset{k_3}{\rightleftarrows}} \text{P - SS - P} + \text{GSH}$$

Equilibrium constants K_1 and K_2 of the two reactions are expressed by

$$K_1 = k_1/k_2 \quad \text{and} \quad K_2 = k_3/k_4$$

Kinetic analysis of these reactions was conducted. Total thiol concentrations in the reaction mixtures were determined by the DTNB method (see Materials and Methods). The concentrations of reduced form of glutathione [GSH] were estimated from the free thiol concentration in the ultrafiltrate of the reaction mixture. The concentrations of thiol groups on the polymer, (P-SH), are expressed by

$$[\text{P - SH}] = [\text{Total thiol}] - [\text{GSH}]$$

The concentration of the oxidized form of glutathione [GSSG] is equal to the half of the difference between total thiol concentration in the ultrafiltrate of the reaction mixture before and after the reduction of GSSG by glutathione reductase, [GSH] and $[GSH]_r$, respectively.

$$[\mathrm{G\text{-}SS\text{-}G}] = \frac{1}{2}([\mathrm{GSH}]_r - [\mathrm{GSH}])$$

The concentrations of heterodisulfide, [P-SS-G], and homodisulfide, [P-SS-P], can be calculated from [GSSG], [GSH], and [P-SH] using the respective equations

$$[\mathrm{P\text{-}SS\text{-}G}] = 2([\mathrm{GSSG}]_0 - [\mathrm{GSSG}]) - [\mathrm{GSH}]$$

$$[\mathrm{P\text{-}SS\text{-}P}] = ([\mathrm{P\text{-}SH}]_0 - [\mathrm{P\text{-}SH}] - [\mathrm{P\text{-}SS\text{-}G}])/2$$

where [P-SS-G] and [P-SS-P] are concentrations of each substance and the suffix 0 denotes the initial concentration.

Figure.4 shows the concentration changes of each substance during the reaction between P-SH44 and GSSG over time. The differential equations for the changes in the concentrations with time of the individual substances are as follows:

$$-d[\mathrm{P\text{-}SH}]/dt = k_1[\mathrm{P\text{-}SH}][\mathrm{GSSG}] - k_2[\mathrm{P\text{-}SS\text{-}G}][\mathrm{GSH}] + k_3[\mathrm{P\text{-}SH}][\mathrm{P\text{-}SS\text{-}G}] - k_4[\mathrm{P\text{-}SS\text{-}P}][\mathrm{GSH}] \quad (3)$$

$$-d[\mathrm{GSSG}]/dt = k_1[\mathrm{P\text{-}SH}][\mathrm{GSSG}] - k_2[\mathrm{P\text{-}SS\text{-}G}][\mathrm{GSH}] \quad (4)$$

$$-d[\mathrm{P\text{-}SS\text{-}G}]/dt = -k_1[\mathrm{P\text{-}SH}][\mathrm{GSSG}] + k_2[\mathrm{P\text{-}SS\text{-}G}][\mathrm{GSH}] + k_3[\mathrm{P\text{-}SH}][\mathrm{P\text{-}SS\text{-}G}] - k_4[\mathrm{P\text{-}SS\text{-}P}][\mathrm{GSH}] \quad (5)$$

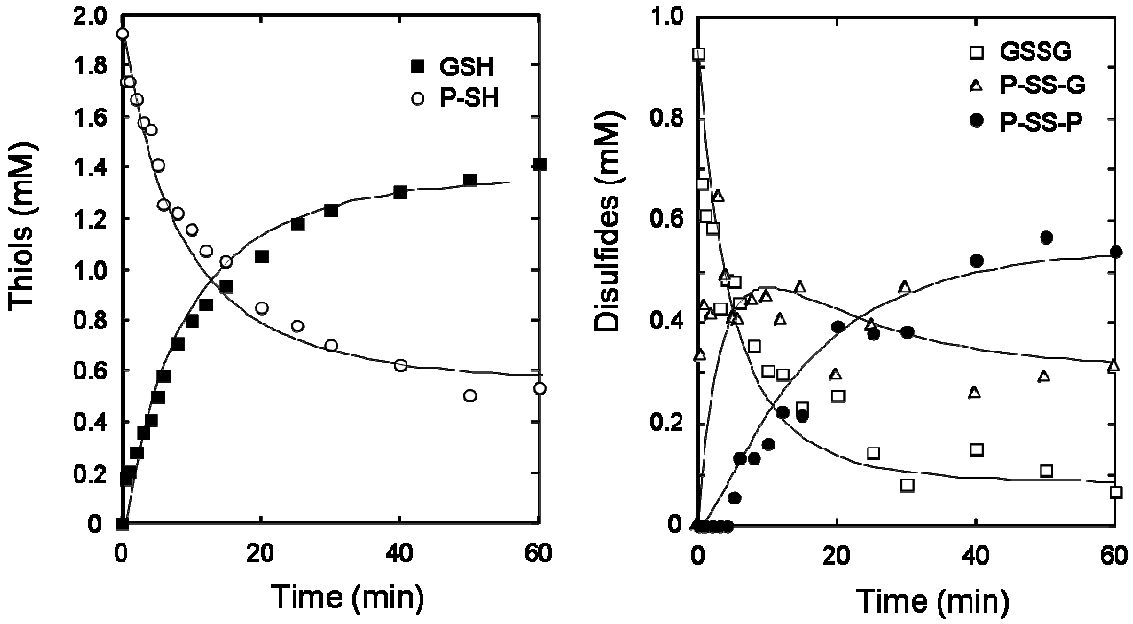

Figure.4 The change in the concentrations of each component (P-SH, GSH, GSSG, P-SS-G, P-SS-P) with time during the thiol-disulfide exchange reaction between P-SH44 and GSSG at pH 7.4 and 37 °C. P-SH44, 0.325, w/v, k_1 = 1.67 $Lmol^{-1}h^{-1}$, k_2 = 0.208 $Lmol^{-1}h^{-1}$, k_3 = 0.833 $Lmol^{-1}h^{-1}$ and k_4 = 0.173 $Lmol^{-1}h^{-1}$. $K_1 = k_1/k_2 = 8.0$, $K_2 = k_3/k_4 = 4.8$.

$$-d[\mathrm{P-SS-P}]/dt = -k_3[\mathrm{P-SH}][\mathrm{P-SS-G}] + k_4[\mathrm{P-SS-P}][\mathrm{GSH}] \qquad (6)$$

These equations cannot be analytically solved. The concentration changes with time were numerically analyzed using Mathematica®. The solid lines in Figure.4 show the concentration changes of each substance calculated using fixed parameters for k_1 = 100, k_2 = 12.5, k_3 = 50.0, and k_4 = 10.4 $M^{-1}s^{-1}$. The calculated values reproduce well the experimentally determined concentration changes of the substances with time. [P-SH] and [GSSG] decreased, whereas [GSH] increased with time simultaneously. The concentration of mixed disulfide, [P-SS-G] reached a maximum and then decreased to an equilibrium concentration. A short lag period was observed in the change of [P-SS-P]. When

the initial molar ratio of $[P\text{-}SH]_0$ to [GSSG]0 was 2, ~60% of thiol groups on polymer, P-SH, was converted to disulfide, P-SS-P, after the reaction reached equilibrium. In the combination of P-SH and GSSG, the equilibrium shifted to the formation of the disulfide linkage. The equilibrium constants, $K_1 = k_1/k_2$ and $K_2 = k_3/k_4$ obtained from these kinetic studies are listed in Table 2.

Table.2 Equilibrium Constants for the Thiol-disulfide Exchange Reaction in pH 7.4 at 37 ^{o}C.

Components	P-SH(% (w/v))	K_1	K_2
P-SH22 + GSSG	0.17	9.3	4.2
P-SH44 + GSSG	0.32	8.0	4.8

Gelation time of P-SH solution

As expected from the kinetic analysis of auto-oxidation of P-SH, the gelation time of the P-SH solution was highly dependent on the solution pH. No gel formation was observed at pH 3 even after 24 h incubation. The gelation time became shorter as the pH increased. The gelation time of P-SH (10%, w/v, was 24 h at pH 7.4 and 6 h at pH 8.8. On the other hand, when GSSG was added to a P-SH solution, the gelation of the P-SH solution was immediately induced due to intermolecular disulfide bond formation between P-SH through the thiol-disulfide exchange. The gelation times of P-SH22 and P-SH44 are summarized in Table 3. With an increase of the fed concentration of GSSG, the gelation time became dramatically shorter. In the case of P-SH22, the gelation time decreased from 4 x 10^4 sec at 1 mM GSSG to 4 sec with 50 mM GSSG. Similarly, for P-SH44, the gelation time in the presence of 50 mM GSSG was 5000 times more rapid than with 1 mM GSSG. These results indicated that the

gelation reaction proceeded by the thiol-disulfide exchange reaction to form intermolecular disulfide bonds without consumption of oxygen at higher concentration of GSSG.

4. 4. Discussion

The rate constants of the thiol oxidation (Figure.3) were obtained under the assumption that the oxidation rate follows first order kinetics with respect to the thiol concentration [10]. Although the rate constants should be independent of the thiol concentrations, their magnitude decreased with increasing thiol concentrations, that is, the polymer concentrations. First it was expected that the decrease of the rate constant in higher thiol concentrations could be explained by insufficient oxygen supply. Even when oxygen bubbling provided an unlimited supply of oxygen, however, the rate constants decreased with increasing the thiol concentration. Thus, the dependence of the rate constants on the thiol concentration could not be explained by oxygen consumption in the reaction mixtures. In our previous study [12], it was found that the rate constants of acetalization of poly(vinyl alcohol) carrying an aldehyde group at a chain end sharply increased with decreasing polymer concentration. This phenomenon can be explained by the second order reaction between -OH and –CHO and taking into account the intramolecular reaction. It was expected that dependence of the rate constants on the thiol concentration can be explained by taking an intramolecular reaction into consideration [12, 13].

The thiol oxidation under the assumption was analyzed that the reaction is

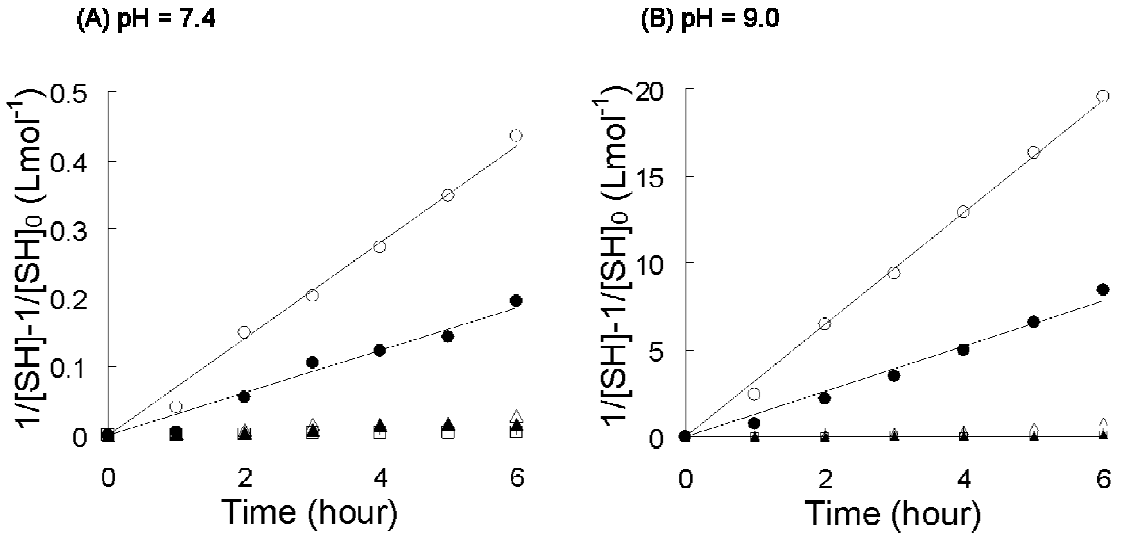

Figure.5 Thiol concentration changes plotted with Eq. (8) under the assumption that the reaction follows second order kinetics with respect to the thiol concentration. Lines in the figure were determined by the linear regression analysis of experimental points using the least-squares method. Measurements were conducted at pH 7.4 and pH 9 at 25 °C. Figure key: (○): 0.05%; (●): 0.1%; (Δ): 0.5%; (▲): 1%; and (□): 2%.

second order relative to the thiol concentration. The oxidation rate of thiol groups is expressed by

$$-\frac{d[\mathrm{SH}]}{dt} = k'[\mathrm{SH}]^2 \qquad (7)$$

$$\frac{1}{[SH]} - \frac{1}{[SH]_0} = k't \qquad (8)$$

where $[SH]_0$ and [SH] are thiol concentrations at time 0 and *t*, respectively and *k′* is the apparent second order reaction rate constant of the oxidation reaction. Changes of thiol group concentrations were plotted against the reaction times using Eq. (8) (Figure.5). The data followed Eq. (8) much better than Eq. (2). Reaction rate constants, *k′*, were obtained from these plots. The rate constant, *k′*,

in the 0.05%, w/v, solution was several hundred times higher than that in 2%, w/v, solution at both pH values.

Dependence of the rate constants on the polymer concentrations can be explained by taking an intramolecular reaction into consideration [12, 13]. A thiol group can react with thiol groups of other polymers as well as with each other within its own polymer. By taking this fact, the thiol concentration in the reaction system which is expressed by

[SH] = { (the number of thiol groups in the reaction vessel) - (the number of thiol groups within the own polymer)}/ (the volume of the reaction vessel) + (the number of thiol groups within the own polymer)/(the volume occupied by the polymer chain)

that is,

$$[SH] = [SH]_{\mathrm{int}er} + [SH]_{\mathrm{int}ra}$$

where $[SH]_{inter}$ and $[SH]_{intra}$ are the concentrations of the inter- and intra-molecular thiol groups. The intramolecular thiol concentration becomes smaller than $[SH]_{inter}$ in a higher concentration, while it becomes predominant at dilute concentration. Eq. (7) could be modified to reflect the contribution of the intramolecular reaction. The consumption rate of thiol groups can be expressed by

$$-\frac{\mathrm{d[SH]}}{dt} = k''([SH]_{inter} + [SH]_{intra})^2 \quad (9)$$

Eq. (9) can be modified as

$$-\frac{\mathrm{d[SH]}}{dt} = k''[SH]_{inter}{}^2(1 + \frac{[SH]_{intra}}{[SH]_{inter}})^2$$

The concentration ratio of inter- and intra-molecular thiol groups can be assumed to be constant throughout the reaction, as expressed by

$$\frac{[SH]_{intra}}{[SH]_{inter}} = \frac{[SH]_{intra0}}{[SH]_{inter0}}$$

where $[SH]_{inter0}$ and $[SH]_{intra0}$ are the initial inter- and intra-molecular thiol concentrations, respectively. The intermolecular thiol concentration, $[SH]_{inter}$, is { (the number of thiol groups in the reaction vessel) - (the number of thiol groups within the own polymer)} / (the volume of the reaction vessel). Here, (the number of thiol groups within the own polymer) is much smaller than (the number of thiol groups in the reaction vessel). It is practically expressed by

$[SH]_{inter}$ = (the number of thiol groups in the reaction vessel) /(the volume of the reaction vessel)

The intermolecular thiol concentration, $[SH]_{inter}$, is numerically equal to a macroscopic concentration [SH] which can be determined by the DTNB method.

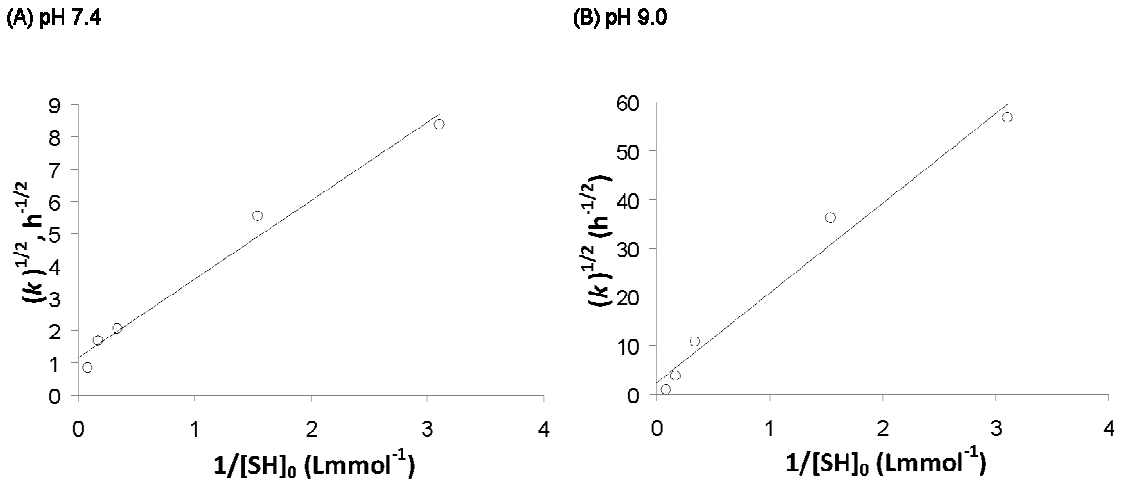

Figure.6 Plot of the square root of the apparent rate constant, *k″*, against the reciprocal of intermolecular thiol concentration, $[SH]_{inter0}$. Rate constants, *k′*, for a second order reaction can be estimated from the intercepts and the intramolecular thiol concentration, $[SH]_{intra0}$, can be estimated from the slope of these plots. pH = 7.4: *k′* = 1.31 $M^{-1}hr^{-1}$, $[SH]_{intra0}$ = 0.35, [P-SH44] = 0.35%, w/v; pH = 9.0: *k′* = 5.64 $M^{-1}hr^{-1}$, $[SH]_{intra0}$ = 7.76, [P-SH44] = 1.27%,w/v.

Eq. (9) can thus be expressed by

$$-\frac{\mathrm{d}[\mathrm{SH}]}{dt} = k''(1+\frac{[SH]_{intra0}}{[SH]_{inter0}})^2[SH]^2 \qquad (10)$$

From this differential equation, the change of thiol group concentration with time can be expressed by

$$\frac{1}{[SH]} - \frac{1}{[SH]_0} = k''(1+\frac{[SH]_{intra0}}{[SH]_{inter0}})^2 t \qquad (11)$$

When Eq. (11) is compared with Eq. (8), the apparent rate constant, *k′*, can be written using the rate constant, *k″*, and the inter- and intra-molecular concentrations of thiol groups by

$$k' = k''(1 + \frac{[SH]_{intra0}}{[SH]_{inter0}})^2 \qquad (12)$$

The intra-molecular thiol concentration, $[SH]_{intra0}$, does not depend on the polymer P-SH concentrations and thus the apparent reaction rate constant, *k′*, increases with decreasing concentrations of polymers, that is, the inter-molecular thiol, $[SH]_{inter0}$. The reaction rate constant, *k″*, and the intra-molecular thiol concentration of P-SH44 were determined from the intercepts of the ordinate and slopes, respectively, of the plots of $k'^{1/2}$ against $1/[SH]_{inter0}$ for the reactions at different P-SH44 concentrations (Figure.6). The intra-molecular thiol concentration was ~5 mM, corresponding to about 0.9%, w/v, of the polymer P-SH44 concentration. Dependence of the rate constants on the polymer concentrations can be explained by the second order reaction mechanism and taking into account the intra-molecular thiol concentration. Unfortunately, it could not be found any preceding work in which the auto-oxidation of thiol to disulfide follows second order kinetics with respect to the thiol concentration.

The disulfide formation rate between P-SH increased with the solution pH (Figure.1). The increased rate of thiol group oxidation with increasing pH is due to the elevation in the concentration of the thiolate anion intermediate $P\text{-}S^-$. As the pH increases, the deprotonation of P-SH is favored, and as indicated by the equilibrium reaction, the concentration of the intermediate anion increases. Thus, the reaction efficiently proceeds under alkaline conditions, but not under neutral or acidic conditions.

In addition, oxygen is consumed in advance of the auto-oxidation of thiol groups. Although the cross-linkage reaction for enclosure of living cells into hydrogel should be carried out under physiological conditions (pH = 7.4), the gelation rate is too slow to enclose living cells into hydrogel as indicated by the reaction rate of disulfide formation at pH = 7.4. Even when cells are successfully enclosed into hydrogel after a long gelation time, the cells hardly survive because oxygen in the reaction mixture is exhausted as the gelation proceeds. It is not practical to enclose living cells or islets of Langerhans (islets) into hydrogel by the auto-oxidation of pendant thiol groups [3].

Cross-linkage formation between P-SHs can be accelerated by the addition of a disulfide compound, GSSG, to a P-SH solution through the thiol-disulfide exchange. Concentrations of the components ([P-SH], [GSH], [P-SS-G], [P-SS-P], [GSSG]) at the equilibrium state under the gelation reaction were calculated using K_1 = 8.0 and K_2 = 4.8. The obtained concentrations are summarized in Table 3. Based on these values, the numbers of disulfide bonds per P-SH chain obtained are also listed in Table 3. The number of disulfide cross-linked bonds per a chain is the important parameter for the formation of gel. When a small amount of GSSG was added to the P-SH solution, the number of disulfide bonds formed was small. On the other hand, when a large amount of GSSG was added to the P-SH solution, disulfide bonds was rapidly formed, resulting in shorter gelation time. The reaction proceeded at physiological pH (= 7.4) without consumption of oxygen. Therefore, the thiol-disulfide exchange reaction is much more suitable for cell encapsulation than the thiol auto-oxidation reaction.

Table.3 Concentrations of each component (P-SH, GSH, GSSG, P-SS-G, P-SS-P) at equilibrium state of thiol-disulfide exchange reaction between P-SHs and GSSG in pH 7.4 at 37 °C. Concentrations of components at equilibrium state of gelation of P-SH solution with GSSG were determined at pH 7.4 and 37 °C.

Solution	$[GSSG]_0$ (mM)	[P-SH] (mM)	[GSH] (mM)	[P-SS-G] (mM)	[P-SS-P] (mM)	[GSSG] (mM)	[SS][c] (per chain)	Gelation time[d] (sec)
	1	97.8	2.0	0	1.0	0	2.09	4×10^4
10% (w/v)	5	89.9	9.9	0.1	4.9	0	10.3	3×10^4
P-SH22[a]	10	80.4	19.4	0.5	9.4	0.1	19.7	5
	50	27.2	72.5	17.5	27.5	5.0	57.5	4
	1	49.3	2.0	0	1.0	0	2.93	4×10^4
10% (w/v)	5	41.5	9.8	0.2	4.8	0	14.1	40
P-SH44[b]	10	32.4	18.9	0.9	9.0	0.1	26.4	30
	50	6.1	45.2	18.5	13.4	15.1	39.3	8

[a] $[P\text{-}SH]_0$ = 99.8 mM. [b] $[P\text{-}SH]_0$ = 51.3 mM. [c] Calculations based on the number average molecular weights. [d] Gelation time is reported in Hisano et al.[3]

4.5. References

[1] H. Iwata, T. Takagi, H. Amemiya, H. Shimizu, K. Yamashita, K. Kobayashi, T. Akutsu, J. Biomed. Mater. Res. 26 (1992) 967-977.

[2] M. Murakami, H. Satou, T. Kimura, T. Kobayashi, A. Yamaguchi, G. Nakagawara, H. Iwata, Transplantation 70 (2000) 1143-1148.

[3] N. Hisano, N. Morikawa, H. Iwata, Y. Ikada, J. Biomed. Mater. Res. 40 (1998) 115-123.

[4] Y. Teramura, H. Iwata, Bioconjugate Chem. 19 (2008) 1389-1395.

[5] Y. Teramura, Y. Kaneda, H. Iwata, Biomaterials 28 (2007) 4818-4825.

[6] J.N. Hansen, Anal. Biochem. 76 (1976) 37-44.

[7] J.N. Hansen, B.H. Pheiffer, J.A. Boehnert, Anal. Biochem. 105 (1980) 192-201.

[8] G.L. Ellman, Arch. Biochem. Biophys. 82 (1959) 70–77.

[9] V.H. Cohn, J. Lyle, Anal. Biochem. 14 (1966) 434-440.

[10] T.J. Wallace, A. Schriesheim, W.J. Bartok, Org. Chem. 28 (1963) 1311-1314.

[11] G. Capozzi, G. Modena, S. Patai, In *The Chemistry of the Thiol Group*, Eds.; Wiley: London, Part. 2 (1974) Chap. 17. “Oxidation of Thiols“

[12] H. Iwata, Y. Ikada, Macromolecules 12 (1979) 287-292.

[13] H. Morawetz, In Macromolecules in solution, Eds.; Jon Wiley & Sons, Inc. (1965) Chap. IX.

Chapter 5

Detection of insulin-releasing cells using in situ immunoblotting

5. 1. Introduction

Many diseases are caused by the disrupted function of particular cells in the human body. For instance, type I diabetes is caused by the destruction of pancreatic beta cells, and Parkinson's disease is caused by the degeneration of dopaminergic neurons. Transplantation of functional insulin or dopamine-releasing cells isolated from human tissue has been performed in clinics to treat patients [1, 2]. However, due to the shortage of human organ or tissue donors, the number of patients treated with cell transplantation has been limited. New cell sources, such as embryonic stem (ES) cells or somatic stem cells, are currently being investigated. ES cells can proliferate indefinitely and can differentiate into the three embryonic germ layers: endoderm, mesoderm, and ectoderm [3]. Because they are pluripotent, ES cells have been thought to be a promising cell source for cellular therapeutic applications. Many studies with mouse and human ES cells have demonstrated effective derivation of insulin-releasing cells [4–6]. In our previous work, we derived ES cell progeny, including many colonies of insulin- and C-peptide-positive cells, from mouse ES cells.

The progeny still contained insulin- and C-peptide-positive cells after nine

rounds of subculturing, but the population of insulin-releasing cells did not increase [7]. It has been reported that beta cells are capable of self-renewal [8-10]. If progenitor or immature insulin-releasing cells with proliferation potential could be isolated from ES cell progeny, a large number of insulin-producing cells could be obtained by in vitro cell expansion. Several methods to isolate specific cells have been developed. ES cell lines that carry a reporter gene have been established to isolate insulin-producing cells [11, 12], but other difficulties must be overcome before these genetically modified cells can be used as gene therapy in human patients. Fluorescence- or magnetic-activated cell sorters (FACS or MACS) are commonly used to isolate specific cells using antibodies against cell surface antigens. However, surface antigens specific to beta cells that can be used in FACS and MACS have not yet been identified. We wished to develop a simple and efficient method to identify and purify insulin-producing cells. In this chapter, we developed a simple method based on *in situ* immunoblotting to identify and isolate bioactive substance-producing cells from a tissue culture dish. Its efficacy was demonstrated using insulin-producing MIN6 cells and alpha-fetoprotein (AFP)-producing Hep-G2 cells as model cell cultures. The cell spots were placed in an orderly array on the culture dishes. A nitrocellulose membrane coated with anti-insulin or anti-AFP antibodies was gently placed on the cell layer to bind to insulin or AFP released from the cells. The location of insulin- or AFP-producing cells was identified by immunostaining the membrane to detect the bound insulin or AFP. The insulin-producing cells could be selectively collected from the culture dish using the cloning ring method and replated onto another culture dish.

5. 2. Materials and Methods

Materials

DMEM, Alexa488-conjugated goat anti-guinea pig IgG(H+L) antibody and Alexa594-conjugated goat anti-rabbit IgG(H+L) antibody were purchased from Invitrogen (Carlsbad, CA, USA). Skim milk, methylcellulose, penicillin-strreptomycin mixed solution (PC/SM), 4% - Paraformaldehyde Phosphate Buffer Solution, 2.5g/L - Trypsin/1mmol/L - EDTA Solution and ethanol were purchased from Nacalai Tesque (Kyoto, Japan). Dulbecco's phosphate-buffer saline (PBS) was obtained from Nissui Pharmaceutical Company (Tokyo, Japan). Mouse anti-human insulin monoclonal antibody was purchased from Sigma-Aldrich (St. Louis, MO, USA). Anti-human AFP monoclonal antibody was purchased from Acris Antibodies GmbH (Herford, Germany). Triton® X-100, 2-amino-2-hydroxymethyl-1,3-propanediol (Tris-HCl), NaCl, Polyoxyethylene (20) Sorbitan Monolaurate (Tween 20) were purchased from Wako Pure Chemical Industries, Ltd (Osaka, Japan). Polyclonal guinea pig anti-swine insulin antibody was purchased from Dako (Glostrup, Denmark). Rabbit anti-human AFP polyclonal antibody was purchased from Sanbio B.V. (Uden, Netherlands). Can Get Signal® Immunoreaction Enhancer Solution was purchased from TOYOBO CO., LTD. (Osaka, Japan). Donkey anti-guinea pig IgG(H+L) antibody conjugated with horseradish peroxidase (HRP) was purchased from Chemicon International, Inc. (Temecula, CA, USA). Goat anti-rabbit IgG(H+L) antibody conjugated with HRP was purchased from Jackson Immuno Research Europe Ltd (West Grove, PA, USA). Konica

Immunostain HRP-1000 was purchased from Konica Minolta Health Care Co., Ltd. (Tokyo, Japan). -Cellstain®- Hoechst 33342 solution was purchased from DOJINDO LABORATORIES (Kumamoto, Japan).

Cell culture

Immortalized mouse pancreatic beta cells, MIN6 [13], were kindly donated by Dr. Miyazaki (Osaka University, Osaka, Japan). Immortalized human hepatoma Hep-G2 cells, which secrete AFP, were obtained from the Health Science Research Resources Bank (Osaka, Japan). Both of these cell lines were routinely maintained using DMEM supplemented with 10% fetal bovine serum and antibiotics (10 U/ml penicillin, and 10 mg/ml streptomycin) in a humidified atmosphere of 5% CO_2/95% air at 37°C.

Preparation of the silicon sheet

A 76-mm × 26-mm slide glass (Matsunami Glass Ind., Ltd.; Osaka, Japan) was cut in half (see Scheme 1). It was washed with ethanol and distilled water, dried by N_2 blowing, and then coated with Barrier Coat (Shin-Etsu Chemical Co.; Tokyo, Japan) using a spincoater for 10 s at 1000 rpm followed by incubation at 120°C for 3 min. A frame made of a 1.0-mm-thick silicon sheet (As One Corp.,; Osaka, Japan) was put on the slide. A 10:1 mixture of a dimethylsiloxane prepolymer and a curing agent (Sylgard 184 Silicone Elastomer Kit, Toray Industries, Inc.,; Tokyo, Japan) was poured into the frame on the glass slide. The slide was left in a desiccator under reduced pressure for 45 min to remove air from the mixture. After another glass slide coated with Barrier Coat was placed

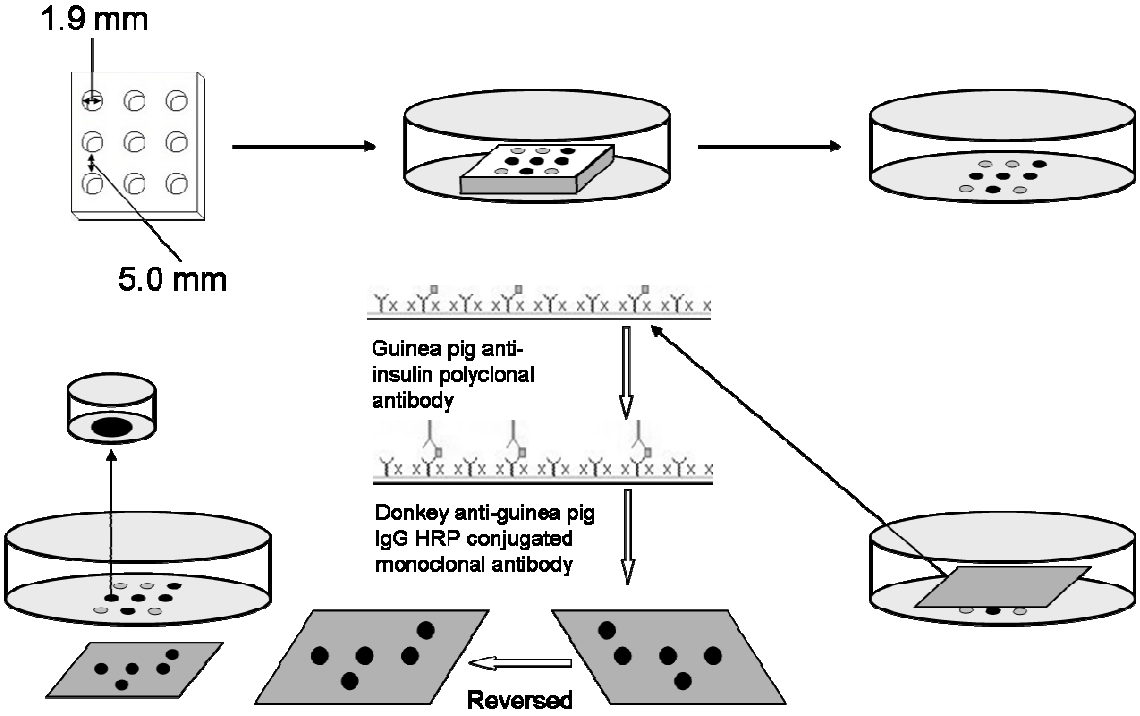

Scheme.1 *In situ* immunoblotting procedure for identifying cells releasing insulin or alpha-fetoprotein.

on the mixture, it was cured at 120°C for 45 min. The cured silicon sheet was removed from the glass plate and nine holes (1.9 mm in diameter) were punched out of the silicon sheet using a stainless steel pipe (1.9 mm inside diameter).

Spotting cells on a culture dish

The silicon sheet with 9 holes was rinsed with 70% ethanol and placed in a 6-cm culture dish. 5 μL of a cell suspension containing 9000 MIN6 or Hep-G2 cells was put into each hole of the silicon sheet. After 700 μl of PBS was left on the periphery of the dish to suppress evaporation of the culture medium, the dish was incubated for 6–7 h at 37°C to allow cells to settle on the surface of the dish. PBS was removed from the dish and 7 ml culture medium was added on top of

the silicon sheet. The dish was left overnight in a humidified atmosphere of 5% CO_2/95% air at 37°C. After cell adhesion onto the dish was confirmed, tweezers were used to remove the silicon sheet from the dish, using care not to disturb the cell spots.

To examine the sensitivity, 5 μl of a cell suspension containing 1000, 3000, 6000, or 9000 MIN6 cells was put into each hole of the silicon sheet and the dish was incubated for 7 h at 37°C to allow cells to settle on the surface of the dish as described above. After the silicon sheet was removed, 4 μl of a cell suspension containing 1×10^6 Hep-G2 cells was applied into the culture dish. *In situ* immunoblotting was performed after 11 h additional culture as follows.

In situ immunoblotting

The outline of the immunoblotting procedure is shown in Scheme 1. A nitrocellulose membrane coated with antibodies against human insulin or against human AFP was prepared as follows. A plain nitrocellulose membrane (Bio-Rad Laboratories, Inc.,; CA, USA) was treated with mouse anti-human insulin monoclonal antibody in PBS (diluted 1:200) or mouse anti-human AFP monoclonal antibody in PBS (diluted 1:200) for 1 h at 37°C. The membrane was blocked with a solution of 3% skim milk in (10 mM Tris–HCl, 100 mM NaCl, 0.1% Tween, pH 7.5), (TTBS) for 1 h at 37°C and then washed twice with PBS. For *in situ* immunoblotting, the membrane carrying anti-insulin antibody or anti-AFP antibody should be placed gently on top of the cell layer. When a membrane directly touches the cell layer, the cells attach to the membrane and will be removed from the culture dish. In Teruya et al.'s study [14], a filter paper was

inserted between the membrane and the cells; however, this procedure caused cells to deteriorate. Therefore, instead of using a filter to form a layer between the membrane and the cells, in this chapter we used a highly viscous culture medium prepared by adding 2% methylcellulose to the medium. The culture medium was removed from a dish that had been placed over the cells, and 1 ml of DMEM supplemented with 2% methylcellulose was added to the culture. The thickness of the medium layer was estimated to be about 470 mm, calculated using the volume of the culture medium added (1 ml) and the surface area of the culture dish (21.3 cm^2). The nitrocellulose membrane carrying anti-human insulin antibody or anti-human AFP antibody was layered over the medium. After a 1-h incubation at 37°C, 5 ml of culture medium without methylcellulose was infused underneath the membrane, and the membrane was carefully recovered with tweezers and washed twice with TTBS. Immunostaining was used to determine the position of immobilized proteins on the membrane. The membrane was treated with guinea pig anti-swine insulin polyclonal antibody (diluted 1:100) or with rabbit anti-human AFP polyclonal antibody (diluted 1:100) diluted with Can Get Signal Solution1 for 1 h at room temperature. After washing with TTBS, the membrane was incubated with donkey anti-guinea pig IgG(H+L) antibody conjugated with HRP (diluted 1:5000) or goat anti-rabbit IgG(H+L) antibody conjugated with HRP (diluted 1:2500) in Can Get Signal Solution2 for 1 h at room temperature. Finally, color was developed using Immunostain HRP-1000.

Immunochemical staining of cells on culture dishes

Cultured cells were fixed with 4% paraformaldehyde solution for 15 min at

room temperature in culture dishes, permeabilized with 0.2% Triton X-100 in PBS, and then blocked with 2% skim milk in PBS for 1 h at room temperature. The cells were treated with a mixture of guinea pig anti-swine insulin polyclonal antibody (diluted 1:100) and rabbit anti-human AFP polyclonal antibody (diluted 1:200) in 2% skim milk in PBS at 4°C overnight. After washing with 0.05% Tween-20 in PBS (TPBS), the cells were treated with a mixture of Alexa488-conjugated goat anti-guinea pig IgG(H+L) antibody (diluted 1:500, Invitrogen Corp.) and Alexa594-conjugated goat anti-rabbit IgG(H+L) antibody (diluted 1:500, Invitrogen Corp.) in 2% skim milk in PBS for 2 h. After washing with TPBS, the cells were treated with Hoechst 33342 fluorescent dye for nuclear DNA staining.

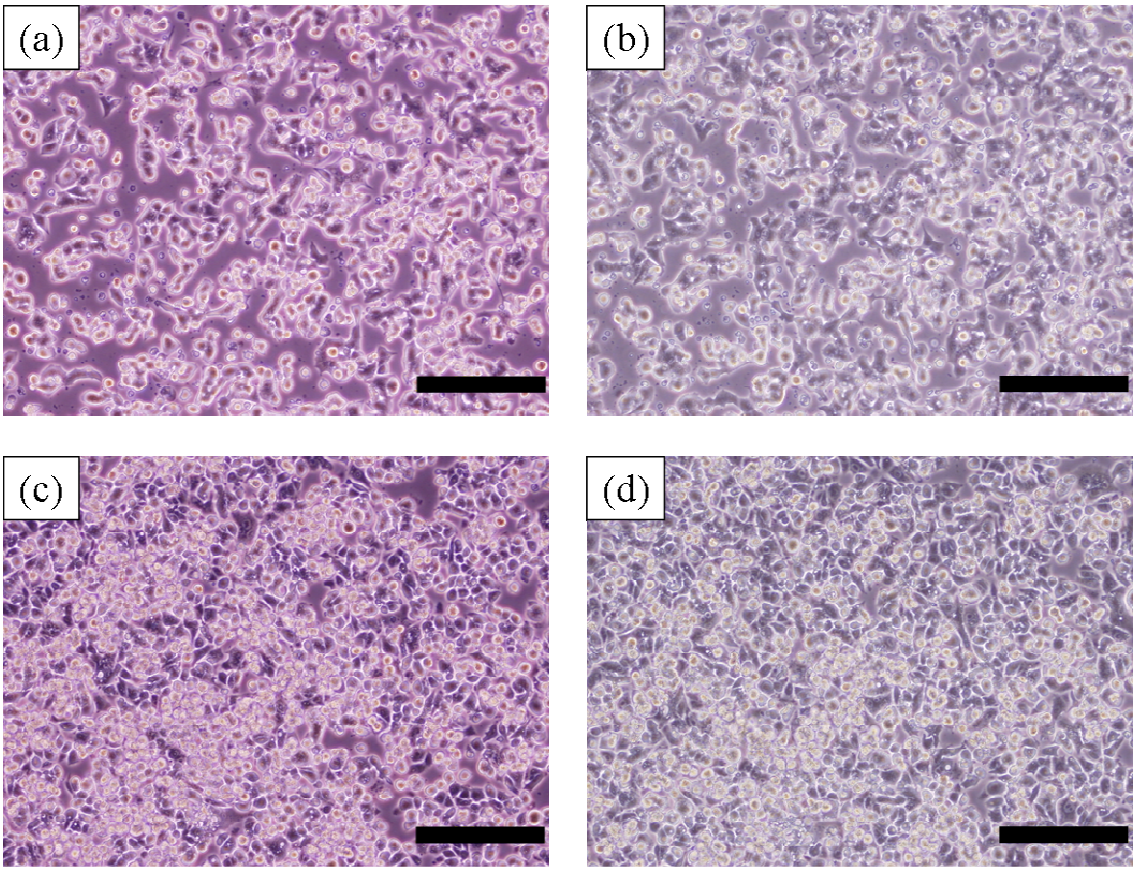

Figure.1 Cell morphology before and after *in situ* immunoblotting. (a) and (b): MIN6 cells;. (c) and (d): Hep-G2 cells. Scale bars: 200 μm.

Collection of insulin-positive cells

Images of the immunostained membranes were collected with a scanner (ES-8000; Seiko Epson Corp., Nagano, Japan). The captured image was reversed by using Adobe Photoshop version 5.0 (Adobe Systems Inc., San Jose, CA). The reversed image was printed and placed under the culture dish. The cells at the immunopositive positions were collected as follows. The culture medium was removed. Then cloning ring (inside diameter 3.4 mm, Asahi Technoglass Corp., Chiba, Japan) with silicon grease (Shin-Etsu Chemical Co.) at its rim was put on the dish at the immunopositive spot. A 0.25% trypsin EDTA solution was added into the cloning rings to detach cells from the culture dish.

Trypsin activity was halted by adding culture medium containing serum into the cloning rings and the cells were collected. The cells were seeded into a well of a 96-well multiwell plate. These collected, plated cells were analyzed by immunostaining using the method described above for cells on a culture dish.

5. 3. Results

***In situ* immunoblotting**

No cell damage was observed for either MIN6 cells or Hep-G2 cells after a series of incubations with membranes (Fig. 1). Insulin and AFP, which were secreted from the cells and diffused to the nitrocellulose blotting membrane, bound to membranes carrying anti-insulin or anti-AFP antibodies, respectively. Those spots were visualized by immunostaining, as shown in Fig. 2 (a) and (b).

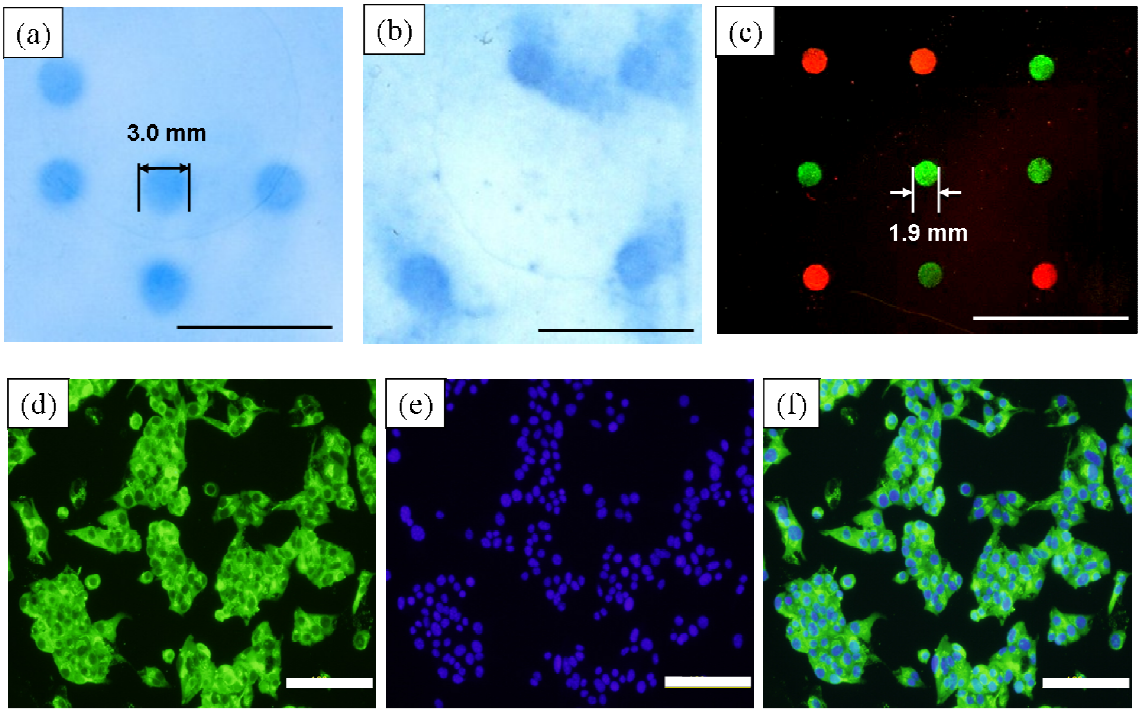

Figure.2 Nitrocellulose membranes used for immunoblotting insulin or alpha˜-fetoprotein, and immunohistochemical staining of cell spots on a culture dish, and collection of MIN6 cells from a spot identified using the *in situ* immunoblotting method. (a): Membrane used for immunoblotting insulin. (b): Membrane used for immunoblotting alpha˜-fetoprotein. (c): Cell spots stained with anti-insulin (green) and anti-AFP polyclonal antibodies (red). Scale bars in panels in (a), (b) and (c): 1 cm. MIN6 cells were collected from the spot using trypsin and a cloning ring, and were replated in a well of a 96-well plate. After incubation for 2 days, cells were immunostained using anti-insulin antibody. (d): Immunostaining image for insulin (green). (e): Nuclear staining image with Hoechst 33342 (blue). (f): Merged image from panels (d) and (e). Scale bars in panels (d), (e) and (f): 100 μm.

The five positive spots could be seen on the membrane as shown in Fig. 3 (a), too. As seen in Fig. 3 (a), 3000 MIN6 cells in a spot (ϕ = 1.9 mm) could be easily detected. The spot containing 1000 MIN6 cells might be possibly found. Thus 1000 MIN6 cells in a spot (ϕ = 1.9 mm) are the limit of detection by this method.

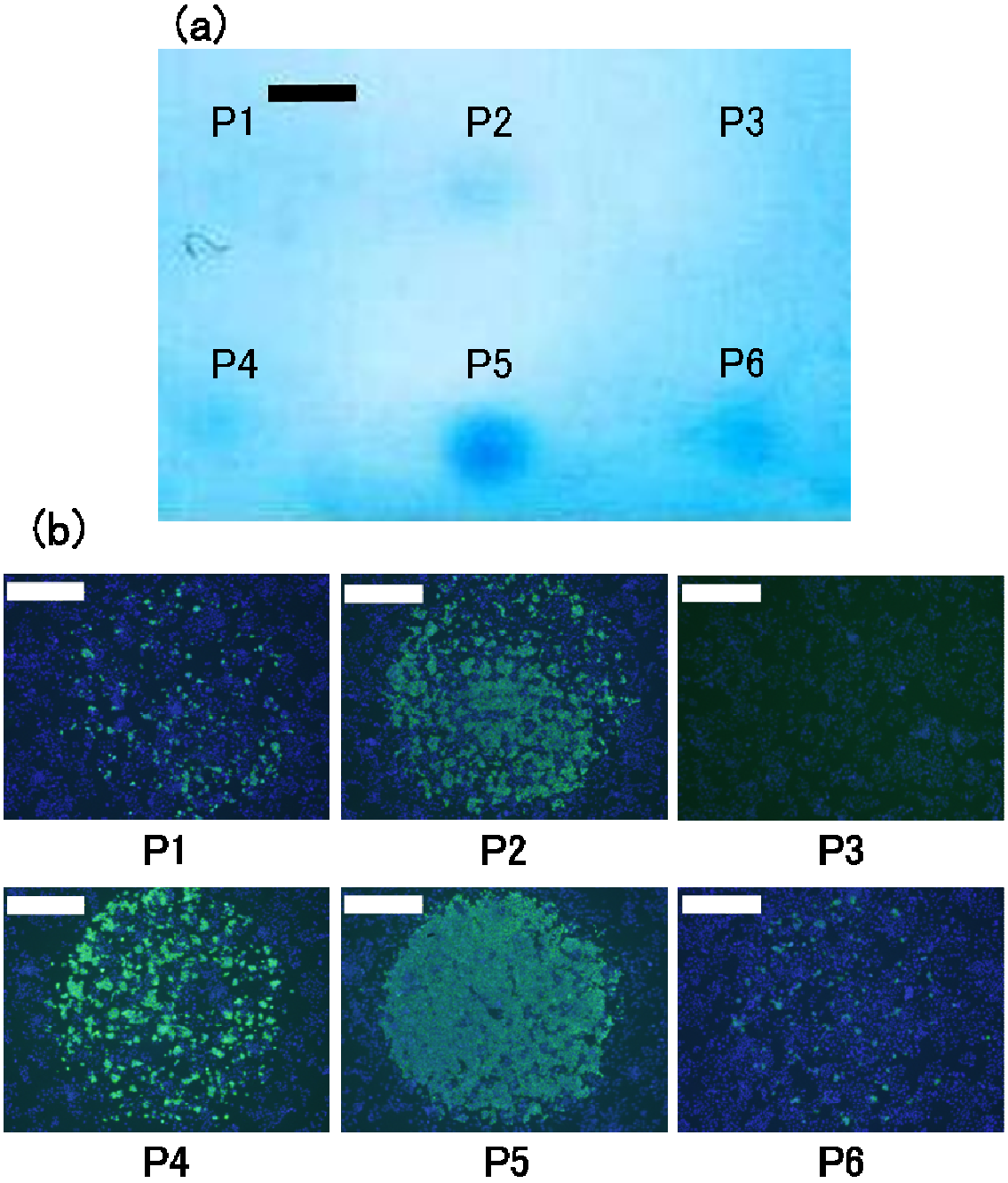

Figure.3 Nitrocellulose membranes used for immunoblotting insulin and immunohistochemical staining of cell spots on a culture dish. (a): Membrane used for immunoblotting insulin. Scale bar: 2 mm. (b): Merged image with the image of immunostained with anti-insulin (green) and that of nuclear staining with Hoechst 33342 (blue). Scale bars: 500 μm. P1-P6 represent the position 1-6. Spots P1, P2, P3, P4, P5 and P6 contained 1000, 6000, 0, 3000, 9000, 1000, respectively.

Immunochemical staining of cells on culture dishes

To verify the correlation of immunoblotted spots on the membrane and cell spots on the culture dish, the cells on the culture dish were fixed and immunostained using anti-insulin antibody and anti-AFP antibody after removal of the membrane. Fig. 2 (c) shows photos of the immunostained culture dish. Insulin-positive (green) and AFP-positive (red) spots can clearly be seen on the culture dish. The immunoblots on the membrane shown in Fig. 2 (a) and (b) formed mirror images of the cell spots on the culture dish. On the other way, different numbers of MIN6 cells (1000, 3000, 6000 and 9000 cells) were put into each hole of the silicon sheet and left for 7 h to adhere to the culture dish. After the silicon sheet was removed, Hep-G2 cells were applied into the culture dish. *In situ* immunoblotting was performed after 11 h additional culture. Fig. 3 also includes micrographs of immunohistochemical insulin staining and nuclear staining of the spots.

Collection of insulin-positive cells

The collected MIN6 cells were reseeded in a well of a 96-well plate and cultured for 2 days in DMEM in 5% CO_2 at 37 ^{o}C. Micrographs of immunohistochemical staining and nuclear staining of the MIN6 cells are shown in Fig. 2 ((d)-(f)).

5. 4. Discussion

Mouse MIN6 cells, which produce insulin, and human Hep-G2 cells, which

produce AFP, were used as model cells to develop an *in situ* immunoblotting method for detecting and isolating protein-secreting cells from cell culture plates. The cells were spotted on a culture dish. In this experiment, five of the nine cell spots were MIN6 cells, and the other four spots were Hep-G2 cells. Highly viscous culture medium, prepared by adding 2% methylcellulose to medium, was added to the culture dish to form a thin layer of medium over the cell spots. A nitrocellulose membrane, previously coated with antibodies that recognize insulin or AFP, was gently placed on top of the cell spots but did not directly contact the cells. The viscous medium served as a 470-μm cushion between the cells and the membrane, preventing the cells from binding to the membrane. After a 1 h incubation at 37°C, the membrane was carefully removed and immunostained for insulin or AFP. In Fig. 2 (a) and (b), the positive spots could be observed on the membrane and they formed the mirror images of the cell spots on the culture dish respectively. The co-existence of Hep-G2 cells in the spots did not interfere with the *in situ* immunoblotting. After removal of the membrane, the culture dish was washed with culture medium without methylcellulose and observed by phase contrast microscopy. The MIN6 cells and Hep-G2 cells did not have damage after the incubation of membrane.

The aim of this chapter was to develop a method to isolate bioactive substance-producing cells from the progeny of stem cells. We have already described the method (*in situ* immunoblotting) used to locate the specific cells. The method used to retrieve the cells from a culture dish is shown schematically in Scheme 1. The reversed image of the immunoblotted membrane was printed and placed under the culture dish. A cloning ring was placed on cells located on

the insulin-positive blots, and trypsin solution was added to the ring. Cells were collected from the dish and reseeded in 96-well plate. The viability of the collected MIN6 cells was greater than 90%, as determined by the trypan blue exclusion test. MIN6 cells adhered well to the dish and formed cell clusters. This indicated that insulin releasing cells could be found and isolated by the combination of the *in situ* immunoblotting and the cloning ring procedure.

To verify the limit of detection of the method and the effect of coexistence of other cells, difference numbers of MIN6 cells spot were prepared and Hep-G2 cells were applied after removed the silicon sheet. *In situ immunoblotting* was performed after 11h additional culture. As a result, positive spot were observed and each color density on the immunoblotting membrane was correlated with the number of MIN6 cells in each spot. The color density increased with increasing numbers of MIN6 cells in the spot and the spot containing 1000 MIN6 cells might be possibly found. Thus 1000 MIN6 cells in a spot (1.9 mm in diameter) are taken as the limit of detection by this method.

In our experimental setup, insulin and AFP released from the cells travelled by diffusion to the blotting membrane and were trapped by the antibodies on the membrane. The time needed for one-dimensional diffusion over distance L can be estimated using the following equation, in which t represents time (in seconds) and D represents the diffusion coefficient (cm^2/sec):

$$t = L^2/2D \qquad (1)$$

The cells and the membrane were separated by 470 μm of culture medium,

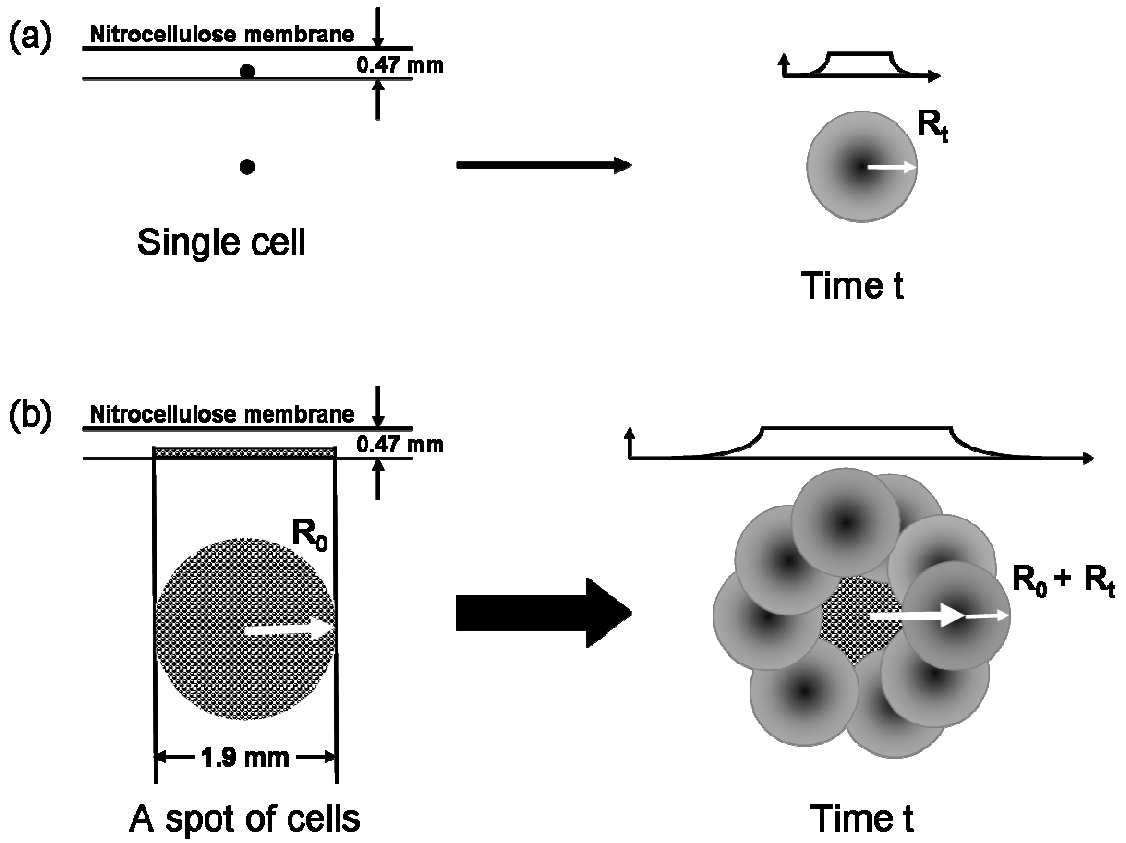

Scheme.2 A secreted substance released from a cell diffuses to the membrane. (a): The substance is released from the cell. After t sec, the substance forms a cloud with radius R_t. (b): The substance is released from a cell spot with radius R_0. A cell at the periphery of the cell culture spot forms a cloud with radius R_t. The diameter of the immunoblotted spot is expressed as diameter = $2R = 2R_0 + 2R_t$.

and the diffusion coefficients of insulin and AFP in water at 20ºC are D = 7.3 x 10^{-7} cm^2/sec and D = 6.6 x 10^{-7} cm^2/sec [15], respectively. Thus, the time required for diffusing 470 μm is estimated using equation (1) to be about 30 minutes for both insulin and AFP. The blotting membrane was left on the culture dish for one hour, allowing sufficient time for the diffused proteins to bind to the blotting membrane.

Note that the diameters of the spots on the immunoblots (3 mm in diameter) are about 1.6 times larger than those of the cell spots on the culture dish. When

insulin and AFP diffuse vertically to the membrane, they also diffuse laterally. Suppose that a single cell adheres to a culture dish and continuously releases a substance as shown in Scheme 2A. Diameter of the area containing the diffused substance after time t is approximately expressed by equation (2) for two-dimensional diffusion, in which R is the radius in cm (and diameter is 2 × R)

$$t = R_t^2/4D \qquad (2)$$

In our experimental setup, each spot contained more than 9000 cells (1.9 mm in diameter). Referring to Scheme 2, a substance released by cells at the periphery of the cell spot diffuses a distance of R_t during time, t. Thus, the diameter of the immunoblotted spots can be roughly expressed by:

$$2R = 2R_0 + 2R_t \qquad (3)$$

where R_0 is the radius of the cell spot, R_t is obtained from equation (2), and R is the radius of a blotted spot on the membrane at time t. In this experiment, the diameter of the immunopositive spot on the immunoblot, 2R, is estimated to be about 3.7 mm after one-hour blotting using equation (2) and (3) and diffusion coefficient. This theoretical value is in agreement with the experimental diameter of the spots observed on the immunoblotted membrane. To obtain a blotting spot similar in size to the cell spot, the distance between the cell layer and the blotting membrane should be as small as possible.

5. 5. References

[1] A.M. Shapiro, J.R. Lakey, E.A. Ryan, G.S. Korbutt, E. Toth, G.L. Warnock, N.M. Kneteman, R.V. Rajotte, Islet transplantation in seven patients with type 1 diabetes mellitus using a glucocorticoid-free immunosuppressive regimen, N. Engl. J. Med. 343 (2000) 230-238.

[2] C.R. Freed, P.E. Greene, R.E. Breeze, W.Y. Tsai, W. DuMouchel, R. Kao, S. Dillon, H. Winfield, S. Culver, J.Q. Trojanowski, D. Eidelberg, S. Fahn, Transplantation of embryonic dopamine neurons for severe Parkinson's disease, N. Engl. J. Med. 344 (2001) 710-719.

[3] J.A. Thomson, J. Itskovitz-Eldor, S.S. Shapiro, M.A. Waknitz, J.J. Swiergiel, V.S. Marshall, J.M. Jones, Embryonic stem cell lines derived from human blastocysts, Science 282 (1998) 1145-1147.

[4] S. Assady, G. Maor, M. Amit, J. Itskovitz-Eldor, K.L. Skorecki, M. Tzukerman, Insulin production by human embryonic stem cells, Diabetes 50 (2001) 1691-1697.

[5] N. Lumelsky, O. Blondel, P. Laeng, I. Velasco, R. Ravin, R. McKay, Differentiation of embryonic stem cells to insulin-secreting structures similar to pancreatic islets, Science 292 (2001) 1389-1394.

[6] Y. Moritoh, E. Yamato, Y. Yasui, S. Miyazaki, J. Miyazaki, Analysis of insulin-producing cells during in vitro differentiation from feeder-free embryonic stem cells, Diabetes 52 (2003) 1163-1168.

[7] T. Ibii, H. Shimada, S. Miura, E. Fukuma, H. Sato, H. Iwata, Possibility of insulin-producing cells derived from mouse embryonic stem cells for diabetes treatment, J. Biosci. Bioeng. In press

[8] S. Bonner-Weir, Beta-cell turnover: its assessment and implications, Diabetes 50 (2001) (Suppl. 1) S20-S24.

[9] G.M. Beattie, A.M. Montgomery, A.D. Lopez, E. Hao, B. Perez, M.L. Just, J.R. Lakey, M.E. Hart, A. Hayek, A novel approach to increase human islet cell mass while preserving beta-cell function, Diabetes 51 (2002) 3435-3439.

[10] Y. Dor, J. Brown, O.I. Martinez, D.A. Melton, Adult pancreatic beta-cells are formed by self-duplication rather than stem-cell differentiation, Nature 429 (2004) 41-46.

[11] B. Soria, E. Roche, G. Berna, T. Leon-Quinto, J.A. Reig, F. Martin, Insulin-secreting cells derived from embryonic stem cells normalize glycemia in streptozotocin-induced diabetic mice, Diabetes 49 (2000) 157-162.

[12] Y. Moritoh, E. Yamato, Y. Yasui, S. Miyazaki, J. Miyazaki, Analysis of insulin-producing cells during in vitro differentiation from feeder-free embryonic stem cells, Diabetes 52 (2003) 1163-1168.

[13] J. Miyazaki, K. Araki, E. Yamato, H. Ikegami, T. Asano, Y. Shibasaki, Y. Oka, K. Yamamura, Establishment of a pancreatic beta cell line that retains glucose-inducible insulin secretion: special reference to expression of glucose transporter isoforms, Endocrinology 127 (1990) 126-132.

[14] K. Teruya, S. Shirahata, T. Yano, K. Seki, H. Tachibana, H. Ohashi, H. Murakami, Secretory cell immunoscreening assay--a highly sensitive screening method for secretory cells, Anal. Biochem. 214 (1993) 468-473.

[15] S. Aliau, J. Marti, J. Moretti, Bovine alpha-fetoprotein. Isolation and characterization, Biochimie 60 (1978) 663-672.

Summary

Chapter.1

When islets were tranlplanted into the portal vein, the exposure of islet surface to fresh blood activated the coagulation and complement system. The majority of transplanted islets are destroyed at early post-transplantation stage by instant blood-mediated inflammatory reactions (IBMIR). Several anticoagulants inhibit IBMIR but they have a high risk of bleeding. The localization of anticoagulant is necessary as an alternative method.

In this chapter, urokinase and TM were immobilized to islet surfaces through a Mal–PEG–lipid conjugate using thiol/maleimide reactions. The thiol groups were introduced to the amine group of enzymes by Traut's reagent. The activities of UK and TM were maintained on the islet surface. Furthermore, the surface modifications did not influence the islets' morphology or ability to secrete insulin in response to changes in glucose concentration. It is expected that the islet graft loss caused by IBMIR at the early stage of islet transplantation can be avoided by this method.

Chapter.2

In chapter 1, it was successful to immobilize urokinase and TM on the islet surface by using Mal-PEG-lipid. Both enzymes kept their activity and released from islet surface with function of time. However, this method can not be applied to low molecular weight drug because the amine group of drug is essential to introduce thiol group.

In this chapter, a low molecular weight anticoagulant, argatroban-loaded liposomes can be immobilized on islet surfaces. OligoDNA were introduced to liposome and islet surface by hydrophobic interaction. Next, liposome and islet were linked by DNA hybridization. Argatroban in the liposome was gradually released, based on measurements of its antithrombin activity. By the observation of single islet cell, few liposomes were internalized into the inside of cell. The surface modification did not influence islet morphology or the islets' ability to secrete insulin in response to changes in glucose concentration. This method may reduce the islet graft loss caused by IBMIR.

Chapter.3

Stem cells are expected as a source of living cell and tissue for regenerative medicine. At the stage of stem cells differentiation, cell-cell interaction is an important factor. On the other way, to control cell-cell reaction is necessary for the generation of cell-type-specific tissues and organs.

In previous chapters, it is possible to immobilize protein or liposome on cell surface. In this chapter, by incorporating complementary DNA sequences attached to amphiphilic PEG-lipids into the membranes of two cell populations, it was induced cell–cell attachments that were mediated by DNA hybridization. The special attachment and control of attached cell ratio can be achieved. This technique was also used to successfully induce cell attachment to a substrate containing immobilized DNA. This method shows promise for use in analyzing homogeneous and heterogeneous cell–cell interactions.

Chapter.4

Hydorgels that have three dimensionally crosslinked polymer chains are used for various biomedical devices. However, because they are insoluble substances with few crosslinked points for gel formation, they are not still well characterized.

In this chapter, poly(acrylamide-*co*-*N*-acrylcysteamine)(P-SH) was examined for the preparation hydrogels for biomedical applications. Using only the auto-oxidation of thiols, the gelation rate was too slow to enclose living cells into hydrogel under physiological conditions at pH 7.4. The hydrogel formation rate can be accelerated by addition of disulfides, such as GSSG. The thiol-disulfide exchange reaction is more suitable for cell encapsulation than thiol auto-oxidation.

Chapter.5

It is known that stem cells are investigated as new cell sources. If specific cells with proliferation potential could be isolated from ES cell progeny, a large number of could be obtained by in vitro cell expansion.

In this chapter, a simple and efficient method was developed to identify and purify insulin-producing cells. A nitrocellulose membrane coated with anti-insulin antibody was placed gently on a cell layer to trap insulin released from the cells. The location of the cells releasing the insulin was determined by immunostaining the membrane-bound insulin. The insulin-releasing cells could then be selectively collected from the dish by trypsin treatment using a cloning ring. The method developed in this chapter may be useful for purifying and concentrating insulin-releasing cells from stem cells progeny for clinical applications.

List of Publications

Chapter.1: Co-immobilization of urokinase and thrombomodulin on islet surfaces by poly(ethylene glycol)-conjugated phospholipid.
Chen H, Teramura Y, Iwata H.
Journal of Controlled Release. 150 (2011): 229-234.

Chapter.2: Immobilization of anticoagulant-loaded liposomes on cell surfaces by DNA hybridization
Chen H, Teramura Y, Iwata H.
Biomaterials. *In Press*.

Chapter.3: Control of cell attachment through polyDNA hybridization.
Teramura Y, Chen H, Kawamoto T, Iwata H.
Biomaterials. 31(2010): 2229-2235.

Chapter.4: Kinetic analysis of disulfide formation between thiol groups attached to linear poly(acrylamide)
Hisano N, Iwata H, Teramura Y, Chen H, Ikada Y.
Journal of polymer science. Part A, Polymer chemistry. 49 (2011): 671-679.

Chapter.5: Detection of insulin-releasing cells using in situ immunoblotting.
Chen H, Sato H, Totani T, Iwata H.
Analytical Biochemistry. 366 (2007): 137-43.

Acknowledgements

The present study was carried out from 2007 to 2011 under the continuous guidance of Dr. Hiroo Iwata, Professor of Institute for Frontier Medical Sciences in Kyoto University. The author is grateful to Professor Iwata for his careful guidance, constant encouragement, valuable discussion and details criticism on the manuscript throughout the present work. The completion of the present work has been an exiting project and would not have been possible without his guidance.

The author is also deeply indebted to Dr. Yuji Teramura, Assistant Professor of Institute for Frontier Medical Sciences in Kyoto University, for his sincere advice and valuable discussion on the study.

The author wishes to express his thank to Dr. Koichi Kato, Associate Professor of Institute for Frontier Medical Sciences in Kyoto University, for his constant guidance and helpful suggestions.

The author is also indebted to Dr. Yusuke Arima, Assistant Professor of Institute for Frontier Medical Sciences in Kyoto University, for intimate advice and valuable discussion.

The author wishes to take an opportunity to extend his hearty thank to all staffs and students of Department of Reparative Materials of Institute for Frontier Medical Sciences, Kyoto University, for their kind help.

Finally, the author expresses his gratitude to his parents, Mr. Hongjie Chen and Ms. Aihua Li, his grandfather Mr. Zhenwen Li, his grandmother, Ms. Yufeng

Acknowledgements

Zhu, for their cordial support and continuous encouragement.

Institute for Frontier Sciences

Kyoto University

Hao Chen

2011 August